TAILORED POLYMER LIGAND SORBENTS FOR RADIOANALYTICAL APPLICATIONS

By

AMOL M. MHATRE

CHEM01201304027

Bhabha Atomic Research Centre, Mumbai

A thesis submitted to the
Board of Studies in Chemical Sciences
In partial fulfillment of requirements
for the Degree of

DOCTOR OF PHILOSOPHY

of

HOMI BHABHA NATIONAL INSTITUTE

May, 2019

Homi Bhabha National Institute

Recommendations of the Viva Voce Committee

As members of the Viva Voce Committee, we certify that we have read the dissertation prepared by **Amol Madhukar Mhatre** entitled "Tailored **Polymer Ligand Sorbents for Radioanalytical Applications"** and recommend that it may be accepted as fulfilling the thesis requirement for the award of Degree of Doctor of Philosophy.

Chairman - **Prof. Y.K. Bhardwaj**		**Date:** 03/05/19
Guide / Convener – **Prof. A.K. Pandey**	Pandey	**Date:** 3.5.2019
Examiner - **Prof. Pralay Maiti**	Pmaiti	**Date:** 03.05.19
Member 1- **Prof. Sangita D. Kumar**		**Date:** 03.05.19
Member 2- **Dr. Suparna Sodaye**		**Date:** 03.05.19
Member 3- **Dr. P.G. Jaison**	Jaison	**Date:** 03/05/2019.

Final approval and acceptance of this thesis is contingent upon the candidate's submission of the final copies of the thesis to HBNI.

I hereby certify that I have read this thesis prepared under my direction and recommend that it may be accepted as fulfilling the thesis requirement.

Date: 3.5.2019

Place: BARC, Mumbai

Pandey

Guide

STATEMENT BY AUTHOR

This dissertation has been submitted in partial fulfilment of requirements for an advanced degree at Homi Bhabha National Institute (HBNI) and is deposited in the Library to be made available to borrowers under rules of the HBNI.

Brief quotations from this dissertation are allowable without special permission, provided that accurate acknowledgement of source is made. Requests for permission for extended quotation from or reproduction of this manuscript in whole or in part may be granted by the Competent Authority of HBNI when in his or her judgment the proposed use of the material is in the interests of scholarship. In all other instances, however, permission must be obtained from the author.

Amol M. Mhatre

DECLARATION

I, hereby declare that the investigation presented in the thesis has been carried out by me. The work is original and has not been submitted earlier as a whole or in part for a degree / diploma at this or any other Institution / University.

Amol M. Mhatre

LIST OF PUBLICATIONS ARISING FROM THE THESIS

Journal

1. Phosphate-bearing polymer grafted glass for plutonium(IV) ion-selective alpha spectrometry. **A.M. Mhatre**, S. Chappa, S. Paul, A.K. Pandey, *J. Anal. At. Spectrom.* **2017**, 32, 1566-1570.
2. Thin film of poly (bis [2-(methacryloyloxy) ethyl] phosphate) grafted on surface of poly (ether sulfone) membrane for plutonium(IV)-selective alpha tracks registration in CR-39 detector. **A.M. Mhatre,** S. Chappa, V. Chavan, A.K. Pandey, *J. Radioanal. Nucl. Chem.,* **2017**, 314, 187-196.
3. Phosphate functionalized radiation grafted Teflon for capturing and quantifications of U (VI) and Pu (IV) ions at ultra-trace concentration in aqueous samples. **A.M. Mhatre**, S. Chappa, C.V. Chaudhari, Y.K. Bhardwaj, A.K. Pandey, *J. Radioanal. Nucl. Chem.* **2018**, 317, 1141-1149.
4. Functionalized Glass Fiber Membrane for Extraction of Iodine Species. **A.M. Mhatre**, S. Chappa, S. Ojha, A.K. Pandey, *Sep. Sci. Technol.*, **2019**, 54, NO. 9, 1469–1477.
5. Imprinted tungstosilicic acid-functionalized glass filter membrane for radiocesium sequestration. **A.M. Mhatre**, S. Chappa, A.K. Pandey, *manuscript under preparation.*

Conferences

1. Thin film of phosphate ligand bearing polymer grafted on microporous membrane for registering alpha tracks from Pu^{4+} Ions and fission tracks from UO_2^{2+} ions in CR-39 and Lexan, **A.M. Mhatre** and A.K. Pandey, "Proceedings of 6th DAE-BRNS Interdisciplinary Symposium on Materials Chemistry (ISMC)", BARC, Anushakitinagar-94, Mumbai, December 6-10, 2016, page-201. (Best Paper Award)

2. Thin film of phosphate ligand bearing polymer grafted glass substrate for alpha spectrometric determination of Pu^{4+} ions, **Amol M. Mhatre**, Sankararao Chappa, Sumana Paul and Ashok K. Pandey, “Proceedings of 13th DAE-BRNS Nuclear and Radiochemistry Symposium (NUCAR)” held at KIIT, Bhubaneswar, India, February 6-10, 2017, paper No. E-144.
3. Phosphate-grafted Teflon film for Pu and U determinations by solid state nuclear track detector, **A.M. Mhatre**, C.V. Chaudhari, Y.K. Bhardwaj, A.K. Pandey, “Proceedings of National Conference on Solid State Nuclear Track Detectors and Their Applications” held at Vidya Vikas Institute of Engineering and Technology, Mysuru, October 26-28, 2017, paper No. O-2.
4. Functionalized glass fiber membrane for extraction of iodine species, **A.M. Mhatre**, S. Chappa, S. Ojha and A.K. Pandey, “Proceedings of Eighth DAE-BRNS Biennial Symposium on Emerging Trends in Separation Science and Technology (SESTEC)” held at BITS Pilani, KK Birla Goa Campus, Goa, India , May 23 – 26, 2018, paper No. O-30.
5. Tungstosilicic acid functionalized glass filter membrane for radiocesium sequestration, **A.M. Mhatre**, S. Chappa, A.K. Pandey, “Proceedings of Eighth DAE-BRNS Biennial Symposium on Emerging Trends in Separation Science and Technology (SESTEC)” held at BITS Pilani, KK Birla Goa Campus, Goa, India on May 23 – 26, 2018. paper No. F-8. (Best Paper Award)

Amol M. Mhatre

ACKNOWLEDGEMENTS

I would like to express my deepest gratitude to all the people who have helped get this far. This wouldn't have been possible without them and those involved with research.

First and foremost, I gratefully acknowledge my guide, Dr. Ashok Kumar Pandey, Prof. Chemical Science, Homi Bhabha National Institute for welcoming me within his research team and offering me an opportunity to participate in this interesting work. It has been my honour to work under him. He has provided invaluable guidance, support to me over past years and also encouraged me to be more practical and confident.

I am thankful to Prof. S. K. Ghosh, Prof. B S. Tomar and Prof. A K. Tyagi former and present Deans, chemical sciences, HBNI for permitting me to register for my Ph.D.

I am also grateful to Dr. P. K. Pujari, Associate Director and Head, Radiochemistry Division for his support and keen interest throughout the work. I would like to thank Dr. R. Tripathi for his advice and positive outlook during the course of the work.

I take this opportunity to thank members of my doctoral committee: Prof. Y. K. Bhardwaj (chairman), Prof. Sangeeta D. Kumar, Dr. Suparna Sodaye, and Dr. P. G. Jaison for their valuable suggestions were of immense help in improving the quality of work as well as enriching my knowledge.

A special thanks to my good friends and fellow colleagues Dr. Sankararao Chappa, Mr. Prakash Rathod and Mrs. Shashikala Ojha for their help, assistance in improving the work significantly in many aspects.

I am extremely grateful and highly obliged to Mr. C.V. Chaudury for assisting in substrate preparation. I am also thankful to Dr. A.K. Dubey, Dr. Sumana Paul , Mr. Raju Shah and Mr. Sasi Bhushan, Dr. Bal Govind Vats, Dr. Ruma Gupta, Mr. Rahul Agarwal, Mr. Suhas Phapale, Mr. Srikant Sahoo, Dr. S. N. Achary for providing materials, measurements facilities and help in interpretations.

I am also thankful to the operating personnel of sophisticated Analytical Instrumentation Facility (SAIF), IIT Bombay, Mumbai for providing FE-SEM and EDX facility and Department of chemistry, Savitribai Phule Pune University for providing SEM.

Last but not least, my family. I thank you all for love and support. You made it possible for me to pursue my goals.

Amol M. Mhatre

CONTENTS

SYNOPSIS

Various nuclear anthropogenic activities lead to a possibility of contaminations of the soil, air and groundwater with the radionuclides having different half-lives ranging from sub-second to millions of years. Therefore, the continuous monitoring of radionuclides in the environment around the nuclear activities is important for (i) environmental risk assessment around nuclear facilities such as nuclear power plants, nuclear fuel reprocessing plants and nuclear waste storage sites, (ii) emergency preparedness, (iii) surveillance of contaminated areas from nuclear weapon tests and nuclear accidents, (iv) detection of accidental leaks and migration in the environment, (iv) waste discharge regulation, and (v) nuclear forensics. There are many methods, such as mass spectrometry, α-spectrometry, γ-spectrometry, solid state nuclear track detection and liquid scintillation counting etc., that have been used for quantifying transuranic nuclides in a variety of the process and environmental samples as evident from the recent reviews [1-3]. It is known from these published reviews that these methods have requisite analytical merits for the quantification of actinides, but require a purification step because of the interferences of matrices in the measurements processes. For example, alpha spectrometry commonly used for Pu isotopes in the aqueous samples requires Pu separation using an anion-exchange column, followed by thin sample source preparation by commonly used methods such as evaporation, micro-precipitation or electrodeposition on a metal disc. These multistep sample treatment is cumbersome and lead to the possibility of the cross-contaminations, which is important for the sample having Pu at ultra-trace concentration.

The quantifications of alpha emitting and fissile elements in the aqueous samples such environmental samples, radiopharmaceutical samples derived from fission molly, fuel reprocessing aqueous waste samples and nuclear forensic samples are often requiring a highly sensitive radiation measurement instrumentation hyphenated with appropriate sample purification and source preparation methods for the unambiguous quantification. However, in many such applications, the sample is to be subjected to a preconcentration step for bringing the concentration of analyte in the measurement range of the radioanalytical method. The dangerous level for accumulated Pu in the human body is 10^{-12} g g^{-1} (1000 fg g^{-1}). This highlights the compulsion to monitor much lower levels in the surrounding environment in order to evaluate the possibility of bio-accumulation of radiotoxic elements [4].

Functionalized thin polymer film-based α-spectrometry could combine the sample purification, preconcentration and source preparation. Recently, it has been shown that the thin film surface-grafted ultrafiltration membrane can be used for capturing Pu from a large volume of aqueous sample, and subsequent direct quantification of Pu ions preconcentrated on thin film bearing membrane withα-spectrometry [5]. Solid state nuclear track detectors (SSNTDs) are the most sensitive for recording the energetic charge particles, but lack chemical selectivity and have limited capability to distinguish the particles based on their energies unlike alpha spectrometry. SSNTD has been used for the detection of alpha particles emitting nuclides [6]. This technique can be made highly effective by imparting chemical selectivity using highly selective thin film of the functionalized polymer on a suitable host matrix for registering alpha/fission tracks in the SSNTD. Also, the track registration efficiency would be considerably higher from the thin film as compared to solution medium generally used for the homogeneous track registration.

The present thesis deals with the development of thin film polymer ligands sorbents for Pu anchored on the different host matrices such as glass, membrane and Teflon sheet that can be applied for one step sample treatment for α-spectrometry and SSNTD based quantification of Pu at ultra-trace concentration in the aqueous samples. The poly (vinylpyrrolidone) and silicotungstic acidanchored glass filter membranes have also been developed for the quantifications of radioiodine and radioactive cesium by γ-spectrometry. This thesis is divided into the six chapters, and a brief description of each chapter is given below:

Chapter 1: Introduction

This chapter gives a brief introduction about sources of radionuclides and their possible ways to enter in the environment, and a general account of the different direct instrumental methods being used for the quantifications of radionuclides such as gamma spectrometry, alpha spectrometry, proportional counters, mass spectrometry, liquid scintillation counting and solid state nuclear track detectors have been given. The possible interferences in these instrumental methods such as problems of α-energies peaks overlap in α-spectrometry, isobaric interferences and polyatomic interferences in mass spectrometry, α/β-radiations selectivity in liquid scintillation counting, problem of distinguishing alpha particle tracks having different energies in the SSNTD, and abundance sensitivity interferences have been discussed. The different sample pretreatment methods reported in literature to overcome these problems in the instrument methods, and the advantages of the polymer based direct preconcentration and quantification methods such as extractive scintillation resin/membrane, polymer based sample loading in thermal ionization mass spectrometry and thin polymer sorbents based alpha spectrometry have also been reviewed. Finally, based on the review of available literature, the scope of the present thesis has been outline.

Chapter 2: Experimental

This chapter describes the general synthetic methods used for the anchoring of phosphate functional groups bearing thin films on the host matrixes such as glass, membrane and Teflon sheet. The specific details are given in the respective chapters. The functionalization of the glass matrices requires anchoring of the monomer by sol-gel method first and subsequently polymerizing the double bonds for grafting the polymer chain. Therefore, the basic mechanisms involved in the sol-gel method and UV, ionizing radiations (γ-rays and electron beams) initiated graft polymerizations have been discussed. The ligand bearing thin films anchored on the different host matrixes have been characterized by different techniques such as Atomic Force Microscopy (AFM), Fourier Transform Infrared Analysis (FTIR), Thermo-gravimetric analysis (TGA), Energy dispersive X-ray spectroscopy (EDX) attached to field emission scanning electron microscopy (FE-SEM), UV-Vis spectrophotometry, X-ray diffraction (XRD) and capillary flow porometry (CFP). Therefore, the basic principles and methodologies involved in these characterizations tools have been discussed briefly. The research work carried out in the present thesis involve the use of optical and electron microscopy. Hence, the brief descriptions of these have also been given. Finally, the radiation measurement methods used in the quantifications of the fission products and actinides such as liquid scintillation counting, α-spectrometry, γ-spectrometry and solid state nuclear track detectors have been discussed.

Chapter 3: Thin Film of Phosphate Ligand Bearing Polymer Grafted Glass Substrate for Alpha Spectrometric Determination of Pu(IV) Ions.

This chapter deals with the covalent anchoring of phosphate-bearing polymer thin film on a glass substrate for the alpha spectrometric determination of Pu(IV) ions in aqueous samples. This method combined matrix elimination, preconcentration and source preparation into one-step sample manipulation. The thin polymer film was formed by first coupling 3-(trimethoxysilyl)propyl acrylate (TMSPA) on a hydrolyzed glass substrate by a sol–gel process, and simultaneously utilizing the double bonds of TMSPA for the UV-initiator-induced graft polymerization of bis[2-(methacryloyloxy)ethyl] phosphate monomers. The thin phosphate ligand bearing poly(bis[2-(methacryloyloxy)ethyl]phosphate)(poly(BMEP)) film thus formed was characterized for the homogeneity, elemental mapping, physical morphology, and its affinity toward representative actinide ions such as UO_2^{2+}, Am^{3+}, Th^{4+} and Pu^{4+} in a HNO_3 medium. Alpha track radiography and elemental mapping of the C and P atoms indicated uniform formation of the poly(BMEP) film on the glass substrate. Atomic force microscopy indicated a 10-15 nm thickness of the film, and the alpha spectrum of Pu^{4+}-loaded glass@poly(BMEP) exhibited well defined alpha energy peaks without any significant loss of energy in the host matrix. The glass@poly(BMEP) film was found to sorb Pu^{4+} ions preferentially from 3 mol L^{-1} HNO_3 in the presence of competing UO_2^{2+} and Th^{4+} ions. Am^{3+} ions did not sorb to a significant extent under similar conditions, even in the absence of Pu^{4+} ions. The Pu^{4+} ions loaded on the glass@poly(BMEP) substrate were quantified by isotope-dilution alpha spectrometry. This glass@poly(BMEP)-based alpha spectrometric method was applied successfully to quantify Pu in aqueous samples. The concentrations of Pu measured by this technique were reproducible within 6% and showed a good agreement with those obtained by standard thermal ionization mass spectrometry.

Chapter 4: Anchoring of Phosphate-Bearing Thin Polymer Film on Polymer Based Host Matrices For U and Pu Analyses by SSNTD

Solid state nuclear track detectors (SSNTDs) based analytical methods are highly sensitive for fissile and alpha emitting nuclides but lack chemical selectivity. This chapter contains the research work carried out to develop chemically selective SSNTD by registering the tracks from the thin ligand polymer film. For this objective, two types of the hosts were used i.e. poly(ether sulfone) (PES) microporous membrane and Teflon sheet. Therefore, this chapter has been divided into two sections dealing with the phosphate bearing polymer anchored on the PES membrane (section A) and Teflon (section B) using UV radiation and γ-rays based methods, respectively. The brief descriptions of these sections are given below.

A. Thin Film of Poly(bis[2-(methacryloyloxy)ethyl]phosphate) Grafted on Surface of Poly(ether sulfone) Membrane

A thin film of polymer of bis[2-(methacryloyloxy) ethyl]phosphate (poly(BMEP)) has been anchored on one surface of poly(ethersulfone) (PES) membrane (PES@poly(BMEP)) by UV-grafting to capture the actinides from solution with a high efficiency and subsequent use as a source for registering the particles tracks in CR-39 detector. The SEM images indicated that surface morphology of the PES@poly(BMEP) did not change significantly with respect to the pristine PES membrane, and also through-pores size distribution and void volume remained unaffected. It was observed from alpha spectrometry that alpha peaks corresponding to ^{239,240}Pu and ^{238}Pu were well defined without significant left side tailing, which was indicative of a minimum loss of kinetic energy of the alpha particles in source matrix. The alpha tracks radiography of the ^{mix}Pu-loaded PES@poly(BMEP) sample indicated homogeneity of the poly(BMEP) grafted on PES membrane. Thus, the alpha tracks density on small area of the CR-39 could be taken as a representative of entire CR-39 area (2x1 cm^2) exposed to the ^{mix}Pu-loaded PES@poly(BMEP) sample in 2π contact. The PES@poly(BMEP) sample was found to sorb Pu^{4+}, UO_2^{2+} ions from solution having 3 mol L^{-1} HNO_3 concentration, and Am^{3+}, Ba^{2+}, Sr^{2+} ions uptakes were negligible under similar conditions. This membrane based SSNTD technique was applied to determine conc. of Pu^{4+} ions in the synthetic urine sample spiked with known amount of Pu activity using the standard comparison method.

B. Phosphate-Functionalized Radiation-Grafted Teflon

The phosphate bearing polymer thin film has been anchored on Teflon sheet by gamma grafting of poly(glycidyl methacrylate) and reacting subsequently with phosphoric acid under appropriate chemical conditions. This Teflon@phoshate sheet has been characterized by FTIR, TGA, and AFM. The phosphate groups are known for their affinity towards higher oxidation state actinides such as Pu (IV) and U (VI) ions. Therefore, the uniform distribution of grafted phosphate groups on Teflon has been studied by α-radiography of ^{mix}Pu-loaded and fission tracks distribution in the ^{nat}U-loaded Teflon@phoshate sheets by CR-39 and Lexan track detector, respectively. The degradation of alpha energy in varying extent of the phosphate containing Teflon@phoshate thin film has been optimized by analyzing the shape of alpha particles energies peaks registered from the ^{mix}Pu-loaded Teflon@phoshate sheet using alpha spectrometry. Teflon@phoshate sheet exhibits remarkably selectivity towards Pu (IV) ions in solution having wide concentration range of HNO_3 (0.5-8 mol L^{-1}) with quantitative sorption, and U(VI), Am(III) ions are sorbed quantitatively only form solution having acidity in a pH range. Teflon@phoshate sheet also takes up U(VI) quantitatively from natural water. Therefore, the Teflon@phoshate sheets have been used for quantitative analyses of Pu(IV) and U(VI) in 3 mol L^{-1} HNO_3 solution and natural water, respectively. The standard comparison method based solid state nuclear track detector based technique has been used for the quantifications of Pu(IV) and U(VI) ions by registering alpha tracks from the ^{mix}Pu-loaded Teflon@phoshate sheet in CR-39 and reactor neutron induced fission tracks from the ^{nat}U-loaded Teflon@phoshate sheet in Lexan plastic, respectively. Finally, the Teflon@phoshate based SSNTD method has been used to quantify U in the natural water samples.

Chapter 5: Functionalized Glass Fiber Filter Membranes for Fission Radionuclide Measurements

For the high fission yields products such as iodine and caesium, the glass fibres membranes have been chemically modified to generate highly selective functional moieties for their selective preconcentrations and subsequent quantifications with γ-spectrometry. This chapter has been divided to two section dealing with radioiodine (section A) and radioactive cesium (section B). The contents of these sections are discussed briefly below.

A. Functionalized Glass Fiber Membrane for Iodine Species

Poly(vinylpyrrolidone) (PVP) form complex with molecular iodine which is used extensively in the medical applications. In the present work, PVP has been anchored on the glass fiber membrane for capturing radioiodine in gaseous state as well dissolved in water. For this, the polymerizing double bond bearing 3-(trimethoxysilyl) propyl acrylate (TMSPA) has been anchored by sol-gel method on the hydrolyzed glass fiber membrane. The double bonds of TMSPA monomers attached on glass membrane have been used subsequently for the anchoring of PVP by UV-initiator induced graft-polymerization of monomer 1-vinyl-2-pyrrolidinone. The chemical and physical structures have been characterized by FTIR, SEM, FE-SEM and elemental mappings by EDX attached to FE-SEM. The extent of grafting of PVP on glass fiber membrane has been obtained by TGA. The sorption of molecular iodine dissolved in water and chloroform in the PVP-grafted glass fiber membrane has been studied by UV-Vis spectrophotometry. The sorption efficiencies of iodine species in water and gaseous form have been studied by using ^{131}I radiotracer. The loading capacity and stability of iodine bonded with the PVP-grafted membrane have also been studied by tagging molecular iodine with ^{131}I radiotracer for the quantifications. The experimental results have suggested that the PVP-grafted glass fiber membrane is highly efficient for sorption and storage of radioiodine.

B. Functionalized Glass Filter Membrane for Radiocesium

Silicotungstate, a heteropoly acid, is known for its selectivity towards Cs^+ ions. Therefore, it has been anchored on the poly(3-(trimethoxy silyl) propyl acrylate) grafted glass fibers membrane. The glass fiber membrane has been anchored with coupling monomer 3-(trimethoxysilyl)propyl acrylate (TMSPA) on a hydrolyzed glass fiber by a sol–gel process, and simultaneously utilized the double bonds of TMSPA for the UV-initiator-induced graft polymerization of TMSPA itself. Thereafter, the grafted glass membrane has been treated with silicotungstic acid. This membrane has been equilibrated with cesium salt solution followed by thermal treatment leading to the condensation and formation of Cs^+-selective matrix. The Cs^+ ions have been deloaded in 3 mol L^{-1} HNO_3, and used thus formed membrane for capturing radioactive cesium ions for the different aqueous samples. The functionalized glass filter membrane has been characterized by FTIR, SEM, FE-SEM, elemental mappings by EDX attached to FE-SEM, and XRD. The cesium sorption efficiency and loading capacity have been studied by using ^{137}Cs radiotracer. It has been confirmed from the FTIR spectrum of silicotungstic acid functionalized glass filter membrane that organization of Keggin ion structure of silicotungstic acid in the membrane matrix with Cs^+ templates is mainly responsible for its cesium selectivity. XRD spectrum indicates that the matrix formed has similar crystal structure to that of cesium silicotungstate. The functionalized glass membrane sorbs ^{137}Cs efficiently from aqueous samples in the presence of a large excess of the competing ions such as monovalent alkali and divalent alkaline ions, and could be desorbed quantitatively in 3 mol L^{-1} HNO_3.

Chapter 6: Summary and Future Scope

In this chapter, the conclusions drawn from the research work carried out in the present thesis and future scope of the outcome of this doctoral research work have been discussed. The major conclusions of the present thesis are:

(i) The glass@poly(BMEP) substrate has been found to exhibit reasonably good selectivity towards Pu^{4+} ions with respect to Th^{4+} and UO_2^{2+} ions in a competing mode, and the representative trivalent actinide Am^{3+} does not sorbs from 3 mol L^{-1} HNO_3, even in the absence of competing ions. The glass@poly(BMEP)-based isotope-dilution alpha spectrometric method has been successfully applied to Pu determination in seawater and ground water samples.

(ii) The polymer ligand bearing PES membrane and Teflon substrates could be used for Pu (IV) ions quantification in the aqueous samples by chemically selective alpha or fission tracks registration based SSNTD. The selective preconcentration of Pu(IV) would also enhance the detection limit to sub-ppb conc. U(VI) has been found to preconcentrate selectively in the phosphate group anchored Teflon from natural water, and could be applied for U quantification using fission tracks based SSNTD.

(iii) A new synthetic route has been developed for grafting the crosslinked PVP chains on the glass fiber membrane, and found to capture gaseous radioiodine. The PVP-radioiodine complex remains intact in the membrane over a long period of time indicating its reasonably good stability in the membrane for the storage.

(iv) Cesium selective silicotungstic acid has been immobilized and organized in alkoxysilane grafted glass fibres membrane to capture radioactive caesium at ultra-trace concentration in the presence of a large excess of the competing ions.

Future work could be related to the fine-tuning of developed substrates, hyphenation with instrumental method, processing of a large volume of contaminated solutions using low-pressure filtration to have high-throughput, one-step concentration, purification, and sample mounting process. The anchoring of actinide selective film on surface of the polymer sheets used as SSNTDs such as CR-39 and Lexan would be very effective for the nuclear forensic applications as both detector and source would be combined.

References

[1] N. Vajda, C. K. Kim, Determination of transuranium isotopes (Pu, Np, Am) by radiometric techniques: a review of analytical methodology, *Anal. Chem.* 83 (2011) 4688-4719.

[2] J. Qiao, X. Hou, M. Mirób, P. Roos, Determination of plutonium isotopes in waters and environmental solids: a review, *Anal. Chimi. Acta* 652 (2009) 66-84.

[3] E. Chamizo, M.C. Jiménez-Ramos, L. Wacker, I. Vioque, A. Calleja, M. García-León, R. García-Tenorio, Isolation of Pu-isotopes from environmental samples using ion chromatography for accelerator mass spectrometry and alpha spectrometry, Anal. Chim. Acta 606 (2008) 239-245.

[4] G. Steinhauser, Fukushima's forgotten radionuclides: A review of the understudied radioactive emissions, *Environ. Sci. Technol.* 48 (2014) 4649-4663.

[5] C.E. Duval, A.W. Darge, C. Ruff, T.A. DeVol, S.M. Husson, Rapid sample preparation for alpha spectroscopy with ultrafiltration membranes, Anal. Chem. 90 (2018) 4144-4149.

[6] V. Zorri, R. Remetti, M. Capogni, G. Cotellessa, R. Falcone, Feasibility study on the application of solid state tracks detectors for fast surveys of residual alpha contamination in decommissioning activities, *Rad. Meas.* 107 (2017) 111-114.

LIST OF FIGURES

LIST OF THE TABLES

LIST OF THE SCHEMES

ABBREVIATIONS

HPGe : High-purity Ge

MCA : Multi-channel analyzer

ICP-MS : Inductively coupled plasma mass spectrometry

TIMS : Thermal ionization mass spectrometry

RIMS : Resonance ionization mass spectrometry

AMS : Accelerator mass spectrometry

MC : Multi collector

LSC : Liquid scintillation counting

PMT : Photo multiplier tube

SSNTDs : Solid state nuclear track detectors

TEVA : TEtra valent acinides

UTEVA : U and TEtra valent acinides

TRU : Trans uranium

DGA : Diglycol amide

DIPEX : P,P’,Di(2-ethyl hexyl) methanediphosphoric acid

DIPHONIX : Di(2-ethyl hexyl) alkylene diphosphonic acid

GMA : Glycidyl methacrylate

DEA : Di ethylamino

SFRP : Stable free radical polymerization

ATRP : Atom transfer radical polymerization

RAFT : Reversible addition fragmentation chain transfer

LET : Linear energy transfer

AFM : Atomic force microscopy

SPM : Scanning probe microscopy

STMs : Scanning tunneling microscopes

FTIR : Fourier transform infrared spectroscopy

TGA : Thermogravimetric analysis

TG : Thermogravimetric

FESEM : Field emission scanning electron microscopy

SEM : Scanning electron microscopy

SE : Secondary electrons

BSE : Backscattered electrons

EDS : Energy dispersive X-rays spectroscopy

XRD : X-ray diffraction

CFP : Capillary flow porometry

PPO : 2,5 Diphenyl oxazole

POPOP : 1,4- bis (5-phenyloxazole-2-yl) benzene

TOPO : Tri-octyl phosphine oxide

HD2EHP : Di (2-ethyl hexyl) phosphoric acid

NIM : Nuclear instrument module

SCA : Single channel analyser

MCA : Multi channel analyser

ADC : Analog-to-digital converter

PMT : Photo multiplier tube

CR-39 : Columbia resin # 39

TIMS : Thermal ionization mass spectrometry

DIPEX : P,P'-di(2-ethylhexyl)methane-di-phosphonic acid

BMEP : Bis[2-(methacryloyloxy)ethyl] phosphate

DMF : Dimethyl formamide

DMPA : α,α’-Dimethoxy-α-phenylacetophenone

TOPO : Trioctyl Phosphine Oxide

PIPS : Passivated ion-implanted planar silicon

FWHM : Full width at half maxima

TMSPA : 3-(Trimethoxysilyl)propyl acrylate

MDA : Minimum detectable activity

PES : Poly (ether sulfone)

PIM : Polymer inclusion membrane

AMPS : 2-Acrylamido-2-methyl-1-propanesulphonic acid

FWHM : Full width at half maxima

PVP : Poly(vinylpyrrolidone)

EGDMA : Ethylene glycol dimethylacrylate

DMF : N,N'-Dimethyl Formamide

EDX : Energy dispersive X-ray spectroscopy

CHAPTER 1- INTRODUCTION

1.1 Sources of radionuclides and their possible ways to enter the environment

Various anthropogenic nuclear activities are responsible for the path of nuclear materials or radionuclides to enter in the environment. It is also possible that the radionuclides such as fission products and actinides might be released to environment by the nuclear accidents such as Fukushima Daiichi nuclear disaster (2011), Chernobyl disaster (1986), Three Mile Island accident (1979), and the SL-1 accident (1961). The long-lived fission products and actinides in the environment pose severe health hazards because of their high degree of radiological toxicity, even though they present in ultra-trace levels. The various possible nuclear energy utilization activities, that may result to release of radioactivity in the environment, are broadly categorized as: (1) Nuclear weapon program, and (2) Nuclear reactor.

1.1.1 Nuclear weapons development testing

The development of nuclear weapons and their dismantling produce different categories of radioactive wastes. The nuclear weapon development programme, in general, involves, the recovery of weapon-grade fissile elements (^{239}Pu) from the spent fuel burned in the nuclear reactor, and conversion of thus recovered fissile elements into the required chemical and physical form. The testing of nuclear weapon is usually done underground, releasing radioactivity such as tritium, fission products, activation products and actinides to nearby environment.

1.1.2 Nuclear reactors

The utilization of nuclear energy for the generation of electricity involves several steps in an open or close end cycle that would give rise to the possibility of release of radioactivity in the environment. These are:

Uranium mining and milling: The initial stage of nuclear programme such as mining and milling involves various processes for the extraction of precious nuclear materials from the matrix followed by conditioning which produces different category waste. The milling stage deals with different alpha activity bearing uranium, thorium and their daughter products like radium and radon isotopes. Some of the short-lived radioactive gases are carcinogenic and some may contribute radiation hazards by intense gamma ray emissions. Uranium tailing involves operations associated with significant sulphides and acidic medium which results in radioactive hazards [A. Abdelouas et al. 2006].

Nuclear fuel reprocessing: The different activities in nuclear industries and R&D centres are associated with the generation of nuclear wastes. The freshly removed spent fuel contains very high radiation level which last long for many years. In reprocessing, different category of waste generated and has always risk of radioactivity leakage. Separations/processing's of these nuclear wastes have importance from the point of view of eliminating the exposure of radioactivity to public from the discharge of processed waste streams in the environment. After certification, the processed aqueous waste streams are discharged appropriately [J. Gray et al. 1995, D. Jackson et al. 1998].

Geological repository of high-level nuclear wastes: Depending on the category of the waste, different underground storage facilities are used and active waste (mainly long-lived actinides and fission products)are buried deep in to these facilities. There is a probability of leaking the radioactivity over a very long period of storage time due to some unexpected natural processes.

Nuclear accidents: Radioactivity spillage is a possibility in the accident occurring in nuclear industry. Alpha emitting nuclides are very important in the perspective of toxicology and radioecology and its migration into environment i.e. aquifer, air, soils and sediments through different pathways. The presence and composition of radionuclides released in the environment is dependent upon the system they belong to like atmosphere, terrestrial, aquatic medium. In case of aquatic system, many factors affect the migration of radionuclide like thermo physico-chemical properties, species existing at different acidity and potentials, the presence of complex forming entities and minerals availability and its percentage [M. Dozol et al. 1993, R. J. Silva et al. 1995]. Nuclear materials/actinides accounting in the samples from different origin is important from the point of view of forensic application, discharge regulations and to have idea about its pathways into the environment [H. Hernandez-Mendoza et al. 2011, C. Li et al. 2008, J. Zheng et al. 2013, S. F. Boulyga 2001].

Medical Applications: The various β/γ-emitting isotopes are extensively used for the diagnostic and therapeutic applications. For these objectives, the radioisotope tagged labelled compounds are used for the diagnosis of various diseases of vital organs such as brain, kidney, thyroid etc. The medical waste generated at radiation medicine centres have to be properly disposed as it may contain short lived radioactivity.

1.2. Monitoring of radioactivity in environment

The quantifications of alpha emitting and fissile elements in the aqueous samples such environmental samples, radiopharmaceutical samples derived from fission molly, fuel reprocessing aqueous waste samples and nuclear forensic samples are often require a highly sensitive radiation measurement instrumentation hyphenated with appropriate sample purification and source preparation methods to avoid possible interferences. However, in many such applications, the sample has to be subjected to a preconcentration step for bringing the concentration of analyte in the measurement range of the radioanalytical method. For example, the dangerous level for accumulated Pu in the human body is 10^{-12} g g^{-1} (1000 fg g^{-1}).This highlights the compulsion to monitor much lower levels in the surrounding environment in order to evaluate the possibility of bio-accumulation of radiotoxic elements [C.-P. Huang et al. 2012, M. Gavrilescu 2009]. For Nuclear forensics and decontamination applications also, a very low concentration of Pu at sub-ppb level has to be measured [C. Talmadge, 2007]. The measurement of trace level radionuclide concentration is also very important for monitoring the release of radioactivity from the various operations in nuclear industries [M. Gavrilescu L et al. 2009, A. E. V Gorden et al. 2003].

1.2.1. General account of the different direct instrumental methods

The α, β, γ-radiation measurements are used generally for quantifying the strength of radioactivity in the samples with good precession and accuracy [G. F. Knoll 2010, G. Friedlander 1981, L. A. Currie; 1968]. Semiconductor detectors, gas-filled detectors, scintillation detectors, and liquid scintillation counters are extensively used in the quantifications of these radiations. For detection and quantification of actinides, mostly α/β-radiations are counted as most of the actinides of interest emit low energy γ-radiation having low abundance as shown in Table 1.1. Often, mass spectrometric methods are useful for the long-lived radionuclide and determining isotopic compositions. γ-spectrometry is extensively used for the quantification of the fission products.

Table 1.1. Nuclear properties of actinides of interest.

Actinide	**Half-life (y)**	**Decay mode**	**Specific activity (Bq/g)**
^{233}U	1.5911×10^{5}	α	356.75×10^{6}
^{233}Pa	7.39×10^{-2}	β,γ	7.66×10^{14}
^{236}Pu	2.86	α	1.96×10^{13}
^{238}Pu	87.7	α (γ)	6.34×10^{11}
^{239}Pu	24100	α (γ)	2.30×10^{9}
^{240}Pu	6561	α (γ)	8.40×10^{9}
^{241}Pu	14.3	β (γ)	3.82×10^{12}
^{241}Pu	3.73×10^{5}	α (γ)	1.46×10^{8}

^{235}Np	1.085	EC(X)	5.17×10^{13}
^{236}Np	1.55×10^{5}	EC(X)	3.63×10^{8}
^{237}Np	2.14×10^{6}	α (γ)	2.60×10^{7}
^{238}Np	5.76×10^{-3}	β, γ	9.54×10^{15}
^{239}Np	6.45×10^{-3}	β,γ	8.55×10^{15}
^{241}Am	432.6	α, γ	1.27×10^{11}
^{243}Am	7367	α, γ	7.39×10^{9}
^{242}Cm	0.446	α (γ)	1.22×10^{14}
^{243}Cm	28.9	α (γ)	1.86×10^{12}
^{244}Cm	18.1	α (γ)	2.99×10^{12}

Gamma/ X-rays spectrometry: γ/X-rays spectrometry is used for the detection, identification and quantification of the radioactivity in the sample which is related to the amount of radioisotope [R. Jenkins 1995]. The strength of the radionuclide/ sample can be estimated by knowing absolute efficiencies or comparison with matching standards. Figure 1.1a & b depict the basic mechanism of gamma and X-ray emission by the elements and thus recorded spectra. The most of the γ-spectrometers used for actinide and fission products quantifications are based on high-purity Ge (HPGe) detectors having high energy resolution, typically < 2 at 1332 keV, and can be used for γ-rays having energy in the range of 50 to 2000 keV. The actinides of interest emit γ- and X-rays in the range of 3- 300 keV. In general, the sensitivity of γ-spectrometry is lower with respect to α-spectrometry associated with lower γ-counting efficiency and higher background. However, γ-spectrometry has advantage that bigger sample volume could also be counted. Wolf has shown that the direct analyses by γ-spectrometry give detection limits of 1100, 0.3, and 0.2 Bq for ^{239}Pu, ^{237}Np, and ^{241}Am, respectively.These detection limits are orders of magnitude higher with respect to that obtained by α-spectrometry or mass spectrometry [S. F. Wolf et al. 1998].

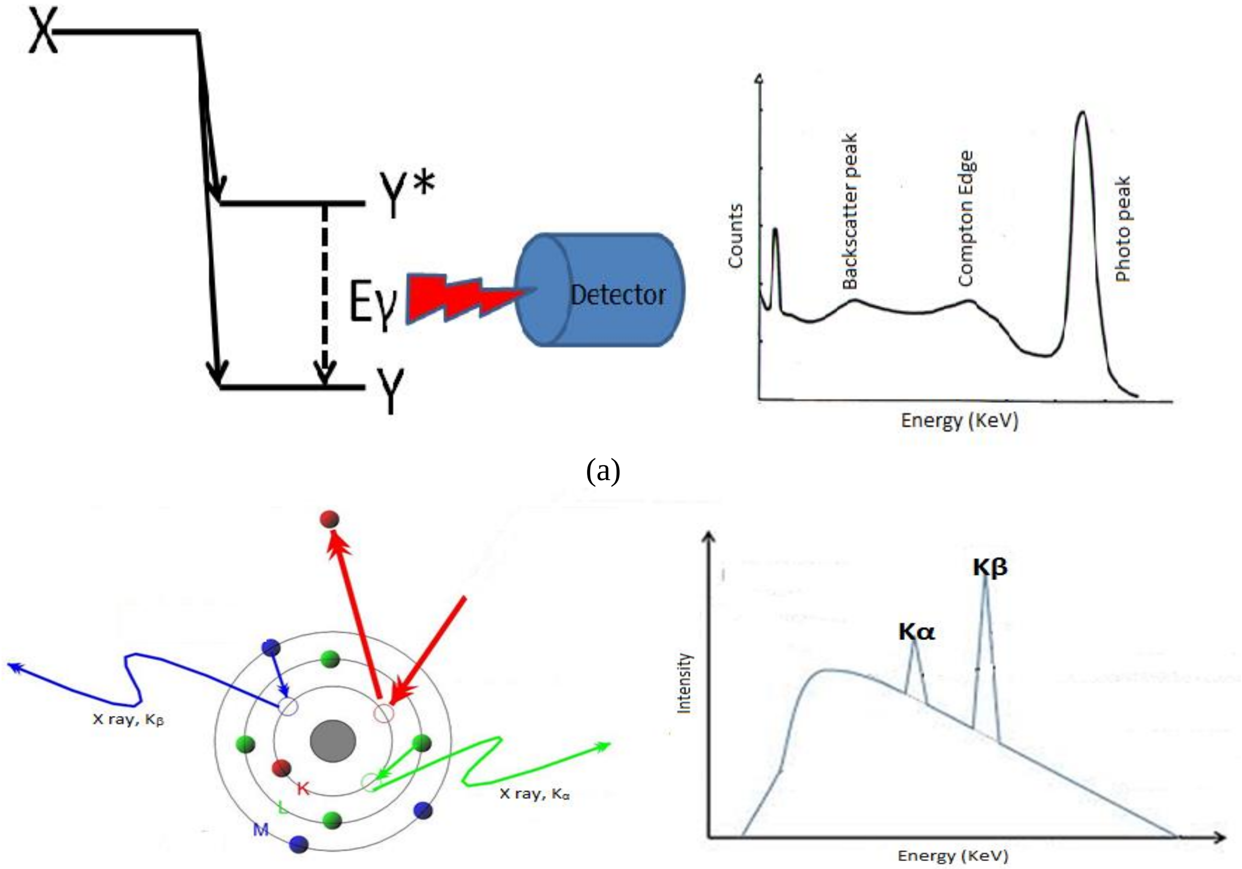

(a)

(b)

Figure 1.1. Illustrations of the basic mechanisms involved in γ-ray (a) and X-ray (b) emission by the elements and their recorded spectra.

Alpha spectrometry: Alpha spectrometry is one of most extensively applied radioanalytical method for the detection and quantification of α-emitting radionuclides in a variety of environmental, biological and nuclear processes samples. In general, the typical α-spectrometer consists of a semi-conductor silicon detector (surfacebarrier or ion-implanted), a charge-sensitive pre-amplifier, a linear amplifier connected to a multi-channel analyzer (MCA) for data acquisition and processing. Alpha spectrometers have many advantages for the quantifications of α-emitting radionuclides such as reasonably lower background, and no significant variation in the efficiency of the detector which obviates the need of standard for the efficiency calibration. However, a thin and homogeneous source is required for obtaining a good quality α-spectrum. The source for α-spectrometry are prepared by using: (i) electrodeposition, (ii) vacuum sublimation, (iii) drop-deposition on suitable metallic disc, and (iv) micro-precipitation. The energy resolution in the range of 30-50 keV allows the complete separation of the α-particles energy peaks of ^{238}Pu, ^{239,240}Pu, ^{242}Pu, and ^{236}Pu. However, the α-particle energy peaks of ^{239}Pu overlaps with that of ^{240}Pu. It is important to consider that the response of a silicon detector with respect to alpha particle energy is not perfectly Gaussian and a low energy tail of the alpha peak is generally observed. A part of the energy is lost to nuclear collisions that would not necessarily create the electron-hole pairs. The extent of peak tailing also arises due to several factors such as size of the detector, energy resolution of the detector, α-activity ratio of high energy to low energy peak, source to detector distance, detector collimation, chamber pressure (10^2 to 10^3 torr), peak analysis window size, and thickness and homogeneity of the source. In general, deconvolution or appropriate algorithm has to be used for overlapped peaks. Aggarwal has reviewed recently about the different parameters involved in alpha-spectrometry [S.K. Aggarwal et al. 2016].

Alpha/Beta detection using gas filled detectors: In this class of radioanalytical instruments, the ionization of gas (generally Ar or He) by radiation is used for the detection and measurement. Depending upon the applied voltage for the collections of the charges thus produced, these detectors can be classified in to three types i.e. ionization chamber, proportional counter and Geiger-Mueller counter. Ionization chamber is based on the measurement of current produced during ionization of gas by radiations, and provides information about the total radiation field useful for the dosimetry application. However, the pulse height obtained by ionization is lower as shown in Figure 1.2. Therefore, a higher potential is applied in the proportional counter to get multiplication by further ionization by collision of higher energy particles producing secondary electrons. This results to higher pulse height obtained in proportional counter and information about the energy and intensity of the radiation can be obtained. In GM counter, a very high voltage is applied that saturate the pulse height as shown in Figure 1.2. Since pulse height is saturated, information only about the intensity can be obtained but not about the energy of the ionization radiation. Alpha spectra collected by gas ionization detectors have basically the same parameters as discussed for alpha spectrometry above.

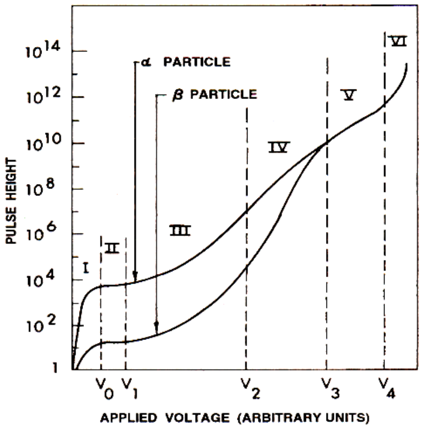

Figure 1.2. Variation of pulse height as function of applied voltage during interactions of radiation with gas-filled detector; chamber, III for proportional counter, and V for GM counter.

Mass Spectrometry: In first step of mass spectrometry, gas phase ions are produced that are subsequently separated by their specific mass-to-charge ratio (m/z), and detector system record the relative abundance of each of the resolved ionic species. A schematic representation of the mass spectrometry-based analysis is illustrated in Figure 1.3. There are four mass spectrometric methods that have employed for the quantification and isotopic composition determination of the actinide isotopes. These are: (i) inductively coupled plasma mass spectrometry (ICP-MS), thermal ionization mass spectrometry (TIMS), resonance ionization mass spectrometry (RIMS), and accelerator mass spectrometry (AMS). It is possible to analyze several isotopes by using sector-field multi-collector (MC). A review on different atomic spectrometric techniques by Zheng et al. showed that TIMS has been gradually replaced by MC-ICP-MS for the application in the radiation protection, nuclear facilities and geochemistry. Inductively coupled plasma source at normal pressure is used in ICP-MS which is well suited for the liquid sample. However, TIMS is well suited for solid sample and extensively used in the nuclear industries. The comparison given by Zheng et al. indicates that there is no significant difference in the limit of detection obtained by these two methods [J. Zheng et al. 2013].

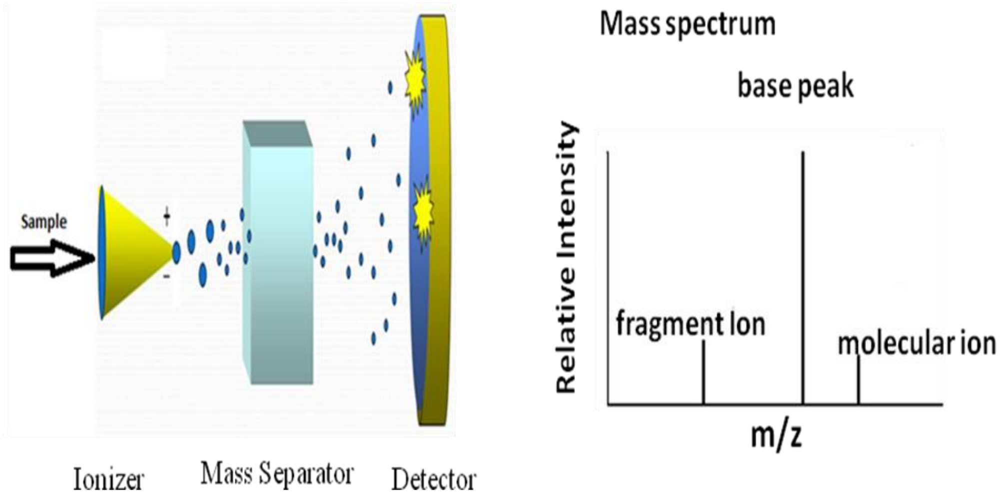

Figure 1.3. Illustration of basic components in mass spectrometer and typical mass spectrum thus obtained.

Liquid scintillation counting (LSC): Liquid scintillation counting is a classical technique in nuclear material accounting by measuring low energy radiation mainly individually alpha, beta radiations or together. The scintillation matrix consists of materials such as solvent for energy deposition, phosphors for transforming of radiation energy to signal in terms of counts or pulses [M.S. Patterson et al. 1965]. This technique provides maximum detection efficiency in low energy radiations emitting radionuclides due to its 4π configuration. This technique is free from radiation self-absorption and problems associated with sample geometries. Organic extractant in scintillation cocktail forms complex with α/β-emitting radionuclides and distribute them uniformly in the scintillation matrix in which extractant is soluble.

Measurement involves detection of radiation emitted in the sequence of process like transfer of radiation energy to solvent molecule followed by absorption of energy by organic phosphor emitted from solvent molecule and followed by detection of light by photomultiplier tube (PMT) as shown in Figure 1.4. The processed signal in the form of counts or pulses is used in getting qualitative and quantitative information about the α/β-emitting radionuclides.

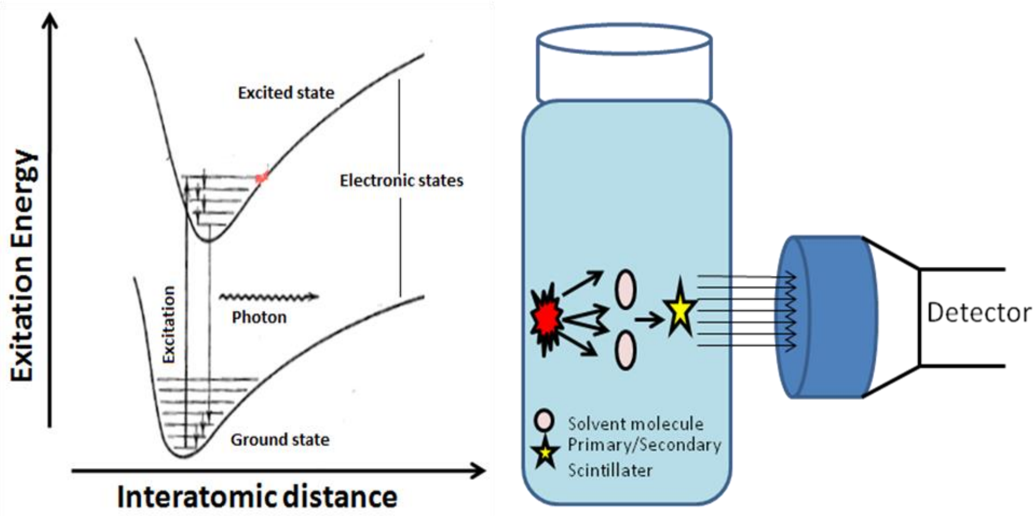

Figure 1.4. Schematic representation of the principle of light emission from organic scintillators produced by α/β-radiations, and subsequent detection using photomultiplier tube.

Solid State Nuclear Track Detection (SSNTD): Solid state nuclear track detectors (SSNTDs) are highly sensitive to record trajectory of a moving charge particle in the form of latent track which can be revealed by chemical etching for the observation of tracks under optical transmission microscope [S.A. Durrani et al. 1987]. Basically, the track profile and track density are two important parameters obtained from SSNTD that can be used for identification of the registered particles and quantifying the event, respectively [Y. L. Law et al. 2008, P. B. Price 2005, P. B. Price 2008, S. F. Boulyga 1999, R. Fleischer et al. 1975]. The sensitivity of the SSNTD has made it possible to measure the fission cross-sections in a nanobarn range and study of the exotic radioactive decay [R. H. Iyer et al. 1993, S. P. Tretyakova et al. 1991, S. P. Tretyakova et al. 2001].The different steps involved in SSND based technique, and alpha and fission tracks cluster recorded in the plastic detectors are shown in Figure 1.5.

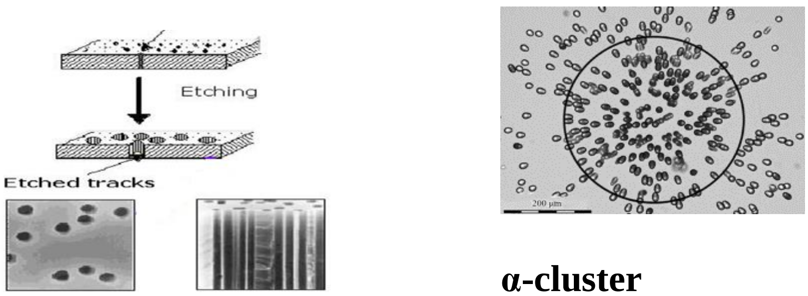

α-cluster

AFM Image of Etched Tracks

Fission Fragments cluster

Figure1.5. The different steps involved in the charge particle detection in SSNTD polymers, and photo-micrograph of developed alpha, fission fragments clusters.

1.2.2. Major problems associated with direct instrumental radioanalytical methods

Although the discussed techniques exhibit excellent analytical performance in radiation measurements, there are several problems in quantifying low amount of radionuclides such as high background, overlap in alpha peaks in alpha spectrometry, isobar and combination of atoms in mass spectrometry, individual radiation detections in liquid scintillation counting (LSC), and error associated with nuclides having poor abundance in γ-spectrometry [Y. A. Zolotov et al. 2005, N. Guérin et al. 2011]. The major drawbacks of individual instrumental methods are briefly discussed below.

Gamma spectrometry: γ-spectrometry measurements of nuclear materials deal with large sample sizes and even small sample with a high concentration of nuclear material has significant self-absorption. An absolute measurement requires the detector efficiency as a function of source position and energy, sample size, shape and accurately known gamma emission rates. However, it is tedious to characterize detector efficiency with sufficient accuracy, and there are still significant uncertainties in the value of the specific activities for many important gamma rays. The use of calibration standards reduces or eliminates the need to accurately known the detector efficiency, the counting geometry, and the specific activities. Because of size and shape of nuclear materials samples vary widely, it is difficult to construct appropriate calibration standards. Accurate gamma assays demand accurate corrections for both electronic losses and losses caused by sample self-attenuation [Doug Reilly, et al, 1991].

Alpha spectrometry: The resolution is very important property of detector which discriminate neighboring alpha peaks. Unfortunately, the achieved excellent resolution in semiconductor detectors used in alpha spectrometry is limited by ion pairs resulted from alpha interaction with semiconductor matrix [E. Steinbauer et al. 1994)]. Further to eliminate contributions from overlapped peaks, there is requirement of deconvolution methods which further complicate the measurement. Another major problem measuring alpha bearing radionuclides using alpha spectrometry is attenuation for alpha radiation in sample matrix itself and inconsistent recovery/losses of radionuclide of interest. Therefore, it is very important to have very thin and uniform sample [P. Roos 2002, G. Sibbens et al. 2007, H. Klemenčič et al. 2010, M. T. Crespo et al. 2012].The major problems associated with alpha spectrometry are summarized in Table 1.2 [S Pommé, 2015].

Table 1.2. Major interferences in the determination of actinides by direct alpha spectrometry.

Instrumental method	**Analyte actinide (Energy in MeV)**	**Interfering actinide (Energy in MeV)**
Spectral interferences	^{239}Pu (5.244)	^{240}Pu (5.255)
	^{228}Th (5.520)	^{241}Am (5.464), ^{243}Am (5.438)
	^{229}Th (5.168)	$^{239-240}$Pu (5.244-5.255)
	^{234}U (4.856)	^{237}Np (4.957)
	^{235}U (4.679)	^{244}Pu (4.665)
	^{237}Np (4.957)	^{242}Pu (4.983), ^{234}U(4.856)
	^{228}Th (5.520)	^{241}Am (5.464)
Matrix interferences (HF co-precipitation)	LnF_3, MgF_2, CaF_2, SrF_2, BaF_2, PbF_2	

Mass spectrometry: The trace level concentration determination of actinides using mass spectrometry from voluminous sample from natural origin needs preconcentration step. Analysis of complex samples has always poor sensitivity due to contribution from the interfering ions in the solution. The methodologies used in selective preconcentration are time consuming and need sophisticated laboratory [S. Domini et al. 2009]. Other major problems with mass spectrometry are: (i) isobaric peak overlap from the species involving similar mass, [J. Ignacio et al. 1995], (ii) polyatomic ions formed by dominant atomic species in the ionization source, (iii) the contribution from matrix [Interference mass table, copyright Finnigan Mat, (1992)], (iv) abundance sensitivity associated with relative signal nearby to the species of interest, (v) non-spectroscopic interferences associated with matrix. **Alpha/ Beta emitting/Proportional Counters:** The main drawback of these techniques is necessity for very thin substrates so as to have minimum attenuation for radiations emitted from source. Such sample preparation is very time consuming.

Liquid scintillation counting: The disadvantage associated with LSC is pulses recorded from different radiation overlap each other. This problem exists due to different extent of energy conversion by different radiation and complicating situation by interfering individual peak areas. This mainly affects the alpha measurements. To overcome these complications, the sample processing or pulse shape discriminator can be used so that alpha pulses can be monitored in the presence of beta or gamma radiation and from external radiation. Liquid scintillation counting also suffers from different quenching occurring in the sample.

Solid State Nuclear Track Detection (SSNTDs): The analytical application of SSNTD is based on recording alpha tracks or neutron induced fission tracks in the solution medium [R. H. Iyer et al. 1997, V. Uma et al. 1980].The solution medium ensures uniform distribution of nuclides that lead to uniform track density in the detector. Thus, the counting of tracks in the small representative areas could be used for obtaining the tracks density for determining concentration of nuclides by a standard comparison. However, the track registration efficiency is considerably lower in solution media as compared to a thin solid source. Also, it is cumbersome to identify the alpha particles having different energies based on their track profiles in the detector [O. A.Bondarenko et al. 2000, C. Amero et al. 2001].

1.3. Literature on Different Sample Pretreatment Methods

There are several methods reported in literature that involve lengthy sample treatment before subjecting the sample to instrumental methods [G. Choppin et al. 2006]. The methods involving preconcentration/sorption were developed for measuring the concentration of actinides in the samples from environment and also from biological origins [A. Milliard et al. 2011, G. Kim et al. 2000, S. Mekki et al. 2011, V. Chavan et al. 2013]. However, the development of new materials with desired/specific requirements for selective preconcentration of radionuclides from complex matrix has remained as a challenge [P. J. Lebed et al. 2012, P. J. Lebed et al. 2011, M. J. Manos et al. 2012, Y. Sun et al. 2013]. Vajda and kim [N. Vajda et al. 2011], Qiao [J. Qiao et al. 2009] and Zheng [J. Zhen, 2013] have reviewed the various sample treatment methods for the quantification of transuranium elements like Pu, Np and Am reported in the literature. In general, Actinides could be purified and preconcentrated using a variety of separation methods such as precipitation/co-precipitation, liquid-liquid extraction, ion-exchange chromatography, extraction chromatography, and the combination of these methods. The preconcentration of actinides by the co-precipitation is a frequently used method for big volumes of solution. Most of the sample purification methods applied for the instrumental radioanalytical methods are based on anion-exchange column, particularly purification of Pu sample, and extraction chromatography using TEVA, UTEVA, TRU, DGA, DIPEX, DIPHONIX, etc [N. Vajda et al. 2011]. To reduce manual handling of the samples and hyphenation with instrumental methods, the automations of sample treatment procedures are reported employing on-line ion-exchange and/or extraction chromatography using flow injection/sequential injection and multi-dimensional designs [J. W. Grate et al. 2011, N. Gu´ erin et al. 2011, A. Milliard et al. 2011, D. Larivi` ere et al. 2010]. New technique for plutonium measurement based on cloud point extraction has been reported in conjunction with ICPMS and alpha spectrometry [C. Labrecque et al. 2013]. A small volume flow system in chromatographic applications has been reported in plutonium estimation in human urine present in voluminous samples [J. Qiao et al. 2013]. Basic problem in most of these methods is radioactive solution loading for the instrumental analyses. The polymer based loading helps to secure physical transportation, hence reducing the possibility of contamination of instrument or cross contamination of the sample, minimize radioactivity handling, and it is a point source. Also, the polymeric based materials are amenable to direct quantification of the radionuclide by preconcentrating in its matrix and fallowed by conventional radiation/radionuclide measurement. Hence, these could be useful for the reduction of radioactive dose to analyte, matrix elimination, chemically selective preconcentration of analyte. The possibility of high preconcentration of actinide in polymer based solid matrix would make be highly effective for the determination of ultra-trace concentrations of actinide in a variety of biological, geological, environmental and process aqueous samples.

1.4. Literature review of polymer ligand based materials

To combine multiple sample manipulation steps such as purification, preconcentration and source preparation, the polymer sorbent based thermal ionization mass spectrometry has been developed for quantifying uranium(VI) and plutonium(IV) ions from a variety of aqueous samples [S. Paul et al. 2014]. Similarly, thin sorbent films anchored on the silicon, polymer membrane/films, glass have been developed using different approaches for one step sample manipulation and subjecting the thin film sorbents directly to alpha spectrometry [R. S. Addleman. et al. 2005, D. Karamanis et al. 2006, S. Paul et al. 2015, S.K. Hanson et al. 2014, J.M. Mannion et al. 2016, W. D. Locklair et al. 2016, A.M. Mhatre et al. 2017, J.H. Rim et al. 2016]. Some of these approach involves formation of the chemically selective polymer thin film upon the surface of passivated silicon diodes, UV-grafting of bifunctional polymer film on membranes, thin films of Kläui-type tripodal oxygen donor ligands have been prepared by spin-casting solutions onto the glass substrates, ultrathin films (10–180 nm) of quaternary amine anion-exchange polymers anchored on the glass and silicon formed by dip-coating, etc. To process large volume of aqueous samples, a surface grafted poly(ether sulfone) membrane has been developed for ultrafiltration to capture the alpha emitting actinides and subsequently quantifying by subjecting the membrane to alpha spectrometry [C.E. Duval et al. 2018]. The scintillating polymer membranes have been developed that produce scintillation proportion to the alpha particles emitted by the actinides captured in the membrane matrix [S. Sodaye et al. 2004, V. Chavan, et al. 2016]. In another interesting approach, the poly(glycidyl methacrylate) poly(GMA) have been anchored in the porous sheets by radiation induced grafting and subsequently attached diethylamino (DEA) groups. Thus formed discs have been fitted in an empty cylindrical cartridge for separation of U and Pu for their determinations by ICP-MS [S. Asai et al. 2008]. The schematic of the polymer ligands-based substrates for radionuclide preconcentration, and direct quantifications are illustrated in Figure 1.6.

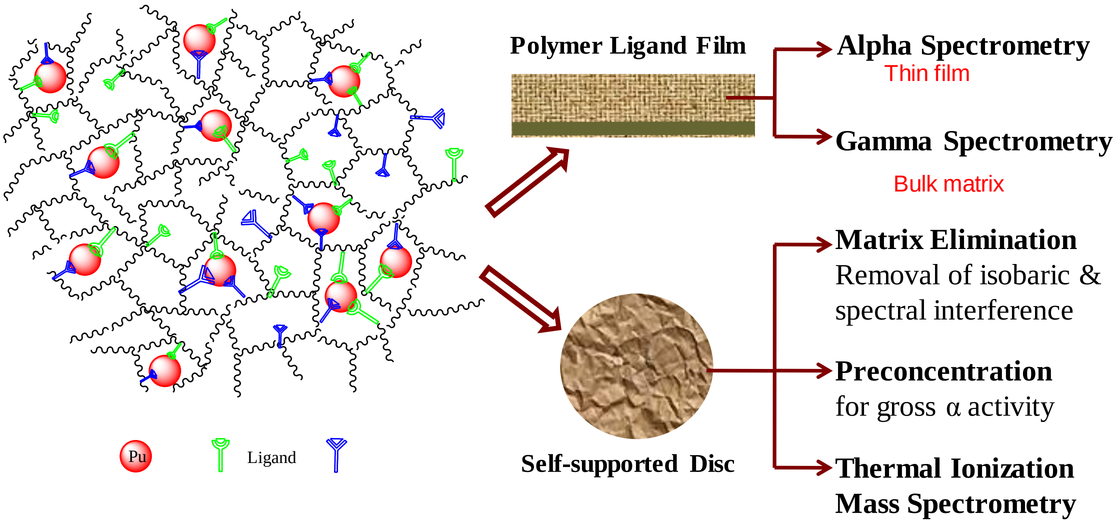

Figure1.6. Development of ligands functionalized sorbents for selective preconcentration of actinides followed by direct quantification from the solid sorbent [S. Paul et al. 2014].

1.5. Scope of the present work

Because of the potential hazards of Pu and fission radionuclides on mankind health, the accurate and reliable determination of these radionuclides in environmental samples is important for (i) environmental risk assessment and monitoring of the environment around nuclear facilities, such as nuclear power plants, nuclear fuel reprocessing plants and nuclear waste storage sites; (ii) emergency preparedness; and (iii) surveillance of contaminated areas from nuclear weapon tests, nuclear accidents, and discharges of nuclear wastes. The quantifications of alpha emitting and fissile elements in the aqueous samples such as environmental samples, radiopharmaceutical samples derived from fission molly, fuel reprocessing aqueous waste samples and nuclear forensic samples are often requiring a highly sensitive radiation measurement instrumentation hyphenated with appropriate sample purification and source preparation methods for the unambiguous quantification. However, in many such applications, the sample has to be subjected to a preconcentration step for bringing the concentration of analyte in the measurement range of the radioanalytical method. The dangerous level for accumulated Pu in the human body is 10^{-12} g g^{-1} (1000 fg g^{-1}). This highlights the compulsion to monitor much lower levels in the surrounding environment in order to evaluate the possibility of bio-accumulation of radiotoxic elements [G. Steinhauser et al. 2014].

Functionalized thin polymer film-based α-spectrometry could combine the sample purification, pre-concentration and source preparation. Recently, it has been shown that the thin film surface-grafted ultrafiltration membrane can be used for capturing Pu from a large volume of aqueous sample, and subsequent direct quantification of Pu ions pre-concentratedon thin film bearing membrane with alpha-spectrometry [E. D. Christine et al. 2018]. Solid state nuclear track detectors (SSNTDs) are the most sensitive for recording the energetic charge particles, but lack chemical selectivity and have limited capability to distinguish the particles based on their energies unlike alpha spectrometry. SSNTD has been used for the detection of alpha particles emitting nuclides [V. Zorri et al. 2017]. This technique can be made highly effective by imparting chemical selectivity using highly selective thin film/polymer on a suitable host matrix for registering alpha/fission tracks in the SSNTD. Also, the track registration efficiency would be considerably higher from the thin film as compared to solution medium generally used for the homogeneous track registration. In gamma spectrometry applications, the bulk functionalized matrix of flat sheet/disc sorbents having the highly porous fibrous architecture would produce materials with a large surface area and densely packed ligating sites. The applications of such materials in the conventional instrumental methods would not only exhibit rapid kinetics, high exchange capacity and capability of the selective extraction of fission products from solution but also would have well-defined counting geometry.

The present thesis deals with the development of thin film polymer ligands sorbents for Pu anchored on the different host matrices such as glass, membrane and Teflon sheet that can be applied for one step sample treatment for alpha-spectrometry and SSNTD based quantifications of Pu at ultratrace concentration in the aqueous samples. The poly (vinylpyrrolidone) and silicotungstic acid anchored glass filter membranes have also been developed for the quantifications of radioiodine and radioactive cesium by gamma-spectrometry, respectively.

CHAPTER 2 - EXPERIMENTAL

2.1 Anchoring of ligating moieties on solid host matrices

The work carried out in the present thesis is based on the selective pre-concentration of the actinides and fission products on the solid matrices having well defined geometry and which can be subjected directly for quantifications by instrumental radiation measurement methods. There two methods used for anchoring ligating functional groups on the solid matrixes are: (1) grafting of ligating groups/precursor groups bearing polymers, and (2) sol-gel anchoring of ligating/precursor groups using appropriate precursor alkoxy silanes. In the present work, γ-ray induced and UV-light induced graft polymerization techniques were used for anchoring polymer ligands on the solid matrix.

2.1.1. Materials and reagents

The monomers bis[2-(methacryloyloxy)ethyl] phosphate (BMEP), 1-vinyl-2-pyrrolidonewere purchased from Sigma-Aldrich, 3-(trimethoxysilyl) propyl acrylate (stabilised with BHT) obtained from Tokyo chemical industry Co. Ltd., Tokayo (Japan), α,α'-dimethoxy-α-phenylacetophenone (DMPA) obtained from FLUKA, Steinheim, Switzerland, glycidyl methacrylate (GMA) (purity >97%) was obtained from M/s Otto Chemie Private Limited, Mumbai, trioctyl phosphine oxide (TOPO) and sodium hydroxide (AR grade) were obtained from S. D. Fine chem. Ltd, Mumbai (India), hydrogen peroxide (30%), *N,N'*-dimethyl formamide (DMF) and hydrazine hydrate (99-100%) obtained from Merk Life science Pvt. limited, Worli, Mumbai (India), sulphuric acid (AR grade 98%) and nitric Acid (AR grade 69-70%) from Thomas Baker (chemicals) Pvt limited, Marine Drive, Mumbai (India), ethyl alcohol (99.9%) was purchased from Changshu Hongssheng fine chemical Co. Ltd., hydroxyl amine (50 wt.% aqueous) was purchased from Lancaster synthesis, Eastgate, More Cambe, (England), chloroform (AR grade) was purchased from Research-Lab Fine Chem Industries, Mumbai (India), Scintillation cocktail W obtained from Sisco Research Laboratories Pvt. Limited, Mumbai (India). De-ionized water (18M cm^{-1}) was used throughout the present work. The micro-concavity glass slides used (cavity diameter- 15 mm, Depth of cavity- 0.5 mm) were obtained from Polar industrial corporation. The microporous host poly(ether sulfone) (PES) membranes (pore size- 0.1µm, thickness-145 µm) from Sartorius Stedim India Private Limited. Teflon sheet (Thickness=0.5 mm) used in the present work was procured from M/s Hindustan Fluro-carbons, Hyderabad, India. The host substrate was glass fibre filter (borosilicate, basic weight: 80-90 g/sq.m., thickness: > 0.4 mm, tensile strength: > 450 gms/cm). CR-39 (allyl diglycol polycarbonate) plastics sheets having 500 µm thickness obtained from Global Nanotech, Mumbai (India). Lexan (bisphenol-A polycarbonate) (200µm thickness) plastics sheets obtained from General Electric Co., USA. The Pu stock solution was obtained from the Radiochemistry Division, BARC, Mumbai, India. Cesium radiotracer was obtained from Board of Radiation and Isotope Technology, Mumbai, India. The grafting was done in a multilamps photo-reactor obtained from Heber Scientific, Chennai, India (model no. HML-SWMWLW-888).

2.1.2 Radiation induced grafting

The polymer can be grafted on the backbone of host matrix by different approaches using appropriate monomer. In general, the free radical polymerization is a preferred route for the controlled formation of the polymer chains. The free radical based polymerization methods normally utilizes free radicals which are produced by initiators (chemical, thermal, or UV-radiations), ionizing radiations such as γ-rays and electron beam, and plasma. The controlled free polymerizations are based on: (i) stable free radical polymerization (SFRP), (ii) atom transfer radical polymerization (ATRP), and (iii) reversible addition fragmentation chain transfer (RAFT). Atom transfer radical polymerization (ATRP) is similar to atom transfer radical addition, and used for controlled formation of the C-C bonds using appropriate transition metal catalyst. RAFT involves conventional free radical polymerization of a substituted monomer in the presence of a suitable chain transfer (RAFT) reagent.

Grafted copolymers consist of a linear backbone of one composition and randomly distributed polymer branches of another composition. The polymer grating is carried out by using different approaches such as: (a) “grafting to”, (b) “grafting from”. “Grafting to” permits incorporation of macromonomers, formed by other controlled polymerization processes into a host polymer backbone chain. The primary requirement for “grafting from” reaction is a initiating functionality on the host polymer chain. Therefore, “Grafting from” involves attachment of amine/hydroxyl groups bearing monomer covalently by the esterification, amidation or similar reactions, and then growing desirable graft polymer chains. “Grafting to” is used for the preparation of graft copolymers using various "click" chemistries.

In the most of polymer grafted material, the ionizing radiations have been used to attach monomer segment to polymer backbone of the matrix having porous architecture. The electron beam, lower wavelength UV-light, RF frequency plasma exposure, and gamma irradiations are used to produce reactive sites (free radicals) on polymer backbone of the matrix. During irradiation or after irradiations, the desired monomers are allowed to come in contact with the active sites to form grafting of monomer and subsequent polymerization to form the grafted polymer chains. The contact of monomer during irradiation leads to the formation of homo-polymerization [Xu et al. 2002, 2003, liu et al. 2005]. However, the formation of homo-polymer is suppressed if monomer is allowed to come in contact after irradiation. In absence of monomer, the active sites form peroxides in the presence of air, and these peroxides are converted back to radicals after heating at appropriate temperature.

The grafted substrates produced by radiation induced are very stable and possess desired and advantageous physical properties [Bhattacharya et al. 2004]. The schematic representation of synthesis for the grafted membrane is given in Figure 2.1.

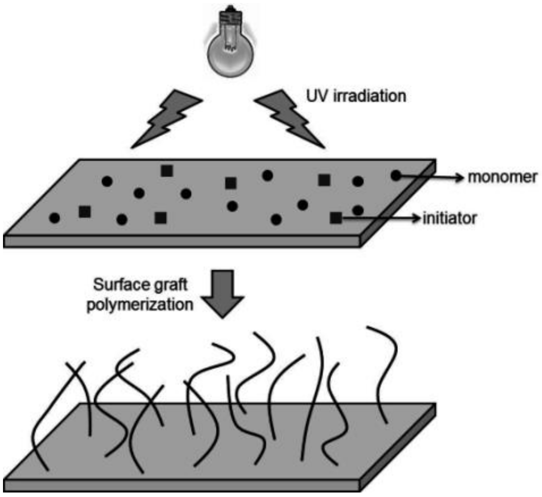

Figure 2.1. The schematic representation of synthesis for the grafted thin ligand bearing film.

2.1.2.1 Radiation induced polymerization using ^{60}Co source

GC-900 gamma irradiator was used for polymer functionalization in the present study contained ^{60}Co source supplied by Board of Radiation and Isotope Technology, Mumbai having dose rate of 1 kGy h^{-1}. GC– 900 is one of the standard gamma irradiator for research applications. The photographs of this γ-irradiator are shown in Figure 2.2. The chamber of γ-irradiator used for graft polymerization consists of ^{60}Co source pencils loaded in a cylindrical array in a source cage, and the source cage assembly is stored at the centre of a lead flask. The central drawer is a long cylinder consisting of two stainless steel clad lead shields with a hollow sample chamber situated in between them. The central drawer can be raised or lowered by a wire rope passing over a system of pulleys and wound on a drum by a geared motor. For irradiation, the drawer is lowered until the sample chamber is at the centre of the source cage. The movement of the sample chamber is controlled from the control panel through an electrical control circuit.

Figure 2.2. GC-900 gamma irradiator used for monomer grafting on Teflon.

2.1.2.2 Calibration of GC-900 gamma irradiator

Fricke dosimeter was used for the dose calibration of GC-900. It is most useful method to measure directly the dose rate in solution [Spinks et al. 1991, Farhataziz et al. 1987] Fricke dosimeter is generally accepted as a primary standard in radiation chemistry due to its accuracy and reliability. Fricke dosimeter relies on oxidation of ferrous ions in to ferric ions in an irradiated ferrous sulphate solution. The amount of ferric ions produced in the solution measured by absorption spectrometry with ultraviolet light at 304 nm, which is strongly absorbed by the ferric ions. Fricke dosimeter depends on an accurate knowledge of the radiation chemical yield of the ferric ions, measured in moles produced per joule of energy absorbed in the solution. The chemical yield is related to a parameter G value, defined as the number of ferric molecules produced in the ferrous sulphate solution by 100 eV of absorbed energy. An accurate value of chemical yield is difficult to ascertain because the chemical yield is dependent on the energy of the radiation, dose rate, and temperature of the solution during irradiation and readout. The best G value for ^{60}Co gamma rays is 1.6 molecules per 100 ev; corresponding to a chemical yield of 1.607 x 10^{-6} mol/J (^{60}Co gamma rays). The typical measurement range for ferrous sulphate Fricke dosimeter is from a few Gy to 400 Gy. Density is 1024 g L^{-1} at 15-25 ^{0}C. The primary radical chemical reactions involved in Fricke dosimeter are conversion of all e_{aq}^- to $H^\bullet$ and finally to $HO_2^\bullet$. Thus, each $H^\bullet$ produces 3 Fe^{3+}(1st via $HO_2^\bullet$, 2nd via H_2O_2 produced from $HO_2^\bullet$ via HO_2^-, and 3rd via $^\bullet OH$ produced from H_2O_2), Each H_2O_2 (radiolytic) will produce 2Fe^{3+} (1st direct, 2nd via $^\bullet OH$ produced from H_2O_2), Each $^\bullet OH$ (radiolytic) will produce 1Fe^{3+}, Each $HO_2^\bullet$ (radiolytic) will produce 1Fe^{3+} [Farhatazizet et al. 1987, Ralph Mathews et al. 1982]. G values of different species formed due to irradiation are available at different pH [Spinks et al. 1991; Farhatazizet al. 1987] The radiation chemical yield of the Fricke dosimeter solution is strongly LET dependent. The above calculation is done for ^{60}Co gamma rays (most commonly used system).

Phosphate functionalized GMA Grafted Teflon (Ph-g-T)

Teflon sheets were washed first with toluene followed by detergent solution, and vacuum dried at 50^0C. To graft poly(glycidyl methacrylate) (poly(GMA)) on only one face of Teflon, Teflon were compression molded into poly(propylene) sheet. The samples were immersed in the GMA containing solution fallowed by irradiation in the gamma chamber. Thus obtained GMA-g-Teflon was refluxed for 3 h at 80 ^0C in a solution of phosphoric acid and tetrahydrofuran. The Ph-g-T samples were washed with acetone for 8 h to remove any trapped homopolymer of GMA in the grafted Ph-g-T. Finally, the grafted matrix was washed with water and dried in vacuum at 50 ^0C for further use.

2.1.3 UV-light induced grafting using multi lamps photoreactor

In the present studies, the UV multilamps photorector was purchased from Heber Scientific (Model: HML-SW-MW-LW-888). The photoreactor consisted of total eighteen lamps (8 Watt each) arranged in circular manner. The eighteen lamps were separated in to six sets with each set consisted of three lamps emitting a fixed wavelength of 254, 312 or 365 nm. The photoreactor and its internal view of array of the lamps and sample holder in UV photoreactor are shown in Figure 2.3 a & b, respectively.

(a) (b)

Figure 2.3. Photographs showing the UV-photoreactor used in polymer grafting (a), and inside view of array of the lamps (b).

2.1.3.1. Glass @poly(BMEP)

Grafting of the polymer film was done on micro-concavity glass slides. The glass slides after pretreatment filled with solution consisting of 3-(trimethoxysilyl) propyl acrylate (TMSPA), bis[2-(methacryloyloxy)ethyl] phosphate (BMEP) and UV-initiator α,α'-dimethoxy-α-phenylacetophenone (DMPA), and irradiated with 365 nm UV light in a photoreactor for 30 min. After grafting, the glass slides were washed with a water/*N, N'*-dimethyl formamide (DMF) mixture at 35-40 ^{0}C to remove the un-polymerized components and dried under vacuum.

2.1.3.2. Poly(BMEP)-grafted PES membrane

The monomer solution sample was made by dissolving monomer BMEP in a mixed solution of water and ethanol and homogenized by ultrasonication for 5 min. One side blocked PES membrane along with monomer solution exposed to UV light. The grafted membranes obtained after irradiation were washed with water ethanol mixture at 35–40^{0}C to remove un-polymerized components and dried in the vacuum oven at 40–45 ^{0}C for 2–3 h.

2.1.3.3. PVP grafted glass membrane filters

First, the glass fiber membranes were treated with piranha solution (H_2O_2:H_2SO_4, 1: 3 v/v) for 15 min to remove the organic impurities, and then washed with distilled water followed by ethanol. These hydrolyzed glass fiber membranes were immersed in ethanolic solution of 3-(trimethoxysilyl) propyl acrylate (TMSPA) for overnight with constant stirring. Thus treated glass fiber membranes were air dried. The details of used sol-gel method for anchoring of TMSPA are described below.

For poly(1-vinyl-2-pyrrolidone) (PVP) grafting, the 3-(trimethoxysilyl) propyl acrylate (TMSPA) anchored host glass fiber membrane was soaked in the polymerizing solution of 1-vinyl-2-pyrrolidone (VP), cross-linker ethylene glycol dimethyl acrylate (EGDMA), and UV-initiator α,α'-dimethoxy-α-phenylacetophenone (DMPA) in DMF for overnight, removed and sandwiched between two transparent polyester sheets. The polymerizing solution filled glass fiber membrane was exposed to 365 nm UV light in a photoreactor for a period of 30 min. After exposure in the photoreactor, the PVP-grafted glass fiber membrane was washed thoroughly with DMF and distilled water to remove the un-grafted material.

2.2. Sol-gel process

In recent years, the tailoring of desired functionality in the host matrix or on its surface with good homogeneity is done using the sol-gel chemistry for developing a variety of materials [C. J. Brinker et al. 1990]. In sol-gel method, the mixing of chemical occurs at very low temperature providing good control at atomic level [L. L. Hench et al. 1990]. The “sol” represents the colloidal form of solid entity in liquid phase of few hundred nm in diameter. The gel is macromolecules formed from condensation of sol suspended in solvent. The sol-gel technique consists of conversion/ transformation of the liquid sol to gel phase. There are two different steps in the sol-gel process to produce the various types of materials. These are:

(i) colloidal process, and (ii) chemical polymerization process. The thin film development based on the sol-gel process is represented in Figure 2.4.

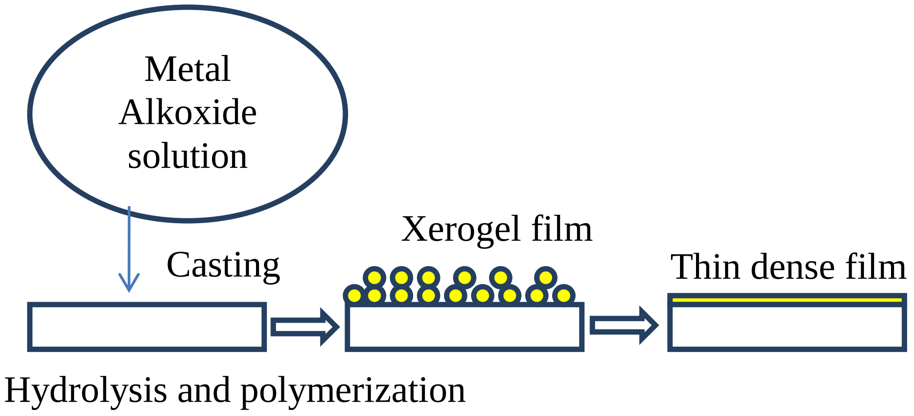

Figure 2.4. Schematic representation of the sol-gel process in thin film material development.

In sol-gel technique, the surface is initially hydrolyzed and then this hydrolyzed silica sites get connected to each other by condensation with removal of water or alcohol. In casting and gelation state, the polymerization process continues and form the three-dimensional network. The extent of gelation is affected by acidity, temperature and the presence or removal of solvent. Liquid expulsion results in the polycondensation process to form the pores. There is decrease in the porosity with increase in the particles size/ neck. During drying, the liquid trapped in the crosslinked network get removed. In dehydration or chemical stabilization, traces of alcohol is removed from silanol backbone to get compound which is chemically stable. The hydrolysis and condensation reaction are represented as follows:

Hydrolysis: $M(OR)_n + H_2O \rightarrow M(OH)(OR)_{n-1} + ROH$

Condensation: $2M(OH)(OR)_{n-1} \rightarrow (RO)_{n-1}M\text{-}O\text{-}M(OR)_{n-1} + H_2O 2M(OH)_n \rightarrow (OH)_{n-1}M\text{-}O\text{-}M(OH)_{n-1} + H_2O M(OR)_n + M(OH)(OR)_{n-1} \rightarrow (RO)_{n-1}M\text{-}O\text{-}M(OR)_{n-1} + ROH$

2.3 Characterization methods used for grafted substrates

2.3.1 Atomic force microscopy (AFM)

The Scanning Probe Microscopy (SPM) is imaging technique which does small dimension probe scans of the specimen. The surface topography and/or surface physical properties are estimated using the probe motion. The technique SPM is mainly used to study the surface properties. The tip used as probe interacts physically with the sample surface, and the image can be constructed by knowing physical quantity of interaction. The SPM includes atomic force microscopes (AFMs) and scanning tunneling microscopes (STMs). In present work, AFM was used to study the morphology of the grafted thin film on the host material.

The working principle is related to use of a micro tip fixed to a cantilever at very close to sample surface [N. Jalili, et al. 2004]. The Atomic Force Microscopy (AFM) mainly measures the extent of interaction between probe tip and the sample. One end of the tip is connected to the cantilever and the tip is brought very close to the specimen under investigation. The cantilever indicates positive or negative bend motion due to interaction of tip with surface due to attractive or repulsive forces. The extent in the bending of the cantilever is probed by measurement with beam of the laser. There is reflection observed for laser beam due to motion of the cantilever. In surface study measurements, the images obtained is of the order of one tenth of nanometer atomic resolution. The AFM gives nanoscale profile of the specimen surface in three dimension at very small distance between probe and surface of the order of 0.2 to 10 nm. The principle of the AFM technique is illustrated in Figure 2.5 (a).The AFM force sensor activates when probe interacts with the surface field. The extent of changes in the forces as function of distance between the probe and the cantilever is shown in Figure 2.5 (b).

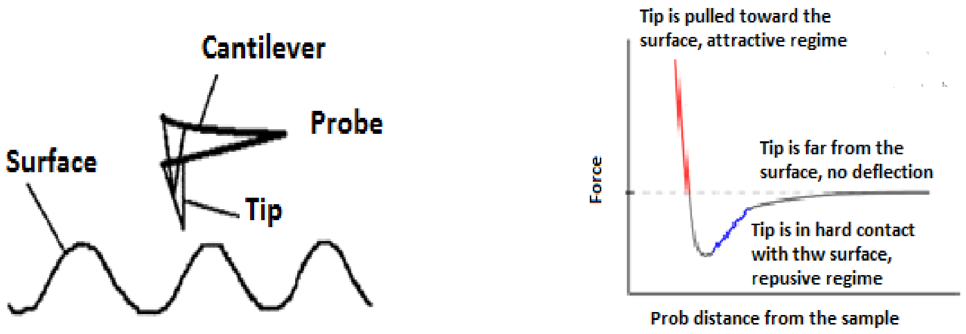

(a) (b)

Figure 2.5. The schematic representation of the principle of AFM technique (a) and nature of forces when tip interact with the sample (b).

2.3.2 Fourier transform infrared spectroscopy

Infrared spectroscopy is employed to study the molecular structure by the application of infrared radiation. When the molecule exposed to infrared radiation, there is change in the molecular vibrations. These changes are measured in the form of absorbed or transmitted infrared intensity as function of wave numbers (ν) (cm^{-1}) of IR radiations. Wave numbers has direct relation with the energy of the vibration, $\Delta E = h\upsilon = hc / \lambda = hc\nu$. Therefore, in principle, each absorption of radiation in the infrared region is quantized and should appear as sharp line. Infrared spectrum of individual compounds represents a fingerprint which is associated with the vibrations of bond between the atoms. Infrared spectrum provides qualitative information associated with different molecular structure of the material and quantification can be deduced from the intensity of the peak. Conventional dispersive grating spectrophotometers are used to get qualitative information. A FTIR instrument has applications in both qualitative as well as quantitative estimation. The FTIR spectrometry is a non-destructive measurement, gives highly reproducible measurement without external calibration, increase speed of measurements, receives and records a scan every second, more sensitivity, and high optical throughput. FTIR provides specific information about the characteristics unsymmetric vibrations of the chemical bonding making it useful for analyzing the molecular structures of organic materials and certain inorganic materials. In present work, the presence of desired functional groups in the thin polymer ligand was confirmed by the FTIR spectroscopy.

2.3.3 Thermogravimetric analysis (TGA)

Thermogravimetric (TG) is a study of the mass changes of a sample as a function of temperature. These changes in the mass of a sample are due to various thermal events (desorption, absorption, sublimation, vaporization, oxidation, reduction and decomposition) occur while the sample is subjected to a program of systematically increase in temperature. Weight of sample continuously monitored in an air, nitrogen, oxygen, or specialty atmosphere in TGA in the range of 30° C to 1000° C. The primary use of this technique in the measurement of thermal stability and elemental composition of the material under study. TGA instruments are potentially used in the many areas including the thermal stability, characterizations of material, quality control, production etc.

The physical changes occurring in the material as a function of heat is monitored using TGA technique. The method interprets the changes in the mass which are due to different transitions occurring in the sample or degradation inside the sample due to heating. The thermo-gravimetric curves are characteristics of the compounds and shows particular sequence in thermo physical reactions in given temperature range at given heating rate. The characteristic properties observed can be correlated with the composition of the sample [R. P. W. Scott, Thermal Analysis Book 5]. TGA in combination with the FTIR can be used to access the gases released during heating of the specimen. TGA analyzer consists of a high-precision balance with a pan (generally platinum) loaded with the sample. The pan is placed in a small electrically heated oven with a thermocouple to accurately measure the temperature. The atmosphere may be purged with an inert gas to prevent oxidation or other undesired reactions. A computer is used to control the instrument. Figure 2.6, shows the typical instrument for TGA (a) and a typical characteristic output (b).

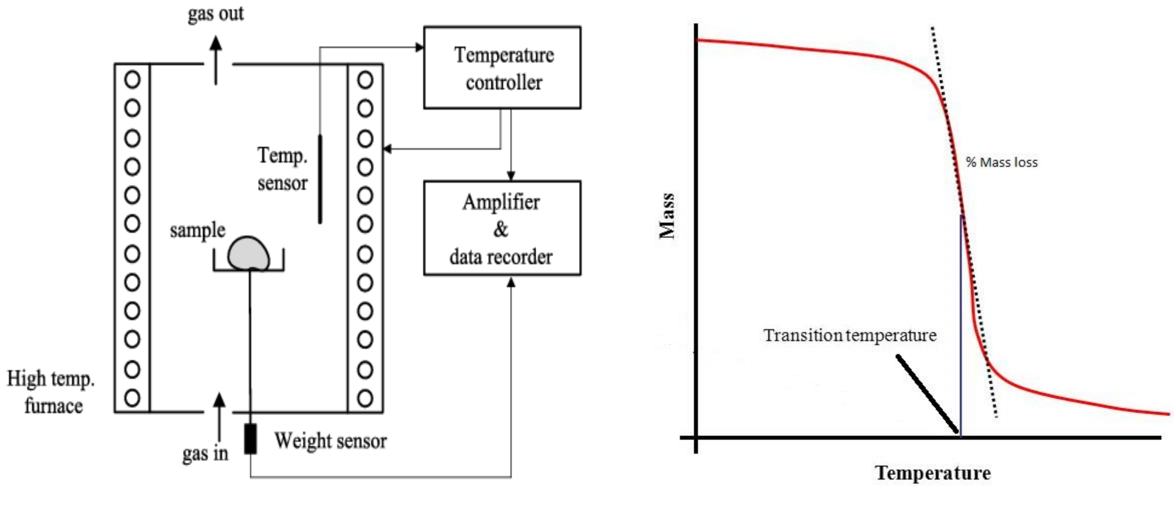

(a) (b)

Figure 2.6. (a) A typical design of instrument for TGA and (b) characteristics thermogram.

2.3.4 Field emission scanning electron microscopy (FESEM)

Electron microscopy is used for studying the morphology of solid surfaces. The high resolved images of the solid objects can be obtained using scanning electron microscopy (SEM). In SEM measurements, the accelerated electrons after interaction with the sample produce a variety of signals when the electrons get slower down in the specimen. The different kinds of signals obtained provide information about the elements present in the sample and topography of the sample. *Secondary electrons (SE)* normally carry surface information due to its low energy (< 50 eV) which limits its emission from the inside matrix at certain depth. The secondary electrons gives information about specimen morphology and topography. *Backscattered electrons (BSE)* are mainly electrons obtained from incident beam undergoes columbic interaction at angle 90^0 with oppositely charged nucleus. The detection of backscattered electrons gives information about elemental contrast and phase inhomogeniety. The electrons are produced either thermionic emission or electric field gradient emission. In

Field Emission Scanning Electron Microscopy (FESEM), the electric field gradient is used to accelerate the electrons produced from field emission source. This beam of electrons in the presence of high vacuum is dispersed and converted to narrow beam using electronic lenses which focus/deflect the primary beam. This focused narrow beam is used to monitor the specimen. The result of the bombardment of these electrons in producing secondary electrons from each spot on the object gives information about the morphological structure of the sample. The detector generate signal after collecting secondary electrons. The signals are further amplified and processed to get the scan image.

2.3.5 Energy dispersive X-rays spectroscopy (EDS)

The electron beam-sample interactions gives out characteristics X-rays emitted by the atoms in the matrix of the sample. Therefore, EDS is generally fitted with the SEM instrument to get information about the chemical composition of the surface. X-rays are emitted as result of ionization of atoms by electron beam due to removal of electron and creates in inner shell. A set of transition occurs so as to compensate the vacancy in inner shell. The unique energies of electrons in the shell are due to the unique electron binding energy. Therefore, the X-rays emitted are characteristics of the element making specifically the technique very important in the elemental analysis. The sample surface scanned by the electron beam used to produce full range X-ray spectrum for each pixel for the surface. The distribution of elements also can be mapped by scanning the specimen surface by relative intensity ratio. Basically, a typical EDS system consists of three important components: X-ray detector, pulse processor and multichannel analyzer. In the present work, the EDS attached to FESEM was used to ascertain the chemical composition of the grafted polymer on the host matrix.

2.3.6 UV-Vis spectrophotometer

Light absorption can be used as a tool in qualitative and quantitative estimation of the specimen. UV-Vis spectroscopy mainly deals with the absorption measurements in standard and sample solutions. However, it is possible to carry out UV-Vis spectrophotometry of solid samples in the reflection mode. In this technique, the sample is exposed to range of electromagnetic radiations of characteristics wavelength. The part of light is absorbed depending on the species present and some part of light pass through the sample which falls on the detector and monitored as function of wavelength and produce output in the form UV-Vis spectrum. The information obtained from the absorbance is used to quantification of the species. The absorption at characteristics wavelength of light beam corresponding to a component allows determination of its concentration in sample is depicted in Figure 2.7.

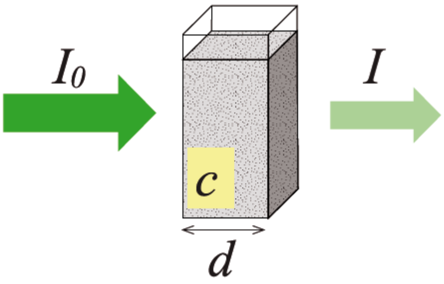

Figure 2.7. The attenuation of light beam allows the determination of sample concentration.

The quantification of the colored species in the matrix (solution or solid) is based on the Beer-Lambert Law which correlates linear variation of Absorbance with concentration as given below:

$$A = \varepsilon\, b\, c$$

Where A = absorbance (unit less), ε = molar absorptivity (M^{-1} cm^{-1}), c= conc. (M cm^{-3})

$$A = -\log T = -\log [I/I_0]$$

Where T is transmission and I is light intensities. However, there are several possibilities where this law cannot be applied and thus quantification cannot be done using UV-Vis spectrometry. In the present work, I_2 and I_3^- concentrations in solutions were determined by UV-Vis spectrometry.

2.3.7 X-ray diffractometer (XRD)

The X-ray interact with the specimen get scatter off of the atoms in a sample. The detection of scattered X-rays gives idea about what atoms are present and how they are arranged in crystal. X-ray diffraction (XRD) is nondestructive technique provides information about orientation of the crystals, crystal phases, structural properties, parameters related to lattice, size of the grains, composition of the phases, idea about transformations is ordered or disordered, thermal expansion, to determine thickness of the films. The unit cell information such as size and shape can be obtained by studying the X-ray interaction with the crystalline material. The path of the X-ray gets modified to different angles after passing through crystal. This scattering of X-rays occurs mainly from the electrons in the medium. The atoms or ions at different inter planer distance scatter X-rays at different angles. X-rays show constructive interference "in phase" when their energies added due to interaction with adjacent layers. The condition for the diffraction can be understood through Bragg's model shown in Figure 2.8. The constructive interference likely happens only when parallel planes with distance d_{hk} exits. This produces dark dots on a detector plate. The space between diffracting planes of atoms determines peak positions. The peak intensity is determined by atoms that are in the diffracting plane. In a crystalline solid, the constituent particles (atoms, ions or molecules) are arranged in a regular order. An interaction of a particular crystalline solid with X-rays helps in investigating its actual structure.

$$\lambda = 2d_{hkl}\sin\theta$$

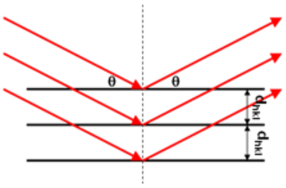

Figure 2.8.Schematic of the X-ray diffraction by a crystal.

Where, λ is wavelength of X-ray, d is inter-planer distance, 2θ corresponds to the angular position of the detector that rotates around the sample.

In the present work, the XRD patterns were studied to understand the crystalline phases of silicotungstate formed in the glass filter membrane for capturing radiocesium ions.

2.3.8 Capillary flow porometry (CFP)

Capillary flow porometry is used for characterization of porous matrix based on the displacement of a wetting liquid from the pores by applying a gas at increasing pressure. The pressure at which liquid is ejected from pore is related to its diameter by capillary equation. Capillary flow porometer measures the most constricted part of through pores. This technique is based on Washburn equation given below:

$$\text{Washburn equation: } \Delta P = 4\gamma \cos \theta / d_p$$

Where where ΔP being applied pressure, d_p the pore diameter, d_p is the pore diameter, γ is the surface tension of the air-liquid interface, and θ is the wetting angle with the solid matrix of the membrane. This method is valid up to 2 nm pore diameter.The schematic representation of this method is shown in Figure 2.9.

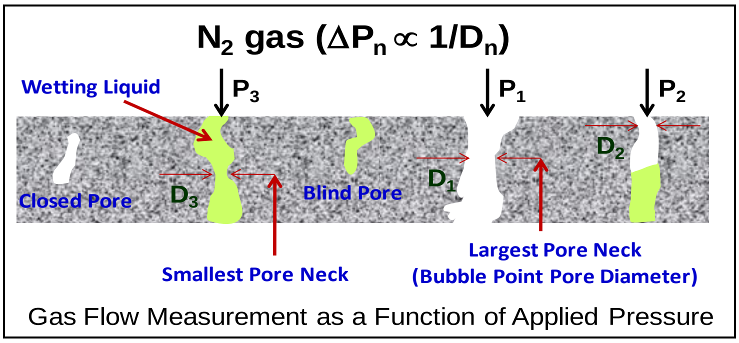

Figure 2.9. The schematic representation of principles of CFP for measuring pore-diameter in a membrane.

To determine the pore size (diameter) distribution by CFP, the plots of N_2 gas flow rates as a function of applied pressure across the membrane with wetting liquid “Porefil” (wet run) and without wetting liquid (dry run) were analyzed. The curves of flow rates as a function of applied pressure are shown in Figure 2.10. The portion of the wet run from a point where first flow of gas was observed (Bubble point) up to a point where it meets the dry run plot was used for determining the pore diameter distribution. Using Washburn equation, the applied pressure was converted to diameter using the experimentally measured surface tension of pore-filled liquid.

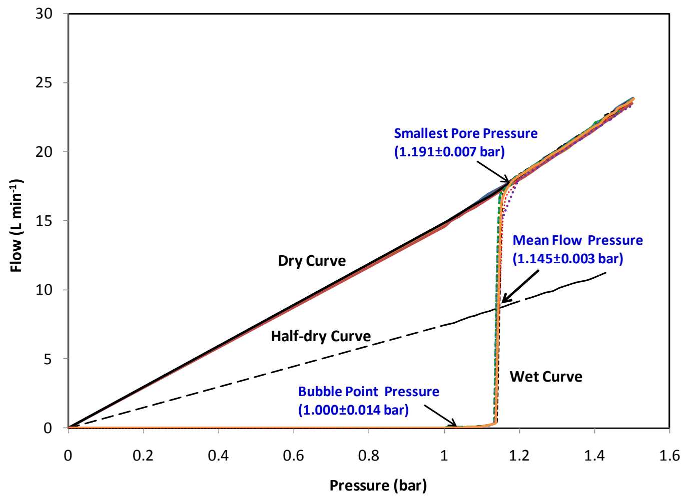

Figure 2.10. The plots showing flow rates as function of applied pressure across dry and wet poly(ether sulphone) membrane subjected to five replicate cycles of measurements.

2.3.9 Optical microscope

The transmission optical microscope is the most widely used method of viewing particle tracks in the plastic or inorganic detector, and making quantitative measurements in solid state nuclear track detector (SSNTDs). The particle tracks in the present work were counted after chemical etching using optical microscope. The developed alpha and fission tracks were observed under Olympus fully motorized transmission optical microscope (model no. BX63, Olympus Tokyo, Japan) attached with QIMAGING QICAM CCD camera and cellSens Dimension Package for image analysis for observable parameters like track length, diameter, number of tracks shown in the Figure 2.11. The detector films after chemical etching are washed under running tap water and air dried. The dry films are mounted on glass slide and placed on the microscope stage and different track parameters were measured with the help of calibrated eyepieces, mechanical stages, transmitted light and different magnifications ranging from 5x, 10x, 40x and 100x available in the microscope. The objective magnification multiplied by the eyepiece magnification results in the visual overall magnification. When damage trails viewed under transmitted light through an optical microscope, these tracks scatter light and show up as dark lines, cylinders, cones or circles. The film is focused under the specific magnification and numbers of tracks per view are counted.

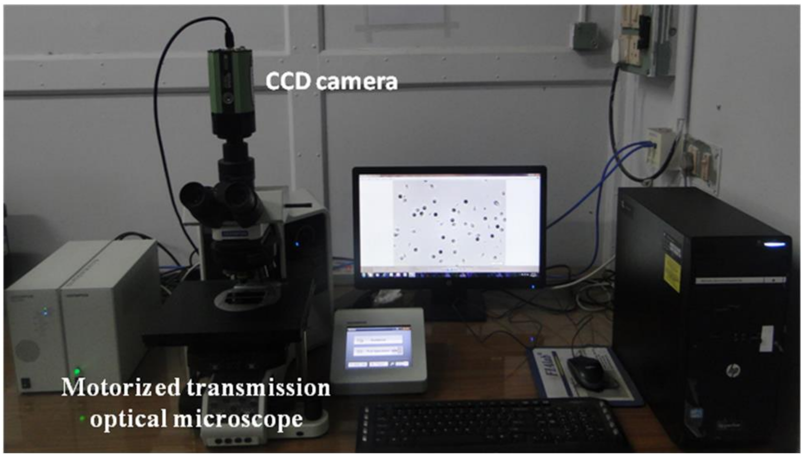

Figure 2.11. Ttransmission optical microscope setup

2.4 Quantification of radionuclides

Different radioanalytical methods used for the quantifications of radionuclides used in the present studies are discussed briefly below:

2.4.1 Liquid scintillation counter (LSC)

The detail of LSC is given in **chapter I**. In the present work, both dioxane and toluene based of scintillators were employed. Dioxane based liquid scintillator consists of 0.1 % (v/v) PPO, 0.025 % (w/v) POPOP and 10 % (w/w) naphthalene. In addition to these, tri-octyl phosphine oxide (TOPO) is added which acts as an anti-quenching agent so as to suppress the effect of acid. Naphthalene was added to increase the shelf life of the cocktail mixture. On the other hand, the toluene based liquid scintillator consists of 10 % (v/v) HD2EHP, 0.7 % (w/v) PPO and 0.03 % (w/v) POPOP. Suitable aliquots (25-100μL) of solutions containing alpha activity were taken in glass vials containing about 5 mL of the liquid scintillator solution. Liquid scintillation spectrometer setup used in the present work is shown in Figure 2.12. The counting setup consists of sample holder where scintlllator /sample is placed and the scintillation from the sample is counted using photomultiplier tube, which is shielded with lead and the output of photomultiplier tube connected to Nuclear Instrument Module (NIM Bin) containing amplifier, Single Channel Analyser (SCA) and counter or pulse hight analysis is done using Multi Channel Analyser (MCA) electronics of the same type used in gamma spectrometry.

Figure 2.12. Liquid scintillation spectrometer set up used in present work.

2.4.2 Alpha spectrometry

The basic principle and application of alpha spectrometry are given in **chapter I**. Figure 2.13 shows a schematic diagram of a typical alpha spectrometer (a) and spectrometer used in sample measurement (b, c).As can be seen from this figure, the alpha source and the silicon-semiconductor detector are placed in the vacuum chamber at fixed geometry. Vacuum pump with the pressure gauge and pressure regulator are used to create desirable vacuum in the chamber. Detector is connected to the input of data acquisition unit via charge-sensitive preamplifier and amplifier. Detector detects alpha radiations and generate signals in the form of charges, detector bias power supply provide electric field to collect detector charges, preamplifier does signal conditioning, electronics of spectroscopy amplifier do digital filters, signal processing of detector signals, Multi-Channel Analyzer (MCA/Analog-to-Digital Converter) is employed to digitize the amplified signal and transfer to computer, ADC ranges from 1, 2, 4, 8, 16 and 32k channels, Control and analysis software configure MCA according to applications, control MCA for data acquisition and spectrum analysis.

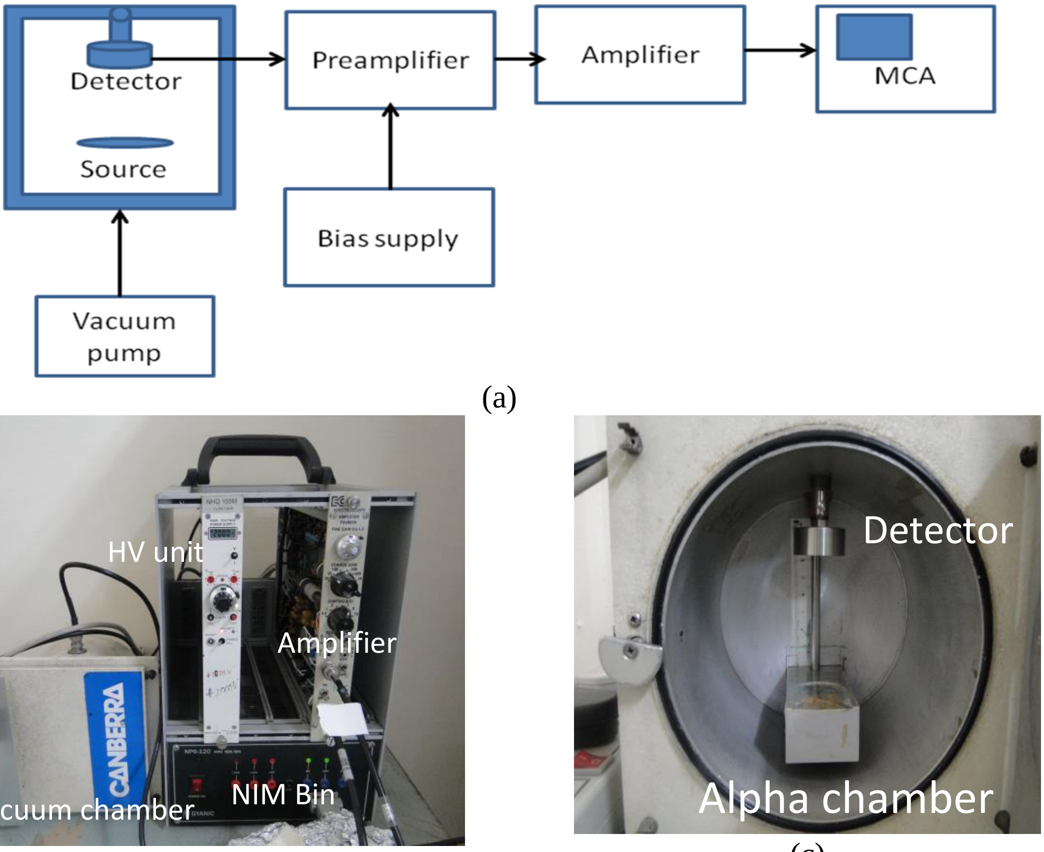

(a)

(b) (c)

Figure 2.13. Photographs showing schematic diagram of a typical alpha spectrometer (a), spectrometer electronics and chamber (b), and inside view of the vacuum chamber (c).

2.4.3 Gamma spectrometry

The γ-rays interact with the medium with different mechanisms [G.F. Knoll, 1980]. These mechanisms are: *Rayleigh scattering:*γ-ray is scattered by medium and results in the change in the direction of gamma radiation which is conserved by the scattering medium. The result of *Compton scattering* is gamma radiation transfer partial energy transfer with electrons in the medium which get recoiled. In case *photoelectric absorption,* gamma radiation interact with the medium electrons with complete energy transfer and gamma radiation is completely absorbed, *Pair production* is associated with the creation of electron positron pair which further get annihilated to give two 551 keV photons. There are two categories of the γ-rays spectrometers i.e. scintillator based and semiconductor based detectors. In the present work, the scintillator based detectors were used.

2.4.3.1 Gamma detection using scintillators (NaI(Tl)) and components

Scintillator is a material that exhibits the property of luminescence [Leo W. R., 1994**].** These materials get excited when exposed to ionizing radiation. Luminescent materials absorb energy of radiation and convert it into the visible or near to the visible energy range photons during de-excitation to ground state. Inorganic alkali halides are very popular scintillating materials which include NaI. Very efficient light output gives attention to NaI. This property is very important and required in the view of good statistics in the number of photons emitted by the scintillator when ionizing radiation interacts with the scintillator. Crystalline sodium iodide, in which a trace of thallium iodide had been added in the melt, produced an exceptionally large scintillation light output compared with organic materials **[**Hofstadter R., 1948**].** Tl doped NaI is commercially obtained in single crystalline form and also in polycrystalline form. In gamma spectrometry, scintillators usually composed of scintillating NaI(Tl) crystal. The reflecting material like MgO or Al_2O_3 covers the NaI(Tl) crystal. The working of the NaI(Tl) gamma detector system is discussed in Figure 2.14(a) along with the system used in the present work Figure 2.14 (b).The light output by scintillator travels through glass window before reaching the detector. The NaI (Tl) scintillators in gamma spectrometric application are used in circular cylindrical geometry. The scintillation produced by the NaI(Tl) absorbed by the photomultiplier tube (PMT) and re-emitted in electron form. These electrons are further amplified which results in electronic signal to be analyzed for the energy and intensity of the radiation which interacted with the scintillator. The function of remaining components of counting system like preamplifier converts absorbed energy into electrical signal and amplify. The electrical signal is further amplified by amplifier and shaped into Gaussian pulse. These pulses processed as per the peak voltage using analog to digital converter (ADC/MCA) which further used to form a energy spectrum.

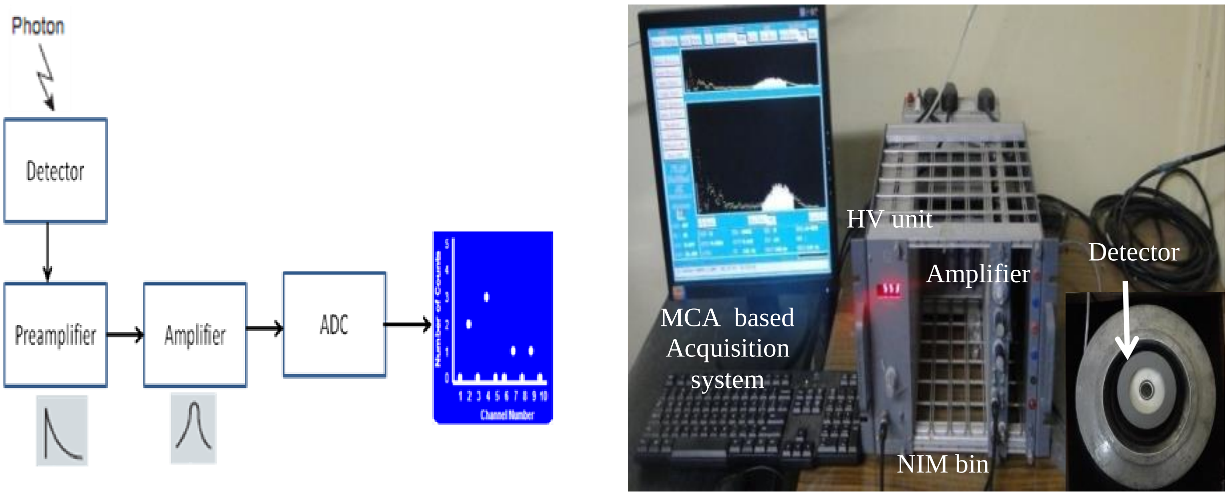

(a)

(b)

Figure 2.14.Generalized detection scheme for gamma measurement (a) and well type NaI(Tl) detection counting setup used in the measurements (b).

2.4.4 Solid state nuclear track detection

Solid State Nuclear Track Detectors (SSNTDs) are insulating solids both naturally occurring and man-made. There are dozens of these detectors including inorganic crystals, glasses and plastics used in energetic charged particles detections [R.L. Fleischer et al. 1975; S.A. durraniet et al. 1987, C. Herburnet et al. 1980)]. Studies on solid state nuclear track detectors are of topical interest because of the wide applications of these detectors in the fields of science and technology [R.L. Fleischer et al. 1965; R. Spohr et al. 1981; B.E. Fischer et al. 1983; E.H. Lee et al. 1991; D. Fink 2004; D. Fink et al. 2005]. Some examples of mineral and crystals detectors category are olivin, zircon, quartz, mica. Inorganic glass materials such as sodalime glass, phosphate glasses and plastic detectors cellulose nitrate, poly allyl diglycol carbonate, polycarbonate, polyethylene terephthalate are also used for the track detection. In most of the applications, the counting of the number of tracks in a specified area of the detector is sufficient for quantifying the events; in specialized applications such as particle identification, quantitative analysis of the track profiles is necessary. When a heavily ionizing charged particle passes through such insulating solids, it leaves a narrow trail of damage about 50 A° in diameter along its path. This is called 'Latent track' as it cannot be seen with the naked eye. It is possible to view this latent track with an electron microscope. The exact nature of the physical and chemical changes occurring at the damage site depends on the charge (Z) and speed ($\beta = v/c$) of the particle, chemical structure of the detector material and also on the environmental conditions like temperature and pressure. These latent tracks can be enlarged / developed and can be viewed under an optical microscope. Cellulose nitrate is used for recording alpha tracks. Polycarbonate detectors such as Lexan, Tuffak (Bisphenol A-polycarbonate) etc. are generally used for recording fission fragment tracks, and CR-39 (Allyl diglycol carbonate) can register all types of tracks ranging from proton recoil to fission tracks. The Lexan and CR-39 are the most commonly used SSNTDs.

2.4.4.1 Mechanism of track recording in SSNTDs

The mechanism of formation of etchable tracks in inorganic solids and organic polymers are different. In the case of ***inorganic solids***, a high concentration of positive ions along the latent track leads to repulsive electrostatic pressures exceeding the mechanical strength of the crystal due to the coherent attractive forces in the atomic lattices. This results in a stressed region which can be chemically etched. This explains why materials with low mechanical strength, low dielectric constant and of low interatomic spacing are good track detectors. It also explains why plastics are more sensitive than glasses which are more sensitive than most inorganic crystals / minerals. If the positive ions produced in the channel either recombine in time scales of the order of 10^{-13} sec (corresponding to the time required for removing the ions from the lattice sites) or have appreciable ion mobility, then the latent track cannot be preserved permanently. Only materials with conduction electron density less than 10^{20} electrons / cm^3 and ion mobility less than 10 cm^2 /volt-sec meet these requirements. This explains why metals (electron density 10^{22} to 10^{23} / cm^3) and semiconductors are not useful as track recording solids. In the case of ***polymers,*** which are much more sensitive to ionsing radiation, the bond-breaking or "scission" of long chain molecules which requires 1-3 eV energy, is mainly responsible for the formation of latent tracks. Scission leads to formation of molecules of smaller length and increased reactivity. It is obvious that the primary physical interaction of radiations with these SSNTDs produces specific damages such as chemical bond scission, free radicals and consecutive cross linking [S. Nouh et al. 1998**].** The efficiency of these changes produced in SSNTDs depends on the structure of the polymer as well as on the experimental conditions of irradiation [R. Mishra et al. 2003].

2.4.4.2 Track development

The quality of information that can be extracted from the tracks depends on how well we can develop the latent tracks and make quantitative measurements on the track profile. 'Developing' or etching the tracks in a given detector depends on a variety of conditions such as the nature of chemical etchant, its concentration, temperature, presence of etch products etc. The underlying principle is that the damage trails, being of a disordered structure are associated with large free energy and are, therefore, preferentially attacked. As in the development of photo prints, there is as much art in track-etching as science.

Etching increases the diameter of the damage trails to micron range comparable to the wavelength of the visible light. When viewed under transmitted light using an optical microscope, these tracks scatter light and show up as dark lines, cylinders, cones or circles.

Etching is done by immersing the detector in the etchant solution for a specified length of time and at a specified temperature. The etchant dissolves not only the damaged portions of the detector (along the damage trail) but also the bulk material. It should be remembered here that all the latent tracks cannot be developed unless certain basic conditions are satisfied. Development of a track for visual observation as well as the nature and shape of the track (track profile) depends on a number of parameters such as: (a) the track-etch rate, V_t, along the track (b) the bulk-etch rate, V_b, along the bulk material and (c) the angle of incidence, Q, of the particle with respect to the detector surface. The films exposed to radiation source are etched in chemical etching bath made of double jacketed glass vessel as shown in Figure 2.15. connected to a constant temperature water bath. The bath is provided with a thermometer, hot water jacket, stainless steel holder and a magnetic stirrer. The apparatus is filled with etchant and heated by external circulation of hot water through the jacket. Once the desired temperature is achieved, the samples are introduced in the solution with a care that whole detector is immersed properly. Constant stirring is used during etching so that the probability of etch products remaining on the detector surface and forming a protective layer was reduced [H.A. Khan, 1973]. During the etching time, the beaker with solution is kept covered so as to avoid the change in concentration of the solution due to evaporation. After etching for fixed time, the samples are taken out and washed firstly under running water and then with distilled water. Finally the samples are air-dried and mounted on glass slide for counting under an optical microscope.

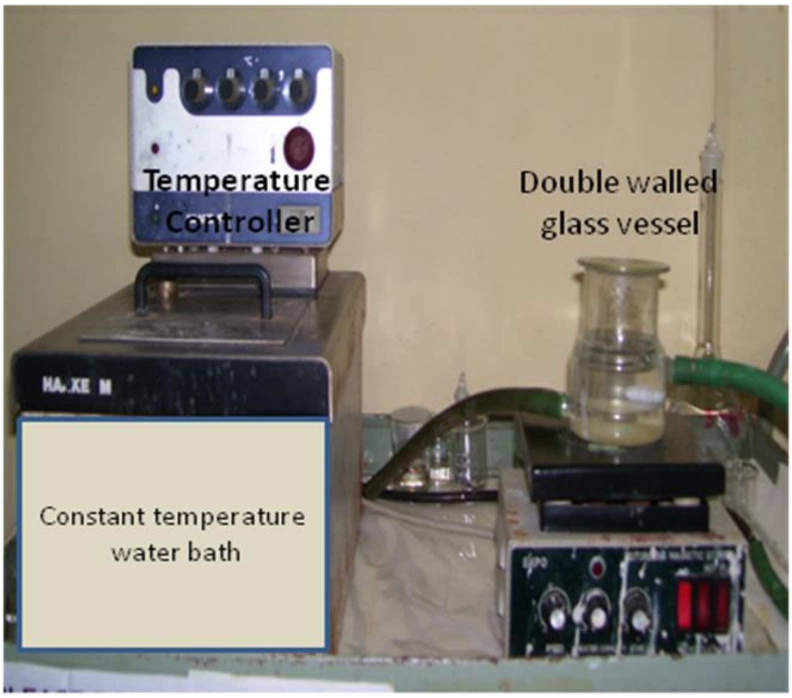

Figure 2.15. Chemical etching setup used in the present work.

CHAPTER 3 PHOSPHATE-BEARING POLYMER GRAFTED GLASS FOR PLUTONIUM (IV) ION-SELECTIVE ALPHA SPECTROMETRY

3.1. Introduction

Actinide monitoring at ultratrace concentrations in aqueous, biological, and geological samples is often required for health physics, nuclear forensics, waste discharge regulation, detection of accidental leaks and migration in the environment, etc. [H. Hernandez-Mendozaet et al. 2011, C. Li et al. 2008, J. Zhenget et al. 2013, S. F. Boulygaet et al. 2001]. There are many methods, such as mass spectrometry, α-spectrometry, solid state nuclear track detection and liquid scintillation counting, that have been used for quantifying Pu in a variety of aqueous and leach liquor samples. Radiometric methods used for the quantification of transuranic nuclides have recently been reviewed by Vajda and Kim, [N. Vajda et al. 2011] Qiao et al. [J. Qiao et al. 2009] and Zheng et al. [J. Zhenget et al. 2013]. It is known from these published reviews that these methods have analytical merit for the quantification of actinides, but often need a purification step. Alpha spectrometry is commonly used for the quantification of Pu in aqueous samples. Recently, the applications of the alpha spectrometric determination of alpha-emitting isotopes in nuclear, environmental and biological samples have been reviewed by Aggarwal [S. K. Aggarwal et al. 2016]. In general, this method requires Pu separation using an anion-exchange column, followed by thin sample source preparation by commonly used methods such as evaporation, micro-precipitation or electrodeposition on a metal disc [N. Vajda et al. 2011]. There are other hyphenated methods for Pu determination in aqueous samples, such as cloud point extraction and automated column extractions that can be coupled to α-spectrometry [C. Labrecqueet et al. 2013, N. Gu´erinet et al. 2011, N. Vajda et al. 2009]. Extractant- filled membranes have been reported for Pu sample introduction in thermal ionization mass spectrometry (TIMS) [S. Paul et al. 2016]. However, this method cannot be used for alpha spectrometry, which requires a thin sample source. Thin polymer film-based α-spectrometry has the possibility to combine the sample purification and source preparation steps. For Pu determination by α-spectrometry, thin films of quaternary amine-bearing polymers, [S. J. M. Mannionet et al. 2016] Kl¨aui ligand thin films, [S. K. Hansonet et al. 2014] and polymer ligand films are formed on glass or silicon substrates using dip-coating or spin-casting methods. [J. H. Rimet et al. 2016, V. Chavanet et al. 2013] For direct α-spectrometry of a liquid, a thin film of polymer containing extractant is formed on the surface of passivated silicon diodes. [Q. T. Tranet et al. 2014, R. S. Addlemanet et al. 2005] A thin polymer surface grafted membrane has also been developed for Pu^{4+} ion determination by alpha spectrometry. [S. Paul et al. 2015] Recently, thin films functionalized with *P,P*′-di(2-ethylhexyl)methane-di-phosphonic acid (DIPEX) have been reported for the alpha spectrometric determination of Pu ions and colloidal Pu in water samples containing trace levels of plutonium [H. Boukhalfaet et al. 2017]. In the present work, a phosphate-bearing thin film has been grafted on the surface of glass substrates. Organophosphorus groups are known for their affinity toward actinide ions. The thin film formed on a glass substrate by the photo-initiator-induced polymerization of 3-(trimethoxysilyl)propyl acrylate and bis[2-(methacryloyloxy)ethyl] phosphate monomers has been characterized by atomic force microscopy (AFM), energy dispersive spectrometry (EDS) attached to a scanning electron microscope, and alpha radiography by a solid state nuclear track detector. The chemical affinity of the phosphate-bearing thin film toward Pu^{4+} ions has been studied in the presence of representative competing ions such as Am^{3+}, Th^{4+} and UO_2^{2+}. The phosphate-bearing thin polymer film grafted glass substrate has been examined for its analytical merits in the α-spectrometric determination of Pu^{4+} ions in a variety of aqueous samples.

3.2. Experimental

3.2.1. Reagents and apparatuses

The details of reagents and apparatus used are given in Chapter 2.

The micro-concavity glass slides used in present work were obtained from Polar industrial corporation (cavity diameter- 15mm, Depth of cavity- 0.5mm), see Figure 3.1.

Figure 3.1. Micro-concavity glass slide used for surface grafting.

The stock solution of Pu was obtained from the Radiochemistry Division, BARC, Mumbai, India having isotopic composition (At. %) as ^{238}Pu (0.16 ± 0.006), ^{239}Pu (68.79 ± 0.03), ^{240}Pu (26.94 ± 0.03), ^{241}Pu (2.09 ± 0.005), and ^{242}Pu (2.02 ± 0.006). The stock solution was purified by the standard anion-exchange column method to remove ^{241}Am ions. The α-activity was measured with a home-built liquid scintillation counter, and alpha spectrometer equipped with a passivated ion-implanted planar silicon (PIPS) detector (Canberra, PD-450-16-100AM) with an area of 450 mm^2 and a resolution of 16 keV (FWHM) at 5.486 MeV of ^{241}Am connected to a multi-channel analyser (Given in Chapter 2).

3.2.2. Experimental

The experimental details are given in chapter 2. Briefly, grafting of the polymer film was done on micro-concavity glass slides with a cavity diameter of 15 mm and depth at centre of 0.5 mm. The glass slides were treated with piranha solution (H_2O_2 : H_2SO_4 (1 : 3 v/v)) for 1 h, followed by overnight immersion in ethanol. After these treatments, the microcavity of the glass slide was filled with 50 µL of a polymerizing solution consisting of 0.2 mol L^{-1} 3-(trimethoxysilyl)propyl acrylate (TMSPA), 0.4 mol L $^{-1}$ bis [2-(methacryloyloxy)ethyl] phosphate (BMEP) and 2 wt% (with respect to TMSPA + BEMP wt) of the UV-initiator α, α'-dimethoxy-α-phenylacetophenone (DMPA) dissolved in DMF, and irradiated with 365 nm UV light in a box-type UV multilamp photoreactor (Heber Scientific, Chennai, India) for 30 min. After grafting, the glass slides were washed with a water/DMF mixture at 35–40^0 C to remove the un-polymerized components and dried under vacuum.

3.2.3. Substrate characterizations

Elemental mapping of the C and P atoms was carried out with a MINI-SEM (SEC Global, Singapore) equipped with a Bruker EDX analyzer. The physical topography of the thin film formed on the glass substrate was studied by atomic force microscopy (AFM). Alpha track radiography was carried out by registering the alpha tracks in the CR-39 detector kept in a 2π geometry on Pu^{4+}-loaded glass@poly(BMEP). The alpha tracks in the CR-39 detector were developed by chemical etching with 6 mol L^{-1} NaOH at 70 C for 5 h. The developed alpha tracks were observed under a transmission optical microscope (Olympus fully motorized microscope model no. BX63, attached with a QIMAGING QICAM CCD camera and cellSens Dimension Package for image analysis obtained from Olympus, Tokyo, Japan).

3.2.4. Uptake studies

Uptake studies of UO_2^{2+}, Am^{3+}, Th^{4+} and Pu^{4+} ions in glass@poly(BMEP) were carried out as described elsewhere, [S. Paul et al. 2014]. The Pu^{4+} ions uptake study was carried out using grafted glass samples by equilibrating with 3M HNO_3 solution (10 mL). The substrate was equilibrated with solution for 4 h. The amounts of Pu^{4+} loaded in the glass substrate was quantified using liquid scintillation counting of aqueous samples (100 µL) taken from solution before and after equilibration of the glass substrates. The sorption efficiency (uptake) of actinide in the glass was obtained from following equation:

$$\text{Uptake (\%)} = [A_b - A_f] / [A_b] \times 100$$

where A_b and A_f are radioactivity (scintillation count rate) of Pu(IV) in the solution before and after equilibration of grafted glass, respectively. The sorption experiments were carried out by stirring the solution for a fixed period of time, and the percentage uptake of Pu(IV) as a function of time was monitored. The Pu loaded glass substrate then washed with 3M nitric acid to remove loosely bound activity on the glass surface and checked for loose contamination. The plutonium loaded thin film glass substrates were monitored at 2 cm source to detector distance by alpha spectrometer equipped with a passivated ion-implanted planar silicon (PIPS) detector, having a resolution of 16 keV (FWHM) at 5.486 MeV, of ^{241}Am connected to a multi-channel analyzer. In order to confirm Pu preconcentration at cavity only, cavity was covered, then by recording the alpha spectrum of front and back surfaces.

The UO_2^{2+}, Am^{3+}, Th^{4+} uptake study was carried out using grafted glass samples by equilibrating with 3M HNO_3 solution (10mL). The substrate was equilibrated with solution for 4 h. The amounts of UO_2^{2+}, Am^{3+}, Th^{4+} loaded in the glass substrate was quantified using liquid scintillation counting of aqueous samples (100 μL) taken from solution before and after equilibration of the glass substrates. Also the uptake of plutonium was studied in presence of uranium at 3M HNO_3. For this the uranium loaded glass was equilibrated with the plutonium solution.

3.2.5. Isotope dilution alpha spectrometry

The analytical applications of glass@poly(BMEP)-based α-spectrometry were studied using Pu-spiked seawater and ground water samples. For the quantification of Pu, an isotope dilution technique involving ^{238}Pu as a spike isotope was used to account for unknown variations in the chemical recovery (uptake) and counting efficiency (intrinsic and geometrical) [S. Paulet et al. 2015]. In this method, a weighed amount of pre-calibrated ^{238}Pu spike solution was added to a weighed amount of the sample. The mixture was treated with conc. HNO_3 for homogeneous mixing of the spike isotopes with the sample, followed by treatment with 3 mol L $^{-1}$ HNO_3 and 20% H_2O_2 to adjust the Pu oxidation state to Pu^{4+}. The aqueous samples were equilibrated with glass@poly(BMEP) for 2 h with continuous stirring. After equilibration, the glass@poly(BMEP) substrates were washed thoroughly with 3 mol L

$^{-1}$ HNO_3, dried and placed directly in front of a passivated ion-implanted planar silicon detector coupled to a PC-based 8K-MCA, to record the alpha spectra. The spectral analyses were carried out using PCA3 software. The Pu concentration in the natural water samples was determined from the change in the ^{238}Pu/(^{239}Pu + ^{240}Pu) alpha activity ratio in the mixture, with respect to that in the sample and the ^{238}Pu spike, using the equation given in a publication [S. Paul et al. 2015].

3.3. Results and discussion

The chemical steps involved in the formation of the monoacidic phosphate group-bearing thin polymer film on a glass substrate are shown in Scheme 3.1. It can be seen from Scheme 3.1 that the polymer film formed by UV-initiator-induced graft polymerization was covalently linked to the glass substrate via coupling of the polymerizable alkoxysilane monomer, TMSPA. The mole proportion of BMEP : TMPSA was kept as 2 : 1. The physical topography of the poly(BMEP) film was examined by AFM, and representative AFM image is shown in Figure 3.2a. It was seen from the AFM images that the poly(BMEP) film formed on the glass substrate had very few defects forming pin-holes as shown in Figure 3.2a. The thickness of the film was obtained from the pin-holes as 10–15 nm. Elemental mapping of the C and P atoms by EDS showed a uniform distribution of the phosphate groups on the polymer thin film formed on the glass substrate, see Figure 3.2b.

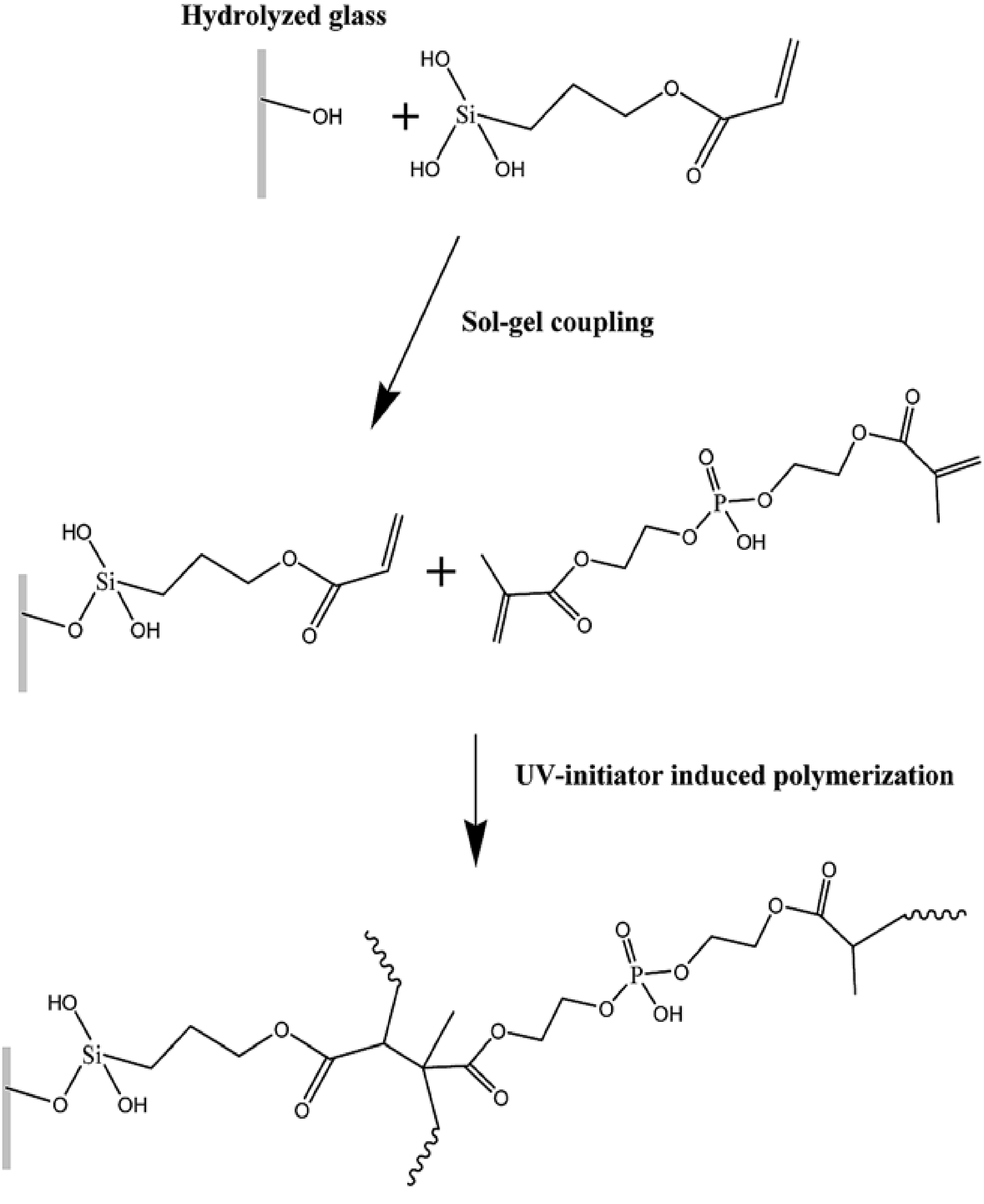

Scheme 3.1.Representative chemical reactions involved in the formation of thin poly(BMEP) film on a glass substrate.

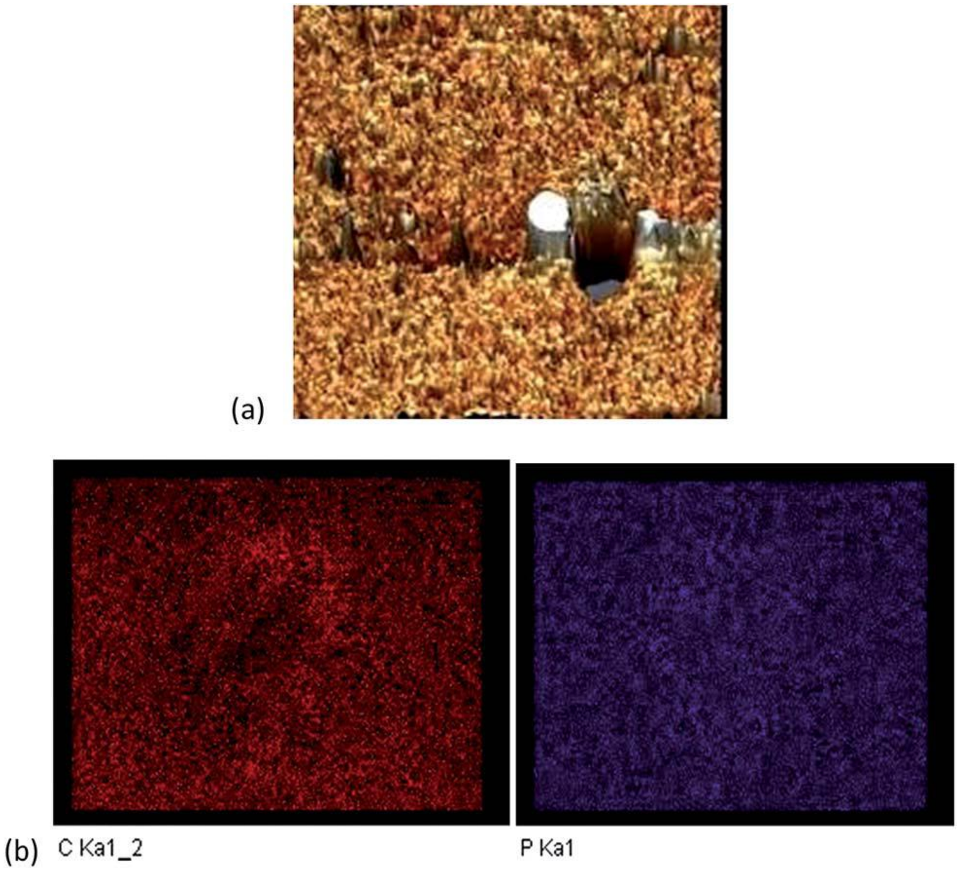

Figure 3.2. AFM image (x = 2.6 µm, y = 2.6 µm and z = 10.4 nm) (a) and elemental mapping of C and P in the 10 × 10 µm grafted area of the microcavity on a glass slide using EDS (b).

The Pu^{4+} ions in glass@poly(BMEP) were loaded from the solution of 3 mol L^{-1} HNO_3. Alpha track radiography of Pu^{4+}-loaded glass@poly(BMEP), shown in Figure 3.3, suggested that Pu^{4+} ions bonded with phosphate groups were uniformly distributed in the CR-39 detector exposed to the poly(BMEP) grafted region. It is evident from the α-spectrum given in Figure 3.4 that the characteristic α-energy peaks of $^{239,240}Pu$ and ^{238}Pu in the alpha spectrum recorded from Pu^{4+}-loaded glass@poly(BMEP) were well resolved without any significant tailing, and were similar to those of the electrodeposited Pu source. This indicated clearly that there was no significant loss of energy of the alpha particles emerging from the poly (BMEP) matrix.

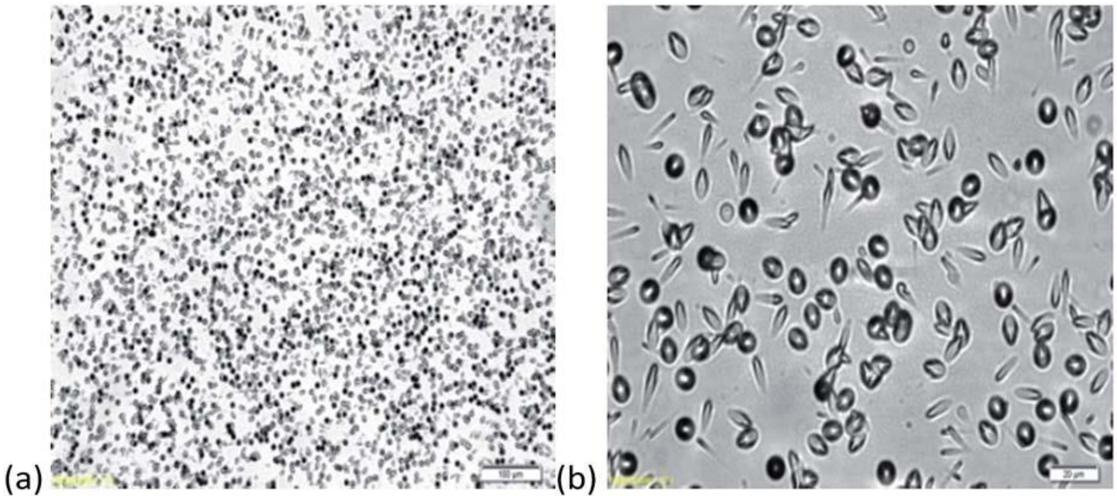

Figure 3.3. Alpha track radiography of Pu^{4+}-loaded glass@poly (BMEP) under 10x (a) and 40x (b) magnifications.

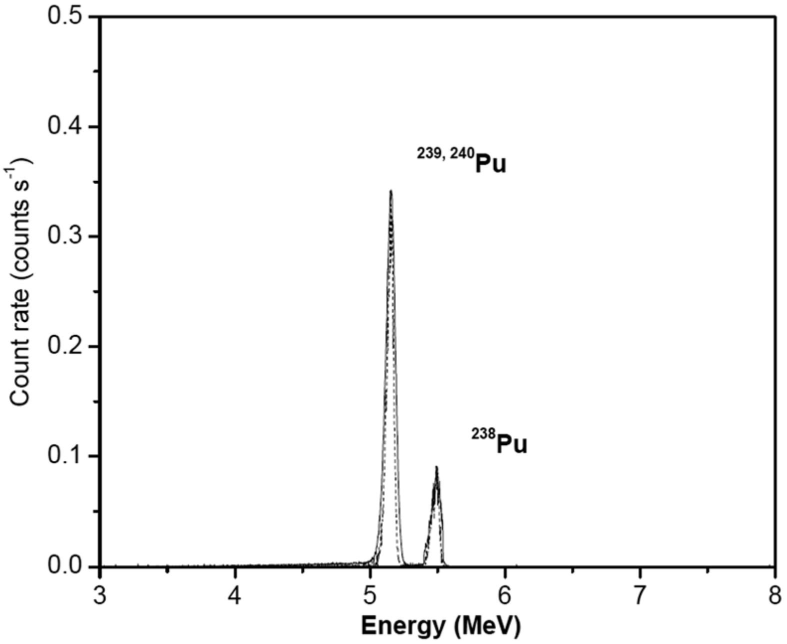

Figure 3.4. Alpha spectrum recorded from the Pu^{4+}-loaded glass@-poly (BMEP) sample (dotted line) and Pu electrodeposited on a stainless steel planchette (solid line) in an equivalent amount.

The control experiment showed that 10–15% of the Pu^{4+} ions were sorbed in the piranha solution-treated glass slide. However, silanization of the glass slide with dimethyldichlorosilane prevented sorption of the Pu^{4+} ions, and the slide could be grafted with poly(BMEP). It was reported that the diacidic phosphate-bearing poly(ethylene glycol methacrylate phosphate) gel sorbed UO_2^{2+} and Pu^{4+} ions from 3 mol L $^{-1}$ HNO_3 solution quantitatively, but not Am^{3+} ions [S. Chappa et al. 2016, T. Vasudevanet et al. 2009]. In the present work, a highly cross-linked polymer with monoacidic phosphate groups was formed, which was expected to exhibit similar behaviour. This was based on the fact that only one ligating site of the phosphate group, either P=O or –OH, participates in the formation of a complex with Pu^{4+} ions due to geometrical constraints [S. Chappaet et al. 2016]. This was confirmed by the formation of a gel of the monomers BEMP and TMSPA by UV-initiator-induced bulk polymerization in a similar 2 : 1 mole proportion. Uptake studies in poly(BMEP-TMSPA) from 3 mol L $^{-1}$ HNO_3 solution showed the expected sorption trend, i.e. the sorptions of Pu^{4+} (95 ± 2%) and UO_2^{2+} (80 ± 2%) ions were quantitative in the 100 mg poly(BMEP-TMSPA) gel sample, but Am^{3+} ions did not sorb quantitatively (<9%) under similar conditions. However, the sorption of all these representative actinide ions in the poly (BMEP-TMSPA) gel from 0.3 mol L $^{-1}$ HNO_3 solution was quantitative (Pu^{4+}= 94%, UO_2^{2+}= 86% and Am^{3+}= 85%). This seems to suggest that poly (BMEP) has an acidity-dependent selectivity toward Pu^{4+} ions. This trend was further confirmed in the present case by recording the alpha spectra from glass@poly(BMEP) samples equilibrated with 3 mol L $^{-1}$ solution containing one of $^{mix}Pu^{4+}$, $^{241}Am^{3+}$, $^{229}Th^{4+}$ or $^{233}UO_2^{2+}$ ions. The alpha spectra showed a trend similar to that observed in the bulk gel. Quantitative characteristic alpha energy peaks were observed in the cases of $^{mix}Pu^{4+}$, $^{229}Th^{4+}$ and $^{233}UO_2^{2+}$ ions, but not in the case of Am^{3+} ions, even at pH = 2, as can be seen from the alpha spectra given in Figure 3.5.

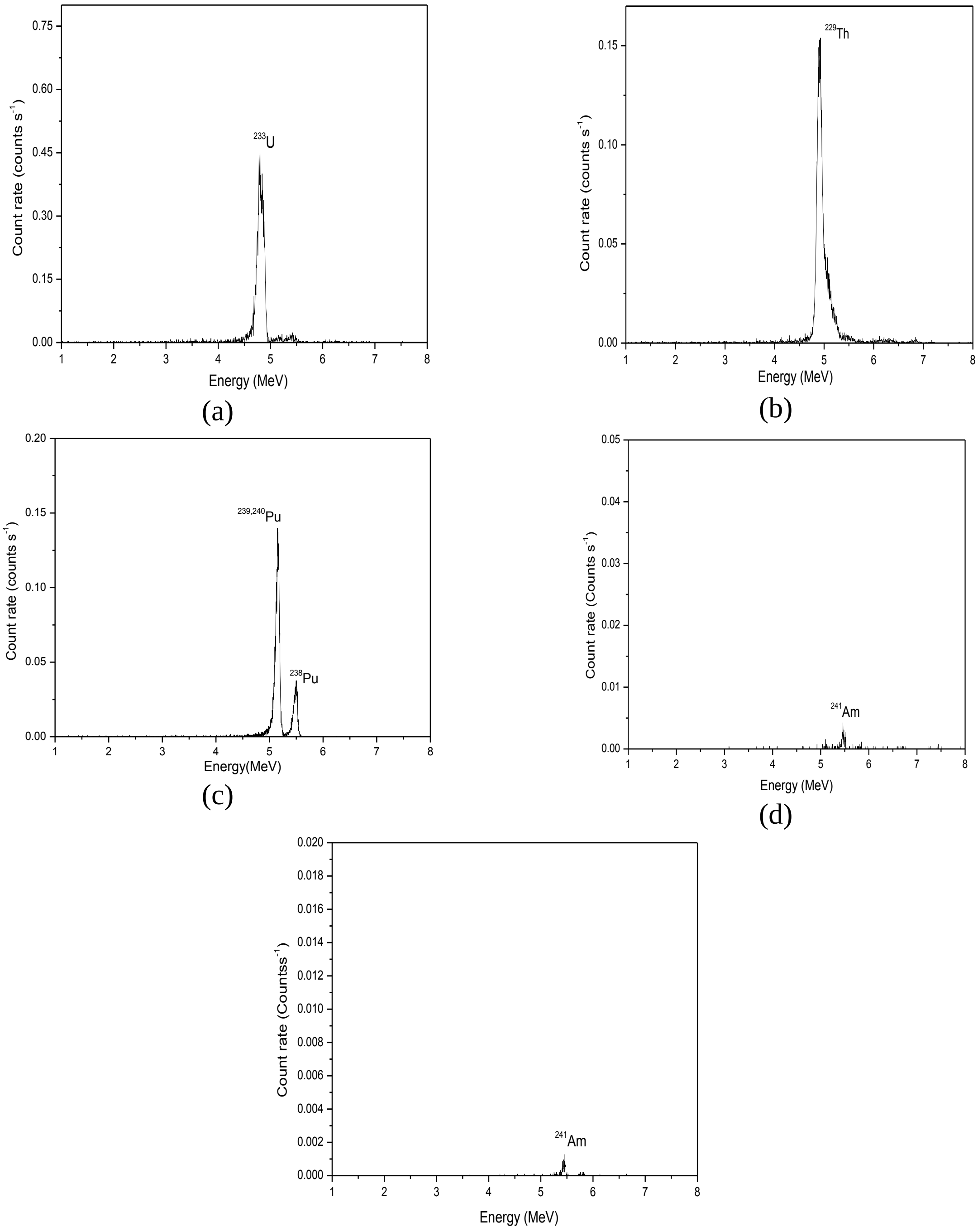

(a) (b)

(c) (d)

(e)

Figure 3.5. The alpha spectra recorded from the glass@poly(BMEP) samples equilibrated with 3 mol L^{-1} HNO_3 containing either of UO_2^{2+} (a), Th^{4+} (b), Pu^{4+} (c) or Am^{3+} (d) ions, and solution having pH=2 and containing Am^{3+} ions (e).

Thus, glass@poly(BMEP) seems to be more selective toward Pu^{4+} ions with respect to Am^{3+} ions in 3 mol L $^{-1}$ HNO_3 as compared to the bulk gel. This could be attributed to the presence of a large number of binding sites in close proximity in the bulk gel as compared to the thin poly(BMEP) film. To examine the sorption of Pu^{4+} ions in a competing mode, glass@poly(BMEP) was equilibrated with 3 mol L $^{-1}$ HNO$_3$ solution containing a 3 times higher alpha activity of ^{233}UO$_2^{2+}$ ions (6.6 x 10^5 counts min ^{1}) than that of ^{mix}Pu^{4+} ions (2.2 x 10^5 counts min $^{-1}$). It was seen from the alpha spectrum given in Figure 3.6 that the count rate for ^{233}U was 18 times less than that for ^{239,240}Pu. This could be attributed to suppression of the sorption of UO$_2^{2+}$ ions due to the preferential sorption of Pu^{4+} ions in the competing mode. The preferential sorption of Pu^{4+} ions in the competing mode was examined by loading ^{233}UO$_2^{2+}$ ions in glass@-poly(BEMP) from 3 mol L $^{-1}$ HNO$_3$ and equilibrating with 3 mol L $^{-1}$ HNO$_3$ containing Pu^{4+} ions. The alpha spectra were recorded before and after equilibration of UO$_2^{2+}$-loaded glass@-poly (BMEP) with Pu^{4+} ions. It was obvious from the alpha spectra given in Figure 3.7 that the UO$_2^{2+}$ ions were replaced by Pu^{4+} ions quantitatively, suggesting a higher affinity of glass@-poly(BMEP) toward Pu^{4+} ions in the case of competition for the available binding sites. It is also seen from the alpha spectra given in Figure 3.7 that the alpha energy peaks of ^{233}U and ^{239,240}Pu overlap with each other, and thus peak fitting analysis would be required to segregate the regions of interest of the peaks.

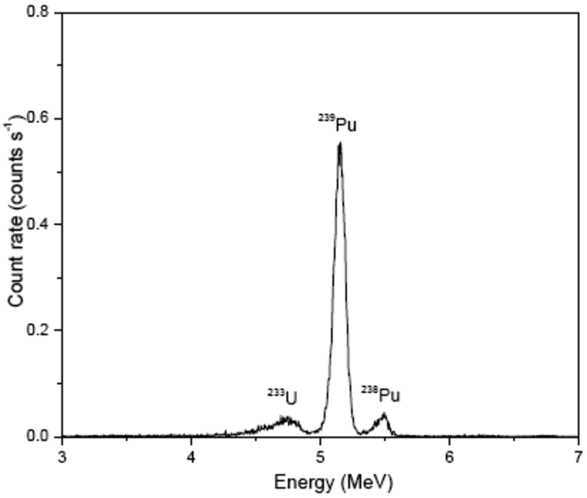

Figure 3.6. Alpha spectrum obtained from glass@poly (BMEP) equilibrated with 3 mol L $^{-1}$ HNO$_3$ containing ^{233}UO$_2^{2+}$ and ^{mix}Pu^{4+} ions in a 20: 1 mole proportion.

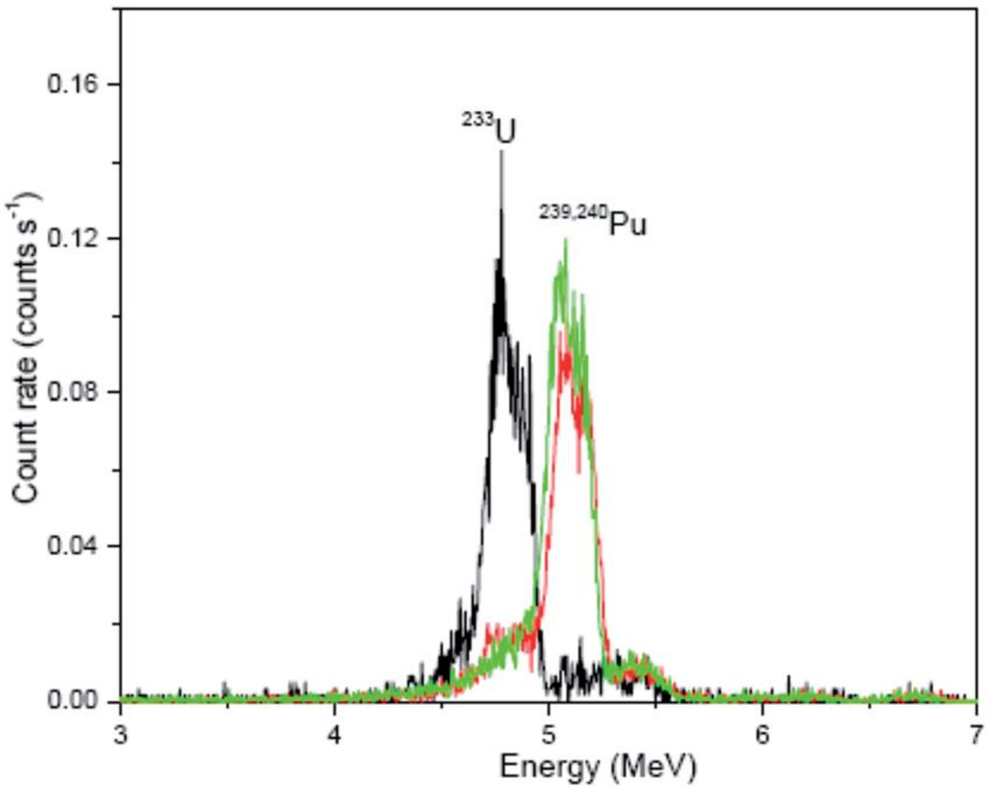

Figure 3.7. Alpha spectra of $^{233}UO_2^{2+}$-loaded glass@poly(BMEP) (black) and after equilibration in 3 mol L $^{-1}$ HNO_3 containing Pu^{4+} ions for 1 h (red) and 2 h (green), indicating quantitative replacement of the $^{233}UO_2^{2+}$ ions with Pu^{4+} ions from the binding sites.

It was observed that Pu^{4+} ions were also preferentially sorbed in glass@poly (BMEP) in the presence of Th^{4+} ions under similar conditions. The variation of HNO_3 concentration indicated that Pu^{4+} ion sorption remains unaffected from 1–6 mol L $^{-1}$ conc. in the presence of 20 times excess of UO_2^{2+} ions, see Figure 3.8.

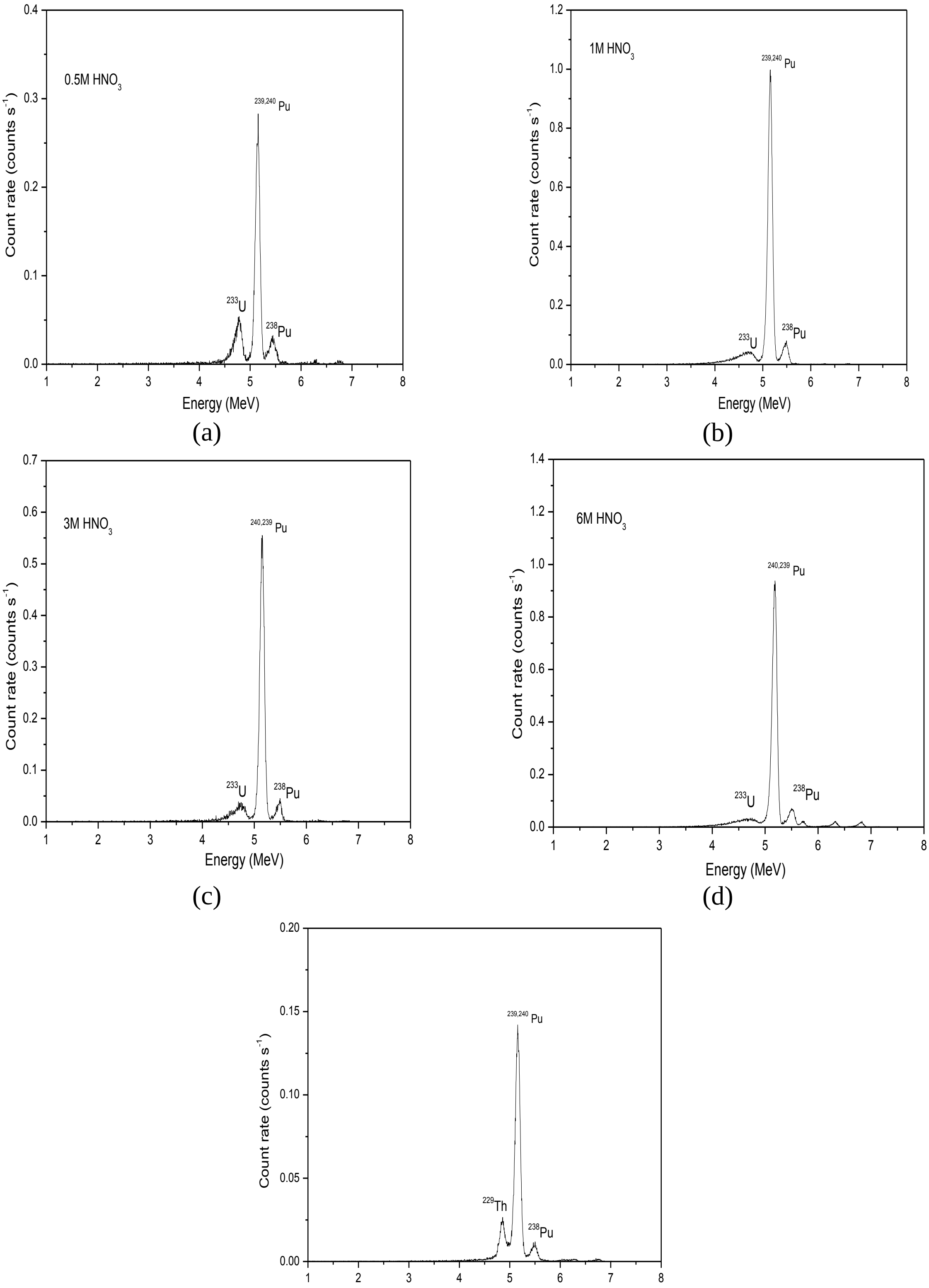

(a) (b)

(c) (d)

(e)

Figure 3.8. Alpha spectra obtained from the glass@poly(BMEP) samples equilibrated with 0.5-6 mol L^{-1} HNO$_3$ containing ^{233}UO$_2^{2+}$ and ^{mix}Pu^{4+} ions in 20:1 mol proportion (a-d), and 3 mol L^{-1} HNO$_3$ containing Th^{4+} and ^{mix}Pu^{4+} ions (e).

The kinetics of Pu^{4+} sorption in glass@poly (BMEP) from 3 mol L $^{-1}$ HNO_3, shown in Figure 3.9 indicated that 95%.sorption was reached in 6 h under constant stirring, and sorption became very slow thereafter.

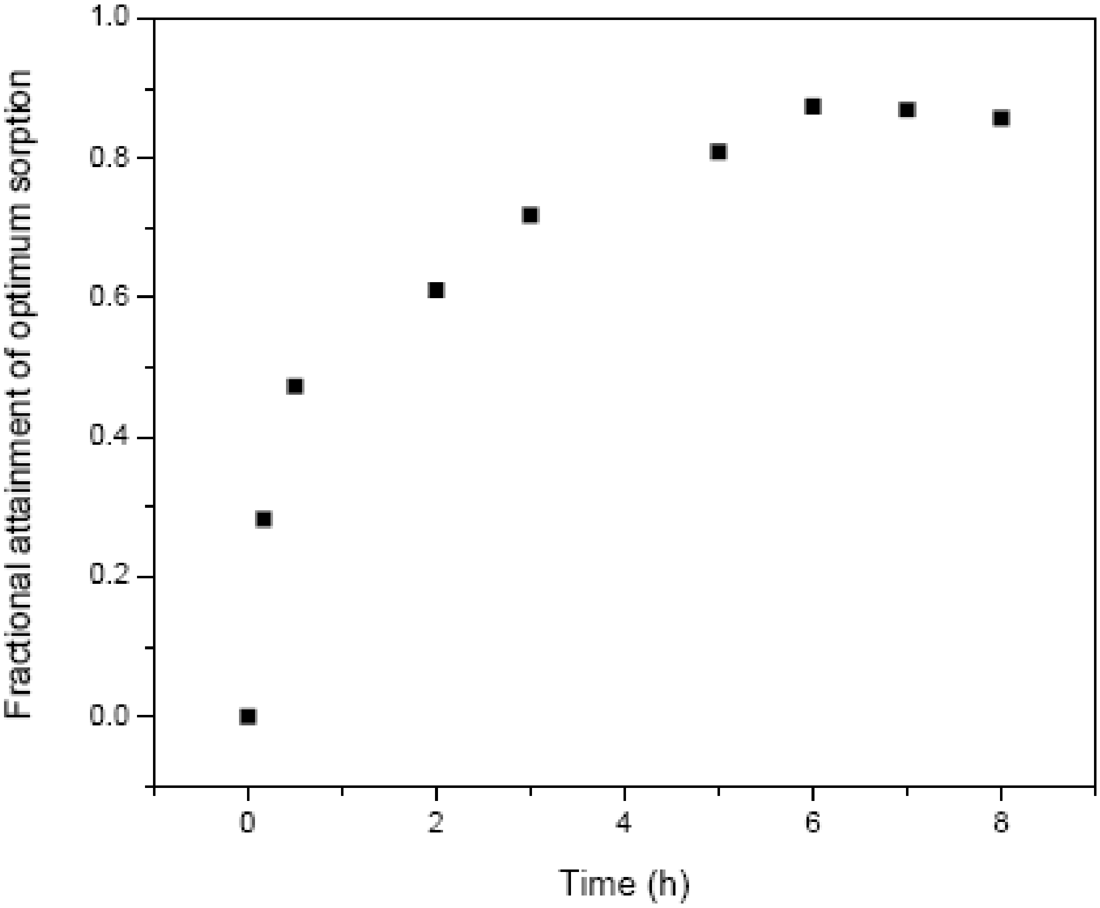

Figure 3.9. Pu^{4+} ions fractional attainment of the optimum sorption in the glass@poly (BMEP) from 3 mol L^{-1} HNO_3.

To examine the consistency of the Pu^{4+} sorption efficiency as a function of its concentration, glass@poly(BMEP) samples were equilibrated with solutions containing 0.2 to 10 ppb Pu^{4+} in 10 mL of 3 mol L $^{-1}$ HNO_3. Alpha spectrometry of these samples showed a linear increase in the count rate as a function of Pu concentration in the equilibrating solution, see Figure 3.10.

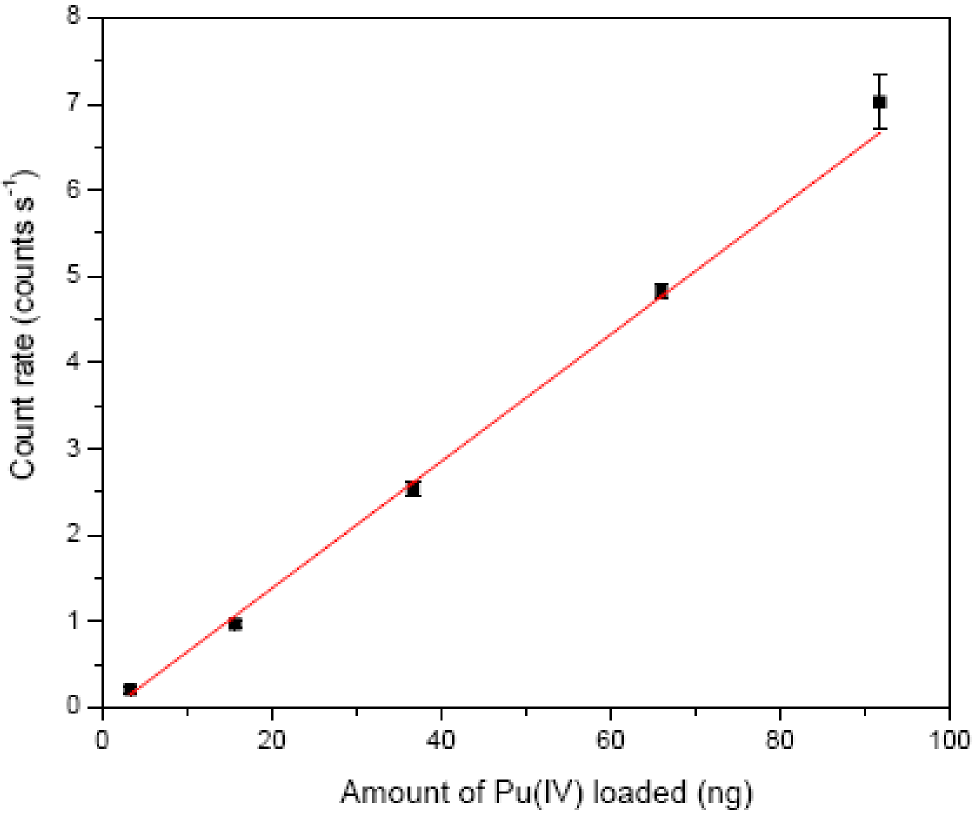

Figure 3.10. Linear variation of alpha count rate obtained by alpha spectrometry of the glass@poly (BMEP) equilibrated with solution having 0.2 to 10 ppb Pu4+ in 3 mol L-1 HNO3.

This seems to suggest that a constant Pu (IV) sorption efficiency was maintained over a wide concentration range from 0.2 to 10 ppb Pu^{4+} in 3 mol L $^{-1}$ HNO_3. The minimum detection limit of Pu by glass@poly(BMEP)-based alpha spectrometry was calculated using the counting efficiency of the detector and the radioactivity measurement limit of detection in counts, which is determined at a 95% confidence level using the Curie equation, [L. A. Currie et al. 1968]. The minimum detectable activity (MDA) for the radionuclide detection by instrumental method can be obtained by following equation:

$$MDA = \frac{Ld}{t \times \varepsilon}$$

Where is MDA is minimum detection limit (Bq) t is counting time (3646 s), is detector efficiency (2%), and Ld is the radioactivity measurement limit of detection in counts, which is determined at the 95% confidence level and obtained by Curie equation, [L. A. Currie et al. 1968] as given below:

$$Ld = 4.653\sqrt{C_b t} + 2.706$$

Where C_b is background count rate (0.572 cps). Using these equations the value of MDA was found to be 2.95 Bq. The minimum amount of Pu required in the glass@poly(BMEP) could be obtained as 1.25 ng using specific activity of Pu having isotopic composition used in the present work. Thus, 1.25 ng Pu has to be preconcentrated in the glass@poly(BMEP) from the appropriate volume of liquid samples.

From this calculation, it was observed that a minimum preconcentration of 2.95 Bq Pu activity in the glass@poly(BMEP) film was required for its detection. The concentration of Pu measured was found to be reproducible within 6% in triplicate measurements using different glass@poly(BMEP) samples for the preconcentration of Pu^{4+} ions from 3 mol L^{-1} HNO_3. The Pu^{4+} ions preconcentrated in glass@poly(BMEP) could be de-sorbed with 0.2 mol L^{1} hydrazine hydrate and hydroxylamine in 1 mol L^{-1} HNO_3 a er two equilibrations, and glass@poly(BMEP) could be reused for Pu^{4+} ion sorption, as shown in Figure 3.11.

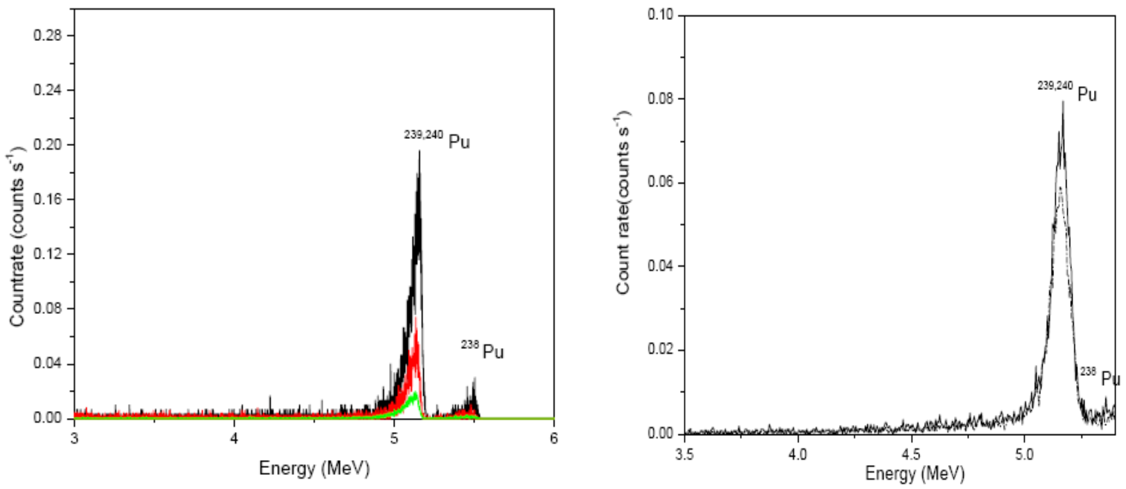

(a) (b)

Figure 3.11. (a) alpha spectrum of Pu^{4+} loaded glass@poly(BMEP) (black line), and alpha spectra after equilibration in 0.2 mol L^{-1} hydrazine hydroxyl amine in 1 mol L^{-1} HNO_3 after 2h (red) and 5 h (green), (b) and reloaded with Pu^{4+} ions.

A single equilibration in 0.2 mol L^{-1} hydrazine and hydroxylamine in 1 mol L^{-1} HNO_3 for 5 h brought about a tenfold reduction in the Pu count rate, but multiple (2–3 times) equilibrations were needed to completely desorb the residual Pu^{4+} ions from glass@poly(BMEP). The glass@poly (BMEP) substrate was successfully used with three reloading cycles of Pu^{4+} ions without a significant reduction in the expected count rate. Thus, the regeneration of glass@-poly (BMEP) would minimize analytical waste handling. For studying its analytical applications, glass@poly (BMEP)-based a-spectrometry was applied to ground water and seawater samples spiked with a known quantity of Pu. An isotope-dilution technique was used to quantify the amount of Pu in these samples, as it could account for the unknown variation in the sorption efficiency and counting parameters (geometry and detector efficiencies, etc.). The Pu concentrations in these natural water samples were determined from a change in the $^{238}Pu/(^{239}Pu + ^{240}Pu)$ alpha activity ratio in the mixture with respect to that in the sample and ^{238}Pu spike. [S. Paul et al. 2015].The Pu concentration in the natural water samples was determined from the change in $^{238}Pu/(^{239}Pu+^{240}Pu)$ alpha activity ratio in the mixture, w.r.t. that in the sample and the ^{238}Pu spike, using the following equation.

$$C_{sa} = \frac{C_{sp}W_{sp}}{W_{sa}} \frac{(R_{sp}-R_m)}{R_{sp}(R_m-R_{sa})} \frac{(\lambda_{238}AF_{238})_{sp}}{(\lambda_{239}AF_{239})_{sa}+(\lambda_{240}AF_{240})_{sa}} \frac{<At.Wt.>_{sa}}{<At.Wt.>_{sp}}$$

Where, C_{sa} and C_{sp} are the concentration and W_{sa} and W_{sp} are the weight of the sample and ^{238}Pu spike, respectively. R_{sa}, R_{sp} and R_m are $^{238}Pu/(^{239}Pu+^{240}Pu)$ alpha activity ratios in the sample, spike and spiked mixture, respectively. The Pu concentrations in the seawater and groundwater sample were found to be 15.14 ± 0.86 ppb and 16.65 ± 0.94 ppb, respectively. which were in good agreement with the values obtained by thermal ionization mass spectrometry, see Table 3.1.

Table 3.1. Comparison of determinations of Pu contents in spiked natural water samples using glass@poly (BMEP) based isotope dilution alpha spectrometry with thermal ionization mass spectrometry. The acidity of sample was adjusted to 3 mol L^{-1} HNO_3 before equilibration with glass@poly (BMEP).

Sample	Pu concentration (ppb)	
	Alpha Spectrometry	TIMS
Seawater	15.14 ± 0.86	15.38 ± 0.62
Groundwater	16.65 ± 0.94	16.45 ± 0.66

3.4. Conclusions

A single-step glass@poly(BMEP)-based isotope-dilution alpha spectrometric method was developed for the quantification of Pu^{4+} ions in 3 mol L^{-1} HNO_3 aqueous samples. The phosphate-bearing thin polymer film was anchored covalently on the glass substrate, which obviated the need for sample purification and source preparation for alpha spectrometry of Pu in solution, and also resulted in achieving a higher preconcentration factor, depending upon the solution sample volume. The other important advantages were minimum radioactive sample manipulation, which minimized radiation exposure to the analyst, low waste generation due to the reusability of glass@poly(BMEP), and it being a one-step process. The glass@poly(BMEP) substrate was found to have reasonably good selectivity towards Pu^{4+} ions with respect to Th^{4+} and UO_2^{2+} ions in a competing mode, and the representative trivalent actinide Am^{3+} did not sorb from 3 mol L^{-1} HNO_3, even in the absence of competing ions. The glass@poly (BMEP)-based isotope-dilution alpha spectrometric method was successfully applied to Pu determination in seawater and ground water samples.

CHAPTER 4. ANCHORING OF PHOSPHATE-BEARING THIN POLYMER FILM ON POLYMER BASED HOST MATRICES FOR U AND PU ANALYSES BY SSNTD

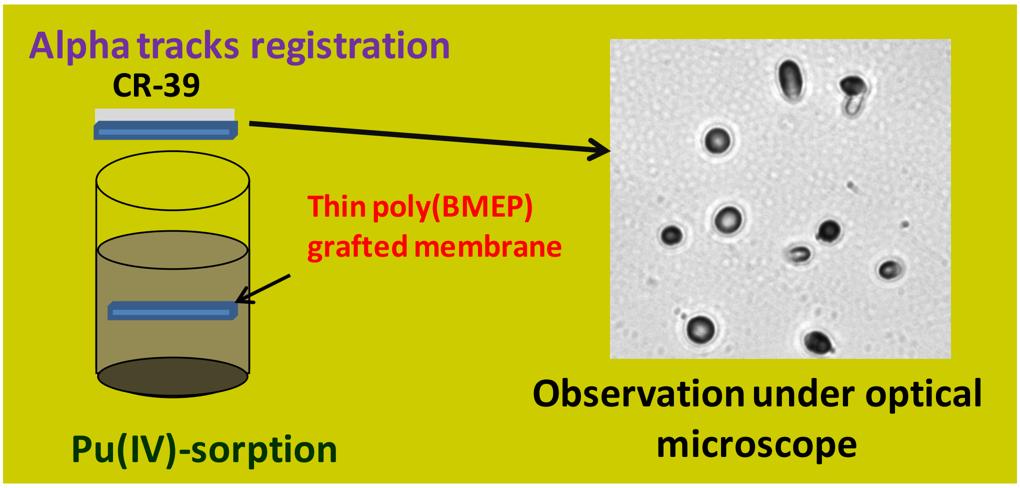

The major objective of the research work carried out in this chapter is to develop thin phosphate ligand polymer film anchored on the host polymer matrix. These substrates can capture higher oxidation state actinides such as UO_2^{2+} and Pu^{4+} ions due to their high affinities toward phosphate function groups. The actinide ions preconcentrated in the phosphate ligand polymer film could be quantified directly using Solid state nuclear track detectors (SSNTDs). This would result in one step process for matrix removal, preconcentration and source preparation. Solid state nuclear track detectors (SSNTDs) based analytical methods are highly sensitive for fissile and alpha emitting nuclides but lack chemical selectivity. This chapter contains the development of chemically selective SSNTD by registering the tracks from the thin phosphate ligand bearing polymer film. For this objective, two types of the hosts were used i.e. poly(ether sulfone) (PES) microporous membrane and non-porous Teflon sheet. Therefore, this chapter has been divided into two sections dealing with the phosphate bearing polymer anchored on the PES membrane (section A (4A)) and Teflon (section B (4B)) using UV radiation and γ-rays based methods, respectively.

The two sections of this chapter are:

SECTION 4A: THIN FILM OF POLY (BIS [2-(METHACRYLOYLOXY) ETHYL] PHOSPHATE) GRAFTED ON SURFACE OF POLY (ETHER SULFONE) MEMBRANE

A thin film of polymer of bis[2-(methacryloyloxy)ethyl]phosphate (poly(BMEP)) has been anchored on the one side surface of poly(ethersulfone) (PES) membrane (poly(BMEP)-grafted PES membrane) by UV-grafting to capture Pu(IV) ions from solution with a high efficiency and subsequent use as a source for registering the particles tracks in CR-39 detector. The SEM images indicated that surface morphology of the poly(BMEP)-grafted PES membrane did not change significantly with respect to the pristine PES membrane, but through-pores size distribution and void volume remained unaffected. It was observed from alpha spectrometry that the alpha peaks corresponding to ^{239,240}Pu and ^{238}Pu were well defined without significant left side tailing which was indicative of a minimum loss of kinetic energy of the alpha particles in the source matrix. The alpha tracks radiography of the Pu (IV)-loaded poly(BMEP)-grafted PES sample indicated homogeneity of poly(BMEP) grafting on the PES membrane. Thus, the alpha tracks density on small area of the CR-39 could be taken as a representative of entire CR-39 area (2x1 cm^2) exposed to the Pu(IV)-loaded poly(BMEP)-grafted PES membrane sample in a 2π contact. The poly(BMEP)-grafted PES membrane sample was found to sorb Pu(IV) ions from the solution having 3 mol L^{-1} HNO_3 conc, and Am(III) ions sorption was negligible under similar condition. This membrane based SSNTD technique was applied to determine the conc. of Pu(IV) ions in the synthetic urine sample spiked with known amount of Pu activity using standard comparison method with a detection limit 0.05 ppb (0.12 Bq mL^{-1}), which could be further improved by preconcentration from a large volume aqueous sample and appropriate blank correction.

SECTION 4B: PHOSPHATE-FUNCTIONALIZED RADIATION-GRAFTED TEFLON

The phosphate bearing polymer thin film has been anchored on Teflon sheet by gamma grafting of poly(glycidyl methacrylate) and reacting subsequently with phosphoric acid under appropriate chemical conditions. This Teflon@phoshate sheet has been characterized by Fourier transform infrared spectroscopy (FTIR), thermo-gravimetric analysis (TGA), and atomic force microscopy (AFM). The uniform distribution of grafted phosphate groups on Teflon has been studied by α-radiography of ^{mix}Pu-loaded and fission tracks distribution in the ^{nat}U-loaded Teflon@phoshate sheets by CR-39 track detector and lexan detector, respectively. The degradation of alpha energy in varying extent of the phosphate bearing polymer thin film grafted Teflon sheets has been optimized by analyzing the shape of alpha particles energies peaks registered from ^{238,239,240}Pu-loaded Teflon@phoshate sheet using alpha spectrometry. Teflon@phoshate sheet exhibit remarkably selectivity toward Pu(IV) ions in solution having higher concentration of HNO_3 (0.5-8 mol L^{-1}) with quantitative sorption, and U(VI), Am(III) ions are sorbed quantitatively only form solution having acidity in a pH range. Teflon@phoshate sheet also takes up U(VI) quantitatively from natural water. Therefore, the Teflon@phoshate sheets have been used for quantitative analyses of Pu(IV) and U(VI) in 3 mol L^{-1} HNO_3 solution and natural water, respectively. The standard comparison method based solid state nuclear track detector based technique has used for the quantifications of Pu(IV) and U(VI) by registering alpha tracks from the ^{mix}Pu-loaded Teflon@phoshate sheet in CR-39 and reactor neutron induced fission tracks from the ^{nat}U-loaded Teflon@phoshate sheet in Lexan plastic, respectively.

SECTION 4A. THIN FILM OF POLY(BIS [2-(METHACRYLOYLOXY) ETHYL] PHOSPHATE) GRAFTED ON SURFACE OF POLY(ETHER SULFONE) MEMBRANE

4A.1 Introduction

The determinations of special nuclear materials such as plutonium and uranium at ultra-trace concentrations (pg) are important for the nuclear forensic and environmental objectives. There are several radioanalytical methods such as scintillation counting, alpha spectrometry, mass spectrometry and proportional counters that can be used for quantifications of Pu in the aqueous samples after subjecting these to appropriate manual/automated procedure for the preconcentration and purification [N Vajda et al. 2011, S Paul et al. 2014, J Eikenberg et al. 2009, J Qiao et al. 2009, A Habibi et al. 2015]. Solid state nuclear track detectors (SSNTDs) are highly sensitive to record trajectory of moving charge particle in the form of latent track which can be revealed by chemical etching for observation the tracks under optical transmission microscope [SA Durrani et al. 1987]. Basically, the track profile and track density are two important parameters obtained from SSNTD that can be used for identification of the registered particles and quantifying the event, respectively [YL Law et al. 2008, PB Price et al. 2005, PB Price et al. 2008, SF Boulyga et al. 1999, R Fleischer et al. 1975].The sensitivity of the SSNTD based techniques has made it possible to measure the fission cross-sections in a nanobarn range and study the exotic radioactive decay [RH Iyer et al. 1991, RH Iyer et al. 1993, SP Tretyakova et al. 1991, SP Tretyakova et al. 2001]. The analytical application of SSNTD is based on recording alpha tracks or neutron induced fission tracks in the solution medium [RH Iyer et al. 1997, V Uma et al. 1980]. The solution medium ensures uniform distribution of nuclides that lead to uniform track density in the detector. Thus, the counting of tracks in the small representative areas could be used for obtaining the tracks density for determining concentration of nuclides by a standard comparison. However, the track registration efficiency is considerably lower in solution media as compared to thin solid source. Unlike alpha spectrometry, it is cumbersome to indentify the alpha particles having different energies based on their track profiles in the detector [OA Bondarenko et al.2000, C Amero et al. 2001]. Thus, the SSNTD based techniques require a chemically selective thin matrix to capture the radionuclides for their unambiguous quantification. However, a combination of alpha spectrometry and fission track analysis can be used for the identification and quantification of the particles [SF Love et al. 1998]. Solid phase extraction has been found to be effective for the selective preconcentration and subsequent direct quantification of the target analyte. This concept has been used to design the highly sensitive radionuclide sensors [V Chavan et al. 2016]. The thin ligand bearing polymer films anchored on mechanically stable polymer support have been reported for the single step chemically selective preconcentration and source preparation methods for alpha spectrometry. Some of these interesting approach involves formation of the chemically selective polymer thin film upon the surface of passivated silicon diodes [RS Addleman et al. 2005], UV-grafting of bifunctional polymer film on membranes [S Paul et al. 2015], thin films of Kläui-type tripodal oxygen donor ligands have been prepared by spin-casting solutions onto the glass substrates [SK Hanson et al. 2014], ultrathin films (10–180 nm) of quaternary amine anion-exchange polymers anchored on the glass and silicon formed by dip-coating [JM Mannion et al. 2016]. In our earlier work, a thin polymer inclusion membrane (PIM) supported on the silanized glass has been developed by physical immobilization of extractant bis-(2-ethylhexyl)-phosphoric acid along with plasticizer tri-(2-ethylhexyl) phosphate [V Chavan et al. 2013]. This PIM supported on glass has been used for the pre-concentration and determination of ultra-trace concentration of actinide ions by α-spectrometry and SSNTDs [V Chavan et al. 2013]. However, the thickness of PIM spin coated on glass substrate is difficult to control, kinetics of actinide sorption is slower, physical bonding of PIM on glass substrate restrict its reusability, and base polymer cellulose triacetate is not stable in high HNO_3 concentration. To overcome this problem, the grafted bifunctional polymer formed by polymerizing the neutral phosphate bearing monomer phosphoric acid 2-hydroxyethyl methacrylate ester and sulphate bearing monomer 2-acrylamido-2-methyl-1-propanesulphonic acid [Paul S et al, 2015]. However, formation of thin bifunctional film was found to be reproducible only under carefully controlled chemical conditions due to solubility reason (AMPS is soluble in polar solvent).

In the present work, these problems have been addressed by using single acidic phosphate bearing monomer for easy grafting, and quantification by SSNTD which is more sensitive to alpha spectrometry and also track density is not affected by the thickness variation in sub-micron range. A thin film of mono-acidic phosphate ligand bearing polymer of bis[2-(methacryloyloxy)ethyl] phosphate (poly(BMEP)) has been anchored on one side of highly porous poly(ether sulfone) (PES) (poly(BMEP)-grafted PES) membrane by UV-grafting. The surface poly(BMEP)-grafted PES membranes have been characterized for the physical structure by scanning electron microscopy, uniformity in grafting by alpha tracks radiography, pore-size distributions by capillary flow porometry, void volume by gravimetry, and loss of kinetic energy of the alpha particle in source matrix by alpha spectrometry. Poly (BMEP) has been found to take up Pu(IV) ions from 3-4 mol L^{-1} HNO_3, and Pu(IV) ions preconcentrated in the poly(BMEP)-grafted PES membrane samples from aqueous samples have been quantified by registering alpha tracks in CR-39 detector kept in a 2π contact. The standard comparison method was used for the quantification using a known amount of Pu (IV)-loaded poly(BMEP)-grafted PES membrane sample having identical dimensions.

4A.2. Experimental

4A.2.1. *Reagents and apparatuses*

The details of reagents and apparatus used are given in Chapter 2.

4A.2.2. Surface grafting

The surface grafting of BMEP on one side of PES membrane was carried out by fixing the 9-cm diameter PES membrane on Petri dish and pouring polymerizing solution (1 mL). The polymerizing solution was made by dissolving BEMP in a mixed solvent containing 1:1 v/v proportion of water and ethanol to keep BMEP conc. as 0.1 mol L^{-1}, and homogenized by ultrasonication for 5 min. The Petri dish containing one-side exposed to polymerizing solution was irradiated with 365 nm light in the UV-photoreactor for 45 min. The grafted membrane, obtained after irradiation, were washed with water ethanol mixture at 35-40°C to remove un-polymerized components and dried in the vacuum oven at 40 - 45 °C for 2-3 h.

4A.2.3. Uptake studies

The Pu(IV)-uptake studies were carried out using grafted PES membrane (2 x 1 cm size) samples by equilibrating with 3 mol L^{-1} HNO_3 solution containing appropriate amount of Pu activity in a 50mL glass beaker kept on magnetic stirrer. The grafted PES membrane was dipped in solution and was stirred with the help of magnetic stir bar for 5 h.The existence of Pu(IV) oxidation state in 3 mol L^{-1} HNO_3 without adding any oxidizing agents such as $NaNO_2$ or H_2O_2 was confirmed electrochemically. This may be because of the presence of HNO_2 in HNO_3. The amount of Pu(IV) in the membrane was quantified by liquid scintillation counting of the aqueous samples (100 µL) taken from solution before and after equilibration of the membrane. The sorption efficiency (uptake) of actinide in the membrane was obtained from following equation:

$$\text{Uptake (\%)} = [A_b - A_f] / [A_b] \times 100$$

where A_b and A_f are scintillation count rates of ^{mix}Pu(IV)/^{241}Am(III)/^{233}U(VI)/^{237}Np in the solution before and after equilibration of membrane, respectively. The concentrations of actinides were in a tracer level. The sorption experiments were carried out by stirring the solution for a fixed period of time, and the percentage uptake of Pu(IV) as a function of time was monitored.

4A.2.4. Alpha tracks registration, revelation and measurements

Alpha tracks were registered from the Pu(IV)-loaded poly (BMEP)-grafted membrane sample (2x1 cm^2 size) in contact with the CR-39 in a 2π contact geometry. After exposure to the Pu(IV)-loaded poly(BMEP)-grafted membrane sample for a fixed period of time, the CR-39 detectors were chemically etched with 6 mol L^{-1} NaOH at 70^{o}C for 5 h to reveal the alpha tracks for observations under optical microscope. The alpha tracks were counted, and the plutonium content in each sample was obtained from the alpha track density by comparison to the track density in the CR-39 exposed to the poly(BMEP)-grafted membrane sample having a known amount of Pu(IV) (standard). The interference from the α-emitting radionuclide in ambient environment such ^{220,222}Rn was minimized by the alpha tracks registration in a such way that the sample along with CR-39 detector was covered in the two polythene sheets, and alpha tracks background caused by ^{220,222}Rn absorbed in the polymer could be eliminated by exposing the CR-39 to blank PES grafted sample for a same period of time in the same geometry.

4A.2.5. Application to aqueous samples

Synthetic urine sample was made according to the composition given in literature [27] [D McCurdy et al. 2005] as: oxalic acid ($H_2C_2O_4.2H_2O$, 0.02 g), pepsin (0.029 g), lactic acid (liquid, 0.094 g), magnesium sulfate ($MgSO_4.7H_2O$, 0.46 g), glucose (dextrose, 0.48g), citric acid (0.54 g), calcium chloride ($CaCl_2.2H_2O$, 0.63g), hippuric acid (0.63 g), sodium metasilicate nonahydrate ($Na_2SiO_3.9H_2O$, 0.071 g), ammonium chloride (1.06 g), creatine ($C_4H_9N_3O_2.H_2O$, 1.1 g), sodium chloride (2.32 g), sodium dihydrogen phosphate ($NaH_2PO_4.H_2O$, 2.73 g), potassium chloride (3.43 g), sodium sulfate (4.31 g), urea (16 g), nitric acid (70.67 g), and distilled water (950 g). Synthetic urine sample (10 mL) was spiked with a known amount of Pu activity (106 Bq mL^{-1}). The other isotopes of Pu were also present but alpha activity of ^{239}Pu was followed as this isotope was major component. The acidity of urine sample was adjusted to 3 mol L^{-1} HNO_3. The poly(BMEP)-grafted membrane sample was equilibrated in the synthetic urine solution under stirring condition for 5 h. Similarly, 10 mL of 3 mol L^{-1} HNO_3 standard sample was made by adding the same amount of Pu activity. The membrane was also equilibrated with standard sample for 5 h. The alpha track density of the CR-39 exposed to the membrane sample equilibrated with Pu(IV) ions spiked urine sample was compared with the track density of CR-39 exposed to the standard Pu(IV)-loaded membrane sample having same dimensions using following equation:

$$[Pu]_{Samp} = \frac{Td_{Samp}}{Td_{Std}} \times [Pu]_{Std}$$

where Td_{Samp} and Td_{Std} are alpha tracks densities in the CR-39 detectors exposed to the urine and standard Pu(IV)-loaded poly(BMEP)-grafted samples, respectively, and $[Pu]_{Samp}$ and $[Pu]_{Std}$ are concentrations of Pu(IV) ions in urine and standard aqueous samples having same 3 mol L^{-1} HNO_3 concentration. The precise sample to detector geometries in the track measurements and accuracy in the exposure time in case of sample as well as standards gave appropriate results by the single point calibration.

4A.3. Results and discussion

PES polymer is UV-active and amenable for the grafting without any initiator [PB Price et al. 2005, A Akbari et al. 2006, H Susanto et al. 2007].The microporous PES membrane was used as a support to provide higher accessibility to the acidic phosphate functional groups for binding with Pu(IV) ions. The photolysis of PES polymer chains on exposure to UV radiations provided free radical sites for the grafting of functional monomer. However, the formation of free radical was not expected to occur at interior matrix of the PES membrane as 352 nm UV radiations would be blocked at a few micron from the surface [PB Price et al.

2005, A Akbari et al. 2006, H Susanto et al. 2007].The chemical structure of monomer BMEP used for surface grafting on the PES membrane is shown in Scheme 4A.1 The functional monomer used in the present work had two polymerizable double bonds. Therefore, BMEP could act as a cross-linker between broken sites of the PES chains or one end of BMEP could be sites for the addition of another BMEP monomer unit.

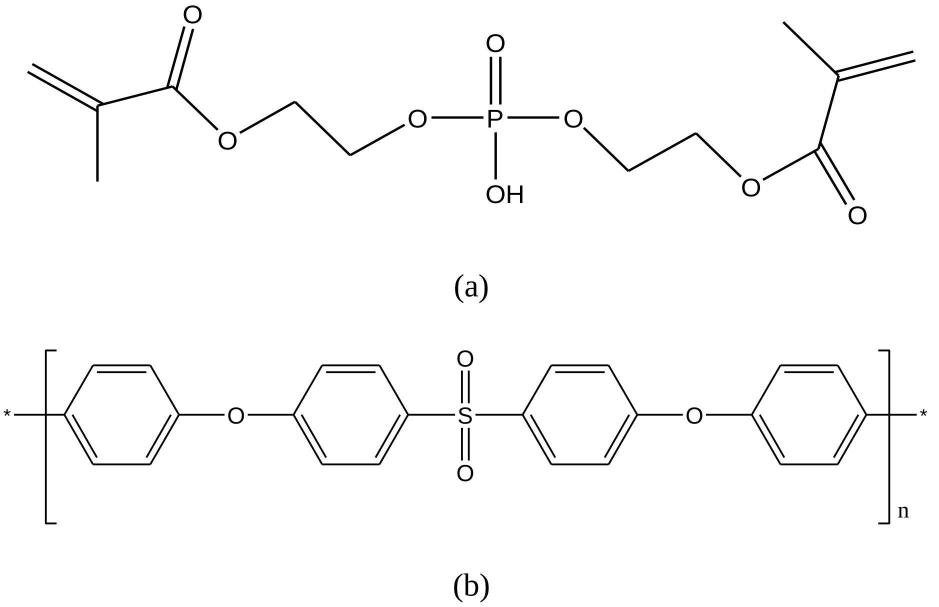

Scheme 4A.1.Chemical Structures of functional monomer BMEP (a) used for surface grafting on base poly(ether sulfone) chain (b).

It was reported that the neutral phosphate groups grafted alone were not efficient and required the presence of sulfonic acid groups in the polymer matrix for fast and quantitative sorption of Pu(IV) ions [S Paul et al. 2014]. As can be seen from Scheme 4A.1, BEMP had mono-acidic phosphate groups that obviated the need for the presence of another acidic groups for the fast and efficient sorption of the Pu(IV) ions.The change in the physical structure of membrane after grafting poly(BMEP) on its one surface was studied by SEM. It is seen from a comparison of the representative SEM images given in Figure 4A.1 that the surface was modified after grafting poly(BMEP) on the PES membrane. The surface of poly(BMEP)-grafted PES membrane was changed distinctly with respect to the surface of pristine PES membrane.

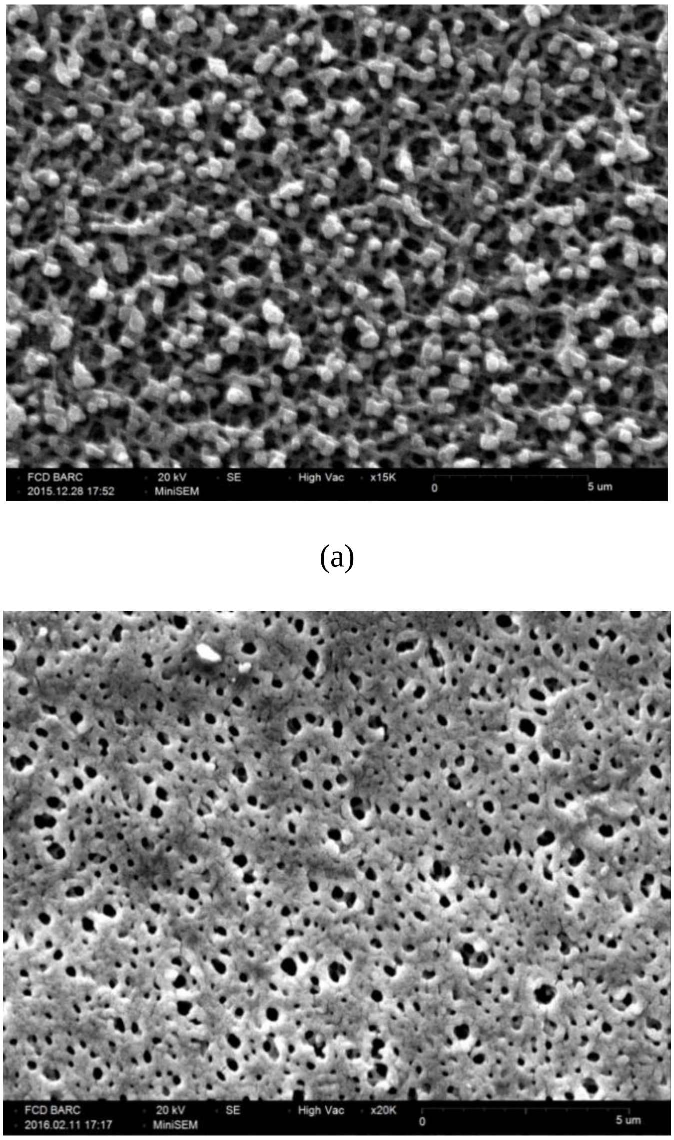

(a)

(b)

Figure 4A.1. Representative SEM images of the pristine PES membrane (a) and one side surface-grafted poly (BMEP)-grafted PES membrane (b).

The pore-size distributions and void volumes in the pristine membrane and poly (BMEP)-grafted membrane were determined as described in our earlier publications [C Agarwal et al. 2012, S Chappa et al. 2017]. The pore-size distributions were measured by capillary flow porometry (CFP) which is based on the measurement of the pressure necessary to blow gas through a liquid-filled porous membrane [C Agarwal et al. 2012]. This pressure could be correlated to the pore diameter using Washburn equation, and gas flow (%) representing number density as function of pore-diameter was obtained as shown in Figure 4A.2. It is seen from Figure 4A.2. that the pore-size distribution in poly(BMEP)-grafted membrane was more spread as compared to the pristine PES membrane. It was possible that the drying process in vacuum oven might have produced a change in the physical structure of membrane. This would have resulted to spread in the pore-size distribution of poly(BMEP)-grafted membrane as shown in Figure 4A.2. However, the major reorganization of the physical structure of the membrane was not observed in the present case as there was chemical bonding of grafted poly(BMEP) on the surface of the membrane, and physical structure of the pristine membrane was quite stable. This is concluded from the total porosity measured using “Pore-fil” liquid as described elsewhere, and chapter II [S Chappa et al. 2017]. It was observed that the void volume was slightly increased from 78 ± 2 vol/vol% in the pristine membrane to 84 ± 2 vol/vol% in the poly(BMEP)-grafted membrane. On UV-grafting, the change in the pore size was attributed to the cumulative effect of solvent, content in the grafting solution, the extent of polymer grafted, and inter/intra chains cross-linking as monomer used was cross-linker. The solvent used in the grafting solution determined the miscibility of monomer used and also responsible for the preferentially opening up of the pores in the membrane. In grafted membrane, the PES host matrix polymer chains were bunched in contact with a non-solvent and due to cross-linking that would be responsible to ≈ 5% increase in the void volume.

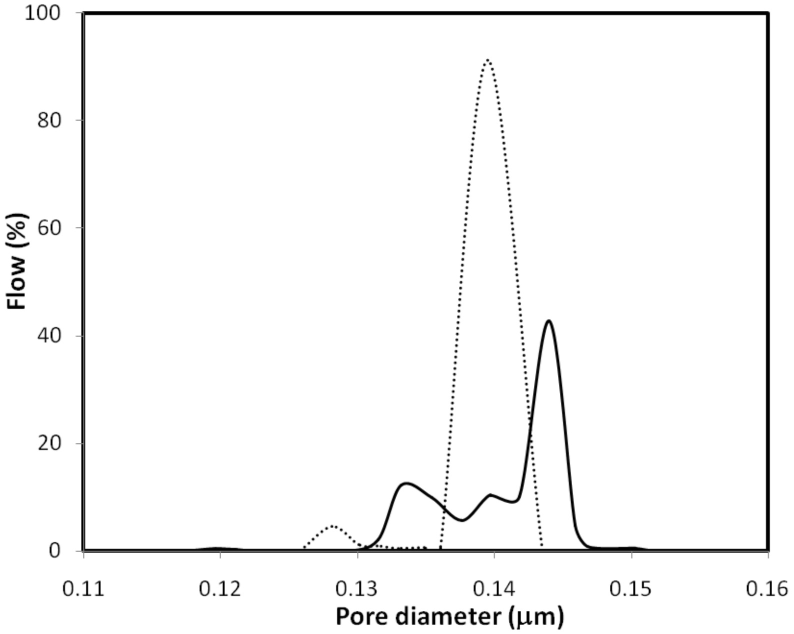

Figure 4A.2.Pore-size distributions obtained by capillary flow porometry in the pristine PES membrane (dotted line) (a) and poly(BMEP)-grafted PES membrane (solid line) (b).

The method of Pu quantification was based on the monitoring alpha particles having characteristic energy by suitable method such as alpha spectrometry or solid state nuclear tracks detector. The porous structure poly(BMEP) grafted on the membrane provided a high accessibility to the binding sites, and location of the binding sites on the surface ensured the minimum loss of energy of alpha particles emitted by Pu(IV) ions held at binding sites. To study the extent of loss of kinetic energy of alpha particles in the source matrix, the Pu (IV)-loaded poly(BMEP)-grafted membrane sample was subjected to alpha spectrometry. It was seen from thus obtained alpha spectrum shown in Figure 4A.3. that the characteristics alpha energy peaks corresponding to ^{239,240}Pu and ^{238}Pu were well resolved, and has Gaussian shape with slight left-side tailing which indicated degradation of the energy of a very small fraction of the alpha particles emerging from the interior matrix of the membrane. This is an indicative of not a significant loss of kinetic energy of alpha particles in the membrane matrix. The quantification of Pu(IV) in the present work was based on solid state nuclear tracks detector. The alpha spectrum was used only to ascertain the minimum loss of alpha energy in the host matrix. It is seen from Figure 4A.3.that alpha spectrometry required a very good control of film thickness. This was not a problem for SSNTD in which degradation in the alpha energy affected the track diameters and not tracks density used for the quantification. The experiments showed fairly reproducible track density (± 5%) in CR-39 detectors exposed to different films equilibrated in the solutions having same concentration of Pu(IV) ions in 3 mol L^{-1} HNO_3.

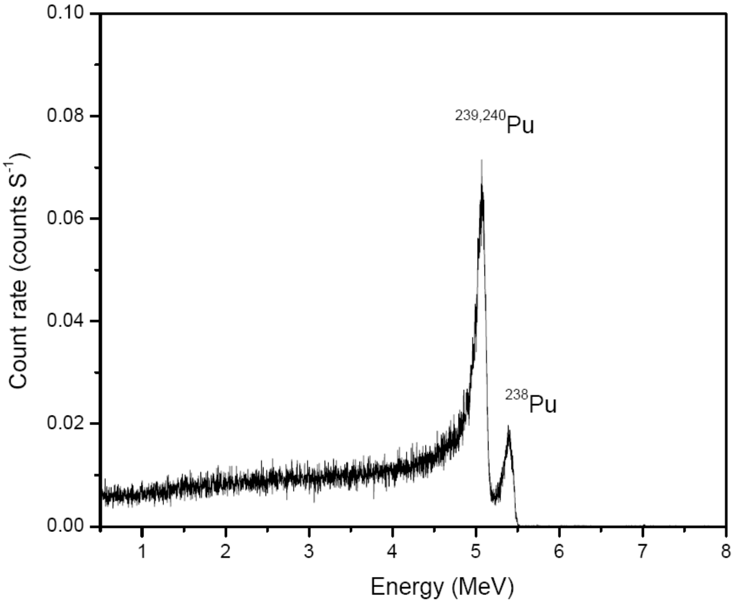

Figure 4A.3.Alpha spectrum of Pu (IV)-loaded poly (BEMP)-grafted PES membrane sample.

The homogeneity of the Pu(IV) ions distribution on the surface of poly(BMEP)-grafted PES membrane was studied by alpha tracks radiography of the Pu-loaded poly(BMEP)-grafted PES membrane sample. The tracks density registered from different locations of the membrane is related to distribution of Pu(IV) ions on its surface. Therefore, a minimum variation in the alpha track densities is an indicator of homogeneous distribution of phosphate groups bearing poly (BMEP) grafted on the surface of PES membrane. At every location, at least 50 areas were scanned for the track density measurements. The mean value obtained for the track density from all the measurements was found to be within ± 5% indicating a reasonably good homogeneity in the grafting, see representative alpha tracks radiography images in Figure 4A.4. Thus, a small representative area could be counted for obtaining alpha track density.

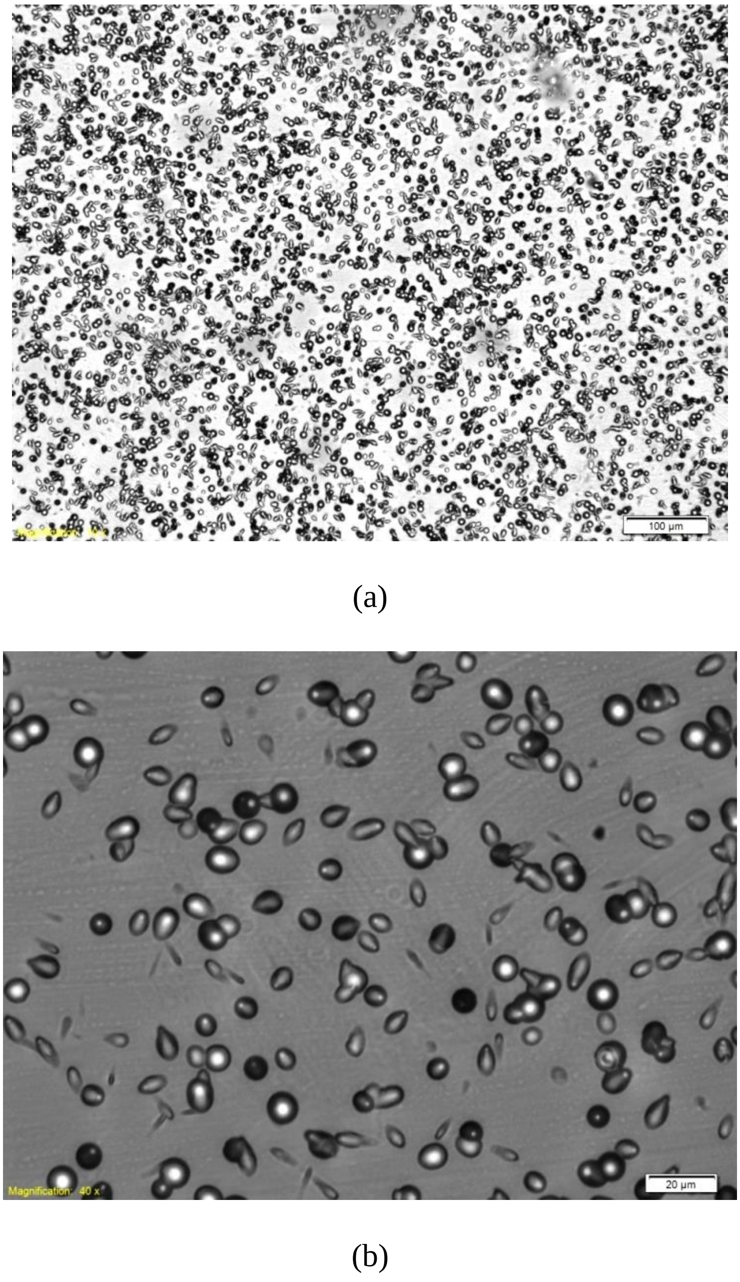

Figure 4A.4. Alpha tracks radiography using CR-39 detector kept in close contact with Pu(IV)-loaded poly(BEMP)-grafted PES membrane sample observed under transmission optical microscope at 10x (a) and 40x (b) magnifications.

^{241}Am is alpha-emitter and likely to be associated with Pu ions. However, ^{241}Am is trivalent actinide ion and likely to be sorbed in the acidic phosphate bearing polymer at a pH range [T Vasudevan et al. 2009]. To confirm this, the poly(BMEP)-grafted PES sample having 2x1 cm^2 area was equilibrated in the solution having ^{241}Am(III) at pH-2 for 5 h. The Am(III) sorption was not carried out above pH-2 to avoid hydrolysis problem. It was observed that ^{241}Am ions were quantitative sorbed (95%) in the membrane under this condition. This ^{241}Am-loaded poly(BMEP)-grafted PES sample was subsequently equilibrated with 3 mol L^{-1} HNO_3 solution. It is seen from a comparison of alpha spectra of the ^{241}Am-loaded poly(BMEP)-grafted PES sample before and after equilibration in 3 mol L^{-1} HNO_3 solution that ^{241}Am ions were quantitatively de-sorbed from the poly(BMEP)-grafted PES sample, see Figure 4A.5. It was observed that Am(III) did not sorb in the solution having pH=2 without Am(III) ions. Same thing happened with Pu(IV) in 3 mol L^{-1} HNO_3. Thus, the sorption did not occurred by the ion-exchange mechanism that followed thermodynamic equilibrium. The blank PES membrane was tested for the Pu extraction in 3 mol L^{-1} HNO_3 condition. The sorption for PES membrane and poly(BMEP)-grafted PES membrane was found to be 5% and 75.3% respectively. The sorption of some Pu in blank membrane was due to ether linkage and sulfone groups in the PES membrane as shown in Scheme 4A.1, and quantitative sorption of Pu in the grafted membrane was due to complex formation with phosphate group involving coordination of O from P=O and P-O$^-$ bonds, and remaining coordination numbers were balanced by nitrate ions at high HNO_3 concentration. Thus, the poly(BMEP)-grafted PES sample would preconcentrate Pu(IV) ions selectively from the solution having 3 mol L^{-1} HNO_3.

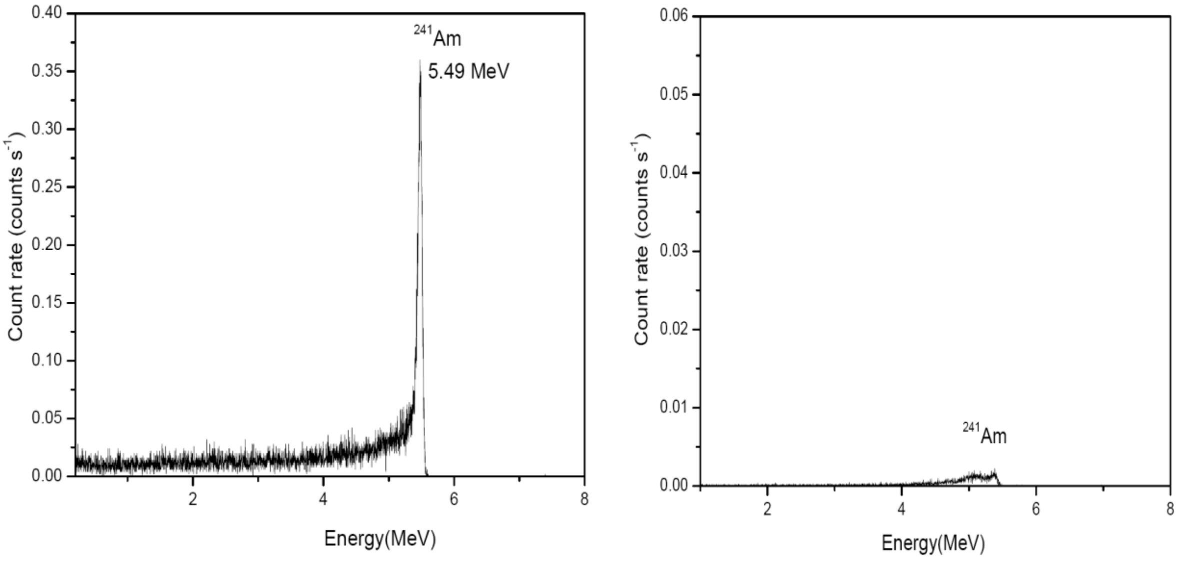

(a) (b)

Figure 4A.5. The poly(BMEP)-grafted PES membrane sample loaded with Am(III) from the solution having pH=2 (a), and after Am(III) deloading from same membrane by equilibrating it in the solution having 3 mol L^{-1} HNO_3 (b).

To ascertain selective binding of Pu(IV), the sorption of representative fission products such as Sr and Cs in the poly(BMEP) film were studied, and technetium and iodine were excluded as these exist as TcO_4^- and I^- anions, respectively, which would not sorb in the cation-exchange matrix. The uptakes of ^{85,89}Sr and ^{137}Cs were found to be 5% and 3%, respectively, from 3 mol L^{-1} HNO_3 solution. This was expected as these are non-complexing ions and sorbed only the by ion-exchange mechanism. The small fraction of these fission products sorbed in the poly(BMEP) film would not affect the quantifications of Pu as these are β/γ emitters and would not be registered in the CR-39 detector. The uptakes of representative ^{233}U and ^{237}Np from 3 mol L^{-1} HNO_3 solutions in the poly(BMEP) film were found to be 80±2% and 40±5%, respectively. To avoid interference from these ions in the Pu(IV)-ions determination, the selective elutions of ^{233}U and ^{237}Np from the poly(BMEP) film with Na_2CO_3 without affecting Pu(IV) was studied. It was observed from the alpha radiography that both ^{233}U and ^{237}Np could be eluted with 0.25 mol L^{-1} Na_2CO_3, but Pu(IV) ions remained complexed in the poly(BMEP) film under similar conditions, see Figure 4A.6.

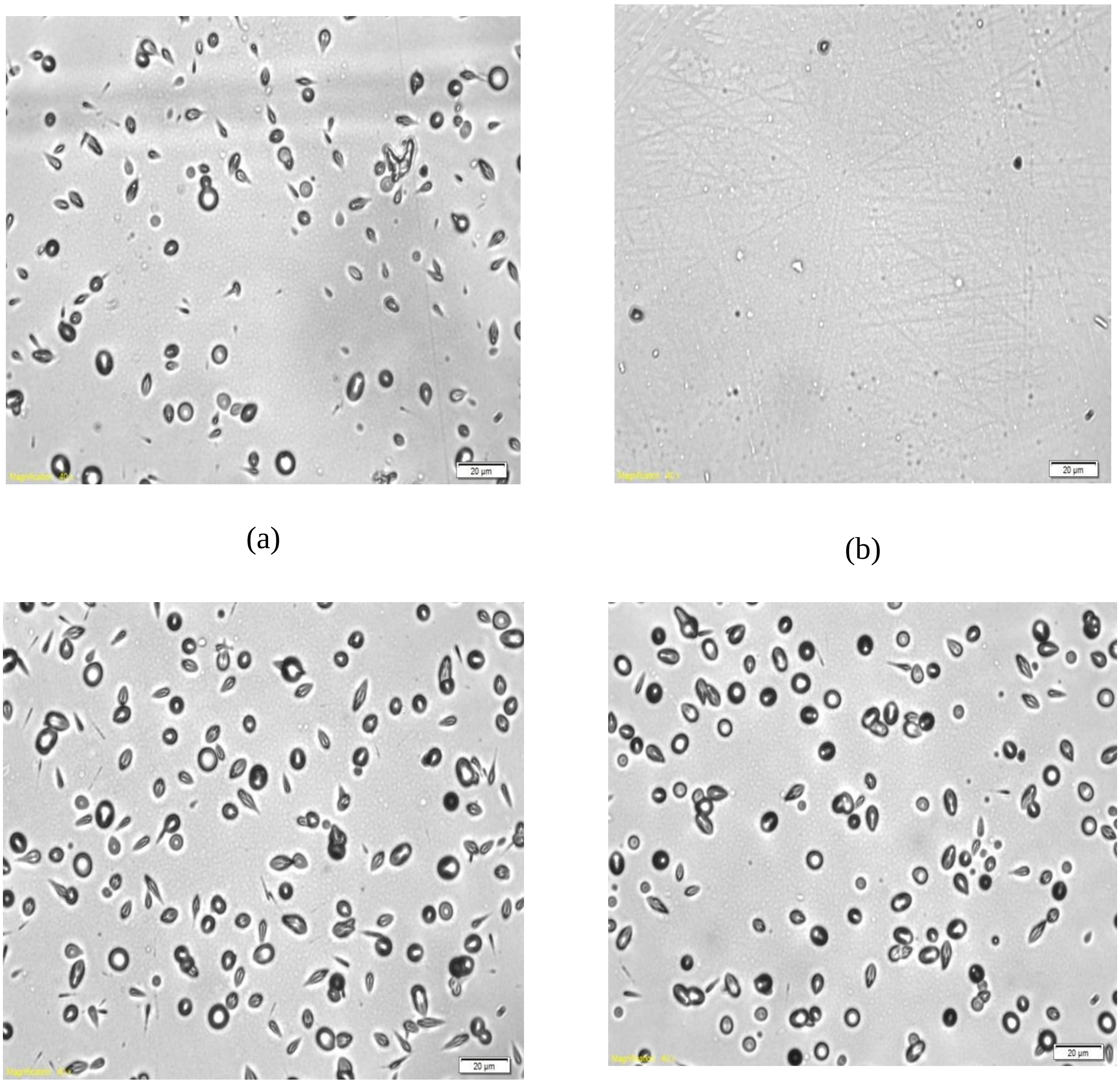

(a) (b) (c) (d)

Figure 4A.6. Alpha tracks radiographs of CR-39 detectors exposed to the ^{233}U(VI)-loaded poly(BMEP)-grafted sample (a), after equilibration of same ^{233}U(VI)-loaded film with 0.25 mol L^{-1} Na_2CO_3, for 5.5 h, ^{mix}Pu-loaded poly(BMEP)-grafted sample (c), and after equilibration of same ^{mix}Pu loaded film with 0.25 mol L^{-1} Na_2CO_3 for 5.5. h (d).

The uptake (%) of Pu(IV) ions in the poly(BMEP)-grafted PES sample from 3 mol L^{-1} HNO_3 solution as a function of time was studied, and Pu(IV)-sorption rate profile thus obtained is shown in Figure 4A.7. It is seem from Figure 4A.7. that the Pu(IV)-uptake reached optimum value 75% in 4 h, and became very slow thereafter. However, it was not clear if the Pu(IV)-uptake efficiency would remain constant over a wide conc. range which was important for the analytical application based on the calibration plot or standard comparison method. Therefore, the calibration plots were constructed by equilibrating the poly(BMEP)-grafted PES samples in the solutions having varying amount of Pu(IV) up to 231 ng in 3 mol L^{-1} HNO_3 concentration. These Pu(IV) samples were subjected to alpha tracks analysis by exposing these to CR-39 detectors for a fixed period of time (SSNTD), and also alpha spectrometry.

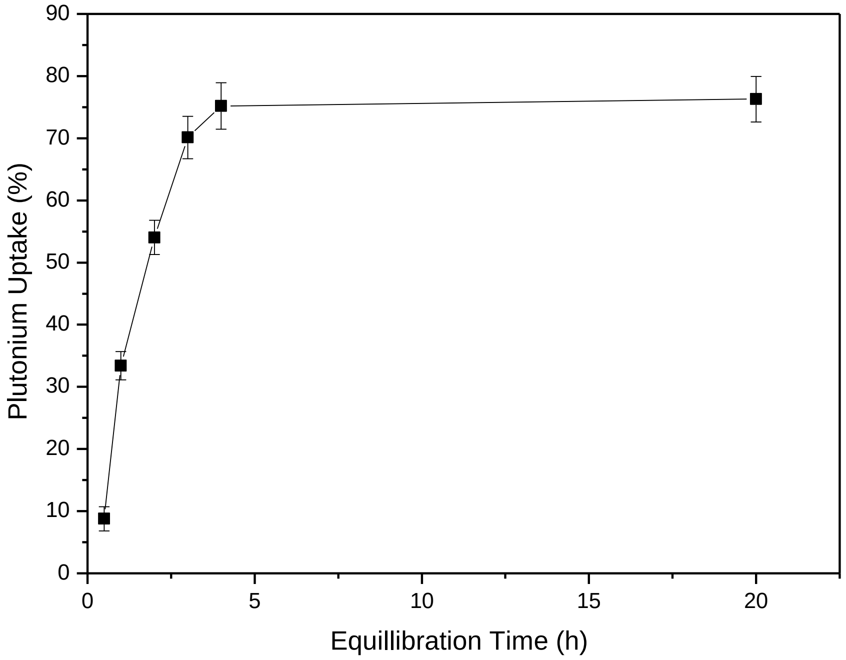

Figure 4A.7. Variation of uptake of Pu(IV) ions in the poly(BMEP)-grafted PES membrane sample from 3 mol L^{-1} HNO_3 solution as a function of equilibration time.

It is evident from the calibration plots given in Figure 4A.8 that the alpha track density and alpha count rate obtained by SSNTD and alpha spectrometry, respectively, varied linearly with the amount of Pu(IV) ions in the equilibrating solution. This seems to suggest that the uptake efficiency remained constant to 75% over the conc. range studied. It is interesting to observe from Figure 4A.8 that the slope of track density was considerably higher in the CR-39 detector (slope=0.140±0.004, R^2= 0.997) as compared to that obtained by alpha spectrometry (0.034±0.002, R^2= 0.982) using the same Pu(IV)-loaded poly(BMEP)-grafted PES membrane samples. This could be attributed to a fact that SSNTD based technique are more sensitive than the alpha spectrometry because of several factors such as semiconductor detector efficiency, geometrical efficiency, and the absence of electronic background.

To examine the possible detection limit, Pu(IV) ions were preconcentrated by spiking known activity of Pu(IV) to make its concentration to 0.05 ppb (0.13 Bq mL^{-1}) and 0.005 ppb (0.014 Bq mL^{-1}) in 15 mL of 3 mol L^{-1} HNO_3. The concentration of Pu(IV) obtained by the poly(BMEP)-grafted PES membrane (2×1 cm^2) based SSNTD were found to be 0.047ppb (0.131 Bq mL^{-1}) ± 0.005 ppb (0.014 Bq mL^{-1}) (8.33 d exposure to register alpha tracks in CR-39) and 0.007 ppb (0.02 Bq mL^{-1}) ± 0.002 ppb (0.005 Bq mL^{-1}) ppb (86 d exposure to register alpha tracks in CR-39), respectively, after blank correction and using a standard comparison method. The higher value of 0.007 ppb (0.02 Bq mL^{-1}) with respect to 0.005 ppb (0.014Bq mL^{-1}) was attributed to long exposure time (86 d) which must have resulted to higher blank correction due to ambient radon/thoron background [G S Pillai et al. 2016, F Fábián et al. 2017]. Thus, the minimum detection limit of 0.005 ppb (0.014 Bq mL^{-1}) Pu conc. in 3 mol L^{-1} HNO_3 solution is possible after appropriate blank correction i.e. CR-39 detector exposed to background for the similar duration.

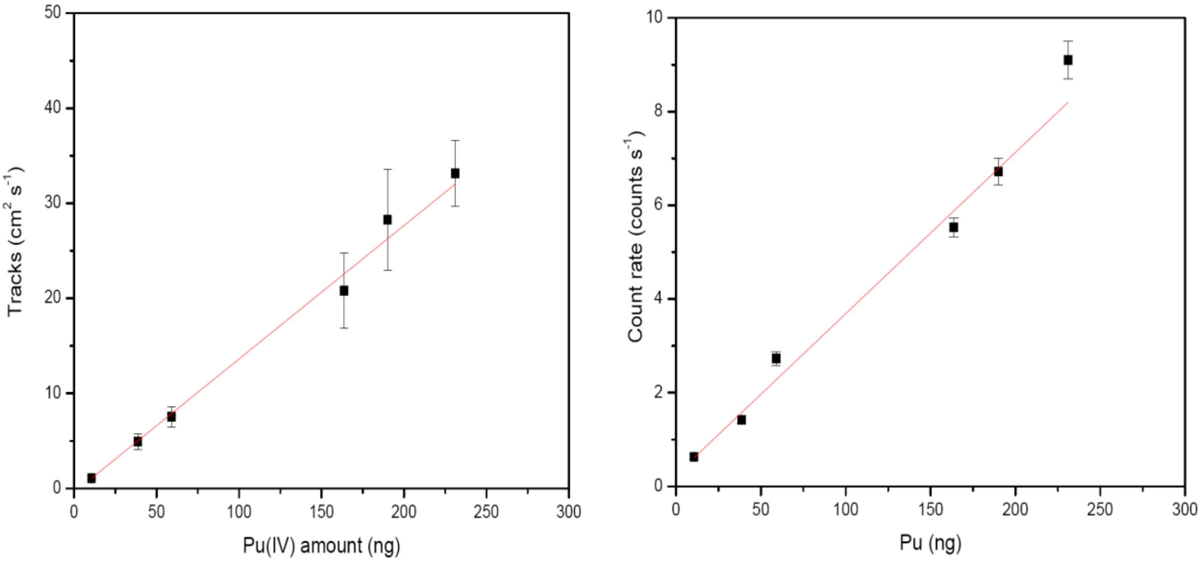

(a) (b)

Figure 4A.8 Calibration plots obtained by subjecting the Pu(IV)-loaded poly(BMEP)-grafted PES membrane samples to SSNTD analysis (a) and alpha spectrometry (b). The experimental points were average of two or three repeated experiments.

Finally, the poly(BMEP)-grafted PES based SSNTD technique developed in the present work was applied to quantification of Pu spiked in the synthetic urine sample after adjusting its acidity to 3 mol L^{-1} HNO_3. The experimental concentration of Pu(IV) in the urine sample was found to be 42±5 ppb (117 ± 14 Bq mL^{-1}). which is in a good agreement with expected concentration 38 ppb (106 Bq mL^{-1}).

4A.4. Conclusions

The thin layer of poly(BMEP) was anchored on the microporous PES membrane by UV-grafting method, which was simple and reproducible method for anchoring the thin layer of acidic phosphate bearing polymer homogeneously. Thus developed poly(BMEP)-grafted PES membrane was found to be selective towards Pu(IV) ions at 3 mol L^{-1} HNO_3, normally encountered in nuclear reprocessing plant and acidified urine to digest the organic components. It was demonstrated that the poly(BMEP)-grafted PES membrane could be used for Pu(IV) ions quantification in the aqueous samples by SSNTD. This would make the chemically non-selective alpha tracks registration based SSNTD technique selective to Pu(IV) ions in aqueous sample. The selective preconcentration of Pu(IV) would also enhance the detection limit to sub-ppb concentration.

SECTION 4B: PHOSPHATE FUNCTIONALIZED RADIATION GRAFTED TEFLON

4B.1. Introduction

The quantifications of alpha emitting and fissile elements in the aqueous samples such as environmental samples, radiopharmaceutical samples derived from fission molly, fuel reprocessing aqueous waste samples and nuclear forensic samples often require highly sensitive radiation measurement instrumentation hyphenated with appropriate sample purification and source preparation methods to avoid possible interferences [N Vajda et al. 2011, J Qiao et a., 2009, E Chamizo et al. 2008, N Guérin et al. 2011, C Labrecque et al. 2013]. However, in many such applications, the sample is to be subjected to a preconcentration step for bringing the concentration of analyte in the measurement range of the radioanalytical method [N Vajda et al. 2011, J Qiao et al. 2009, E Chamizo et al. 2008 , N Guérin et al. 2011, C Labrecque et al. 2013]. For example, the dangerous level for accumulated Pu in the human body is 10−12 g g^{-1} (1000 fg g^{-1}). This highlights the compulsion to monitor much lower levels in the surrounding environment in order to evaluate the possibility of bio-accumulation of radiotoxic elements [G Steinhauser et al. 2014]. To combine multiple sample manipulation steps such as purification, preconcentration and source preparation, the polymer sorbent based thermal ionization mass spectrometry has been developed for quantifying uranium(VI) and plutonium(IV) ions in a variety of aqueous samples [S Paul et al. 2014]. Similarly, thin sorbent films anchored on the silicon, polymer, membrane, glass have been developed using different approaches for one step sample manipulation and subjecting thin film sorbents directly to alpha spectrometry [R S Addleman et al. 2005, D Karamanis et al. 2006, S Paul et al. 2015, S K Hanson et al. 2014, J M Mannion et al. 2016, W D Locklair et al. 2016, J H Rim et al. 2016]. To process large volume of aqueous samples, a surface grafted poly(ether sulphone) membrane has been developed for ultrafiltration to capture the alpha emitting actinides and subsequently quantifying by subjecting the membrane to alpha spectrometry [C E Duval et al. 2018] . The scintillating polymer membranes have also been developed that produce scintillation proportion to the alpha particles emitted by the actinides captured in the membrane matrix [S Sodaye et al. 2004, V Chavan et al. 2016]. Solid state nuclear track detectors (SSNTDs) are the most sensitive for recording energetic charge particles but lack of chemical selectivity and also have limited capability to distinguish the particles based on their energies like alpha spectrometry. However, a combination of alpha spectrometry and fission track analysis could be very effective for nuclear forensic applications [S F Love et al. 1998]. SSNTDs have been used for monitoring alpha particles from radon decay [N M Hassan et al. 2017], detecting residual hot particles after nuclear facility decommission activities [V Zorri et al. 2017], and determination of alpha emitting radionuclides in the marine fish samples to study the pathways of ^{238}U, ^{232}Th, ^{222}Rn, and ^{220}Rn to human body [M A Misdaq et al. 2018]. To improve analytical applications of SSNTDs, a thin polymer inclusion membrane supported on the silanized glass and surface phosphate functionalized polymer grafted membranes has used for pre-concentrating actinides selectively and used as a source for registering the alpha tracks in CR-39 detector [V Chavan et al. 2013]. In general, the phosphate groups are selective to the tetravalent and hexavalent actinides ions at higher HNO_3 concentration but lack the selectivity towards Pu(IV) ions. It has been reported that the selectivity of the phosphate groups for covalent binding with Pu(IV) could be influenced by the functional groups in a close proximity [S Chappa et al. 2016, S Chappa et al. 2016]. In these work, it has been shown that the high selective toward Pu(IV) ions could be achieved by choosing appropriately the chemical architecture of the functional polymer film.

In present work, the GMA has been anchored on the Teflon film by mutual radiation grafting technique reported elsewhere [N K Goel et al. 2011, C V Chaudhari et al. 2016]. The grafting extent of the poly(GMA) on Teflon has been controlled by the exposure to appropriate absorbed γ-dose from ^{60}Co and other experimental parameters. The epoxide ring of the grafted GMA was later converted to phosphoric acid under optimized chemical conditions. Thus synthesized Ph-g-T has been characterized and used for the selective pre-concentration of Pu(IV) and U(VI) in the aqueous samples and subsequent direct determinations by registering alpha and fission tracks in CR-39 and Lexan detector. The schematic representation of the efficacy of the Ph-g-T in combining sample treatment and source preparation for the radiation measurements based analytical methods is illustrated the Scheme 4B.1.

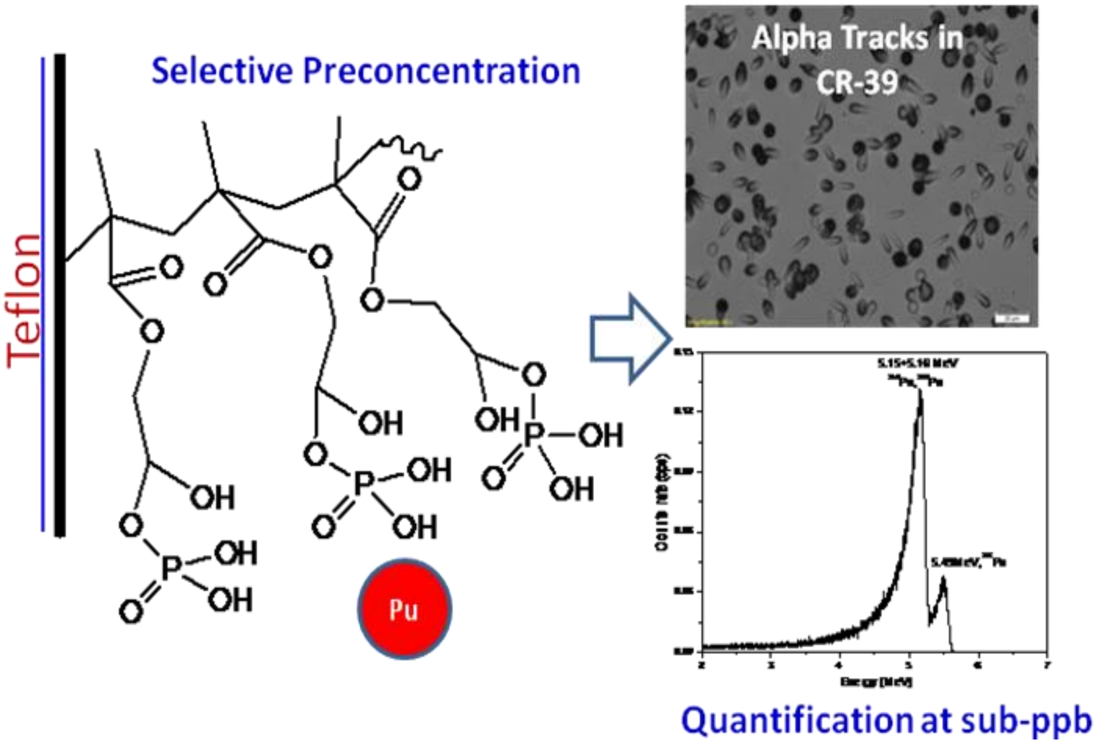

Scheme 4B.1. Phosphate bearing thin polymer film on Teflon sheet and its application in quantifying Pu(IV) ions by alpha spectrometry and solid state nuclear track detector.

4B.2. Experimental

4B.2.1. Reagents and apparatus

The details of reagents and apparatus used are given in Chapter 2.

4B.2.2. One side functionalization of Teflon sheet

Teflon sheets were washed first with toluene followed by detergent solution, and finally vacuum dried at 50 °C and stored in desiccator for further use. The cleaned Teflon sheet had a bulk density=2.1 g/cc, and surface energy=22.5 mJ m^{-2}. In order to avoid contact of one face of Teflon with grafting solution so that grafting occurs on only one face of Teflon, Teflon pieces (1.5 cm x 2.0 cm) of Teflon were compression molded into 0.7 mm poly(propylene) sheet at 180 °C and 98066 pascal pressure. The samples immersed in the GMA containing solution were then irradiated in the gamma chamber for the required doses. Thus obtained G-g-T was refluxed for 3 h at 80 °C in a solution of phosphoric acid and tetrahydrofuran (75:25 v/v). The Ph-g-T samples were Soxhlet extracted with acetone for 8 h to remove any trapped homopolymer of GMA in the grafted Ph-g-T. Finally, the grafted matrix was washed with water and dried in vacuum at 50°C for further use.

4B.2.3. Representative actinide ions sorption studies

The sorption efficiencies of Ph-g-T pieces (1x1 cm^2) toward representative actinide ions were carried out using ^{241}Am(III), ^{233}U(VI) and ^{mix}Pu(IV) in 5 mL of solution having varying concentrations of HNO_3.The extents of Pu (IV), U(VI) and Am(III) sorptions on Ph-g-T were quantified using liquid scintillation counting of aqueous samples (100 µL) taken from solutions before and after overnight equilibration and added in 5 mL scintillation cocktail-W. The sorption efficiency (uptake) of actinide was obtained from equation (1):

$$Uptake\ (\%) = [A_b - A_f] / [A_b] \times 100 \qquad (1)$$

where A_b and A_f were alpha scintillation count rates of ^{mix}Pu, ^{233}U and ^{241}Am in the solution before and after equilibration with Ph-g-T, respectively. The sorption experiments were also carried out by stirring the solution for a fixed period of time, and the percentage uptakes of ^{mix}Pu, ^{233}U and ^{241}Am radiotracers as the function of time were monitored.

4B.2.4. SSNTD experiments

The alpha tracks were registered from Pu(IV)-loaded Ph-g-T sheet (1x1 cm^2 size) in CR-39 in a 2π contact geometry. After exposure to the Pu(IV)-loaded Ph-g-T for a fixed time period, CR-39 detectors were chemically etched with 6 mol L^{-1} NaOH at 70 ^{o}C for 5 h to reveal alpha tracks for the observations under optical microscope. Similarly, the fission tracks were recorded by irradiating Pu(IV)-loaded Ph-g-T sheet (1x1 cm^2 size) with Lexan in a 2π contact geometry in neutron irradiation facility at BARC having neutron flux ≈10^7 cm^{-2} s^{-1}. The fission tracks in Lexan were developed by chemical etching with 6 mol L^{-1} NaOH at 60 ^{0}C for 1 h.

4B.3. Results and discussion

4B.3.1. Radiation induced grafting and chemical conversion of epoxide to phosphoric group

The gamma rays induced mutual grafting of poly(GMA) on one surface of teflon sheet was carried out by blocking one of the teflon surfaces. The details regarding the grafting extent, absorbed dose, dose rate effect, rate of grafting etc. had been provided in our earlier reported work [C V Chaudhari et al. 2016]. The grafted poly(GMA) was reacted with phosphoric acid at elevated temperature to convert epoxide ring of the grafted GMA to generate phosphate groups (Scheme 4B.2). The chemistry of chemical conversion of epoxide to different functional group is well established and reported. Ester bond of epoxide ring can be hydrolyzed or converted to phosphoric group depending on acid used as well as other experimental conditions. In the present work, the method reported by Kalal et al. was used to attach phosphate groups by epoxy ring opeing reaction [J Kalal et al. 1974]. It is clear from chemical structure of thus formed Ph-g-T that hydroxyl groups are in a close proximity and may lead to hydrogen bonding. The hydrogen bonding is known to influence the affinity of phosphate and diglycolamide groups toward f-element ions [B Qiao et al. 2014, V Chavan et al. 2015].

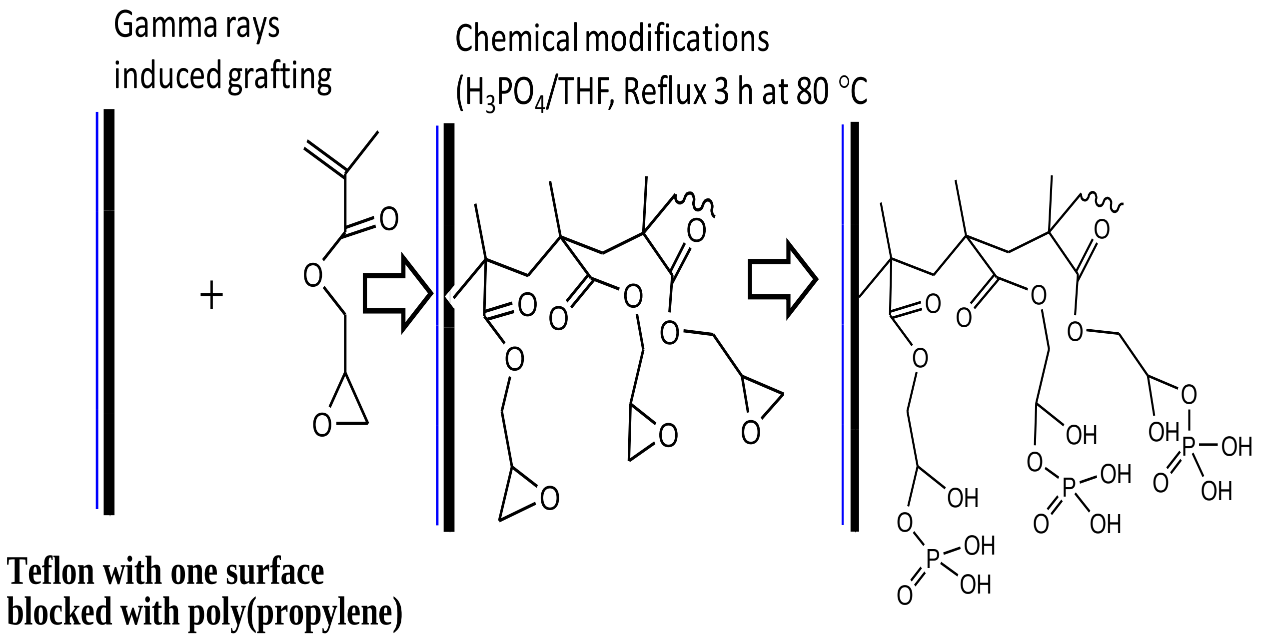

Scheme 4B.2. Chemical reactions involved in the formation of phosphate bearing thin polymer film by gamma-rays induced grafting on Teflon sheet.

4B.3.2. Characterization of grafted matrices

Fourier Transform Infrared Analysis

The presence of -H_2PO_4 in Ph-g-T used for adsorption studies was confirmed comparing FTIR spectra of pristine Teflon, G-g-T and Ph-g-T given in Figure 4B.1. In FTIR spectrum of pristine Teflon, the absorbance at 1145 and 1205 cm^{-1} were assigned to F_2 stretching. Grafting of GMA was confirmed by the presence of absorption band at 1737 cm^{-1} assigned to the C-O stretching of the ester group and symmetrical stretching of the epoxy ring near 1250 cm^{-1}. Another band in the region 950-800 cm^{-1} was attributed to asymmetrical ring stretching in which C-C bond was stretched during contraction of the C-O bond. The C-H stretching vibrations of epoxy rings could be observed in 3050- 2950 cm^{-1} region. The conversion of epoxy to phosphate group was established by appearance of band in the region 900-1040 cm^{-1}

which was assigned to P-OH stretching vibration and was further confirmed by -OH group functionality from peaks at 3200 and 3700 cm^{-1}.

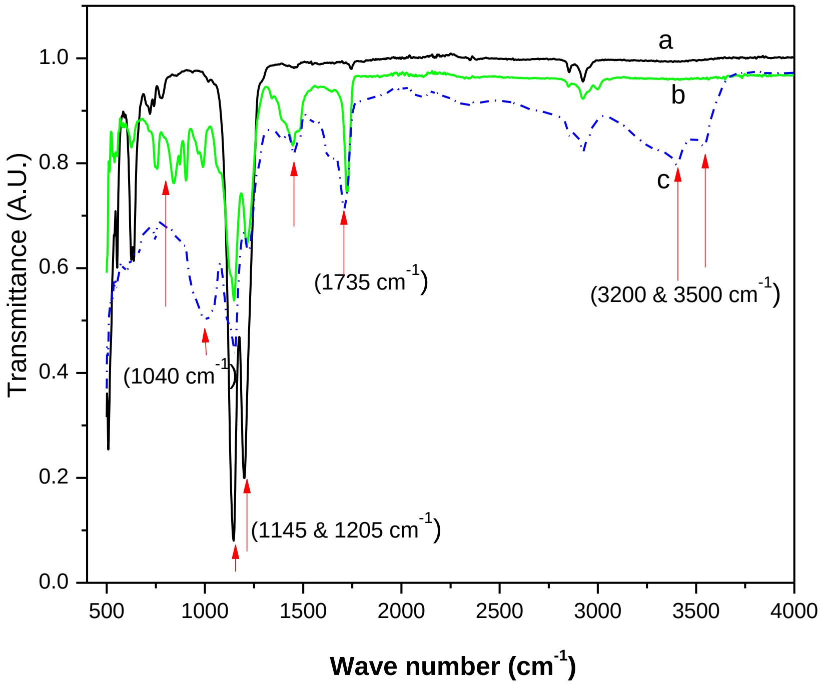

Figure 4B.1. FTIR spectra of (a) pristine Teflon, (b) G-g-T (c) Ph-g-T.

Thermogravimetric analysis

The thermograms of pristine teflon showed sharp weight loss near its decomposition temperature 480 °C which is similar to that reported earlier [C V Chaudhari et al. 2016]. The thermogram of G-g-T showed two step weight loss at temperatures 230 °C and at 480 °C. The additional weight loss step in grafted Teflon was attributed to grafted poly(GMA) chains [C V Chaudhari et al. 2016, M S Iqbal et al. 2009]. The phosphate converted grafted Teflon showed multistep gradual weight loss. The quantitative analyses of weight losses observed due to grafted poly(GMA) and phosphate group were found to be 2.23 wt.% and approximately 0.5 wt. % which were in a good agreement with extent of weight gain measured using gravimetric measurement (Figure 4B.2).

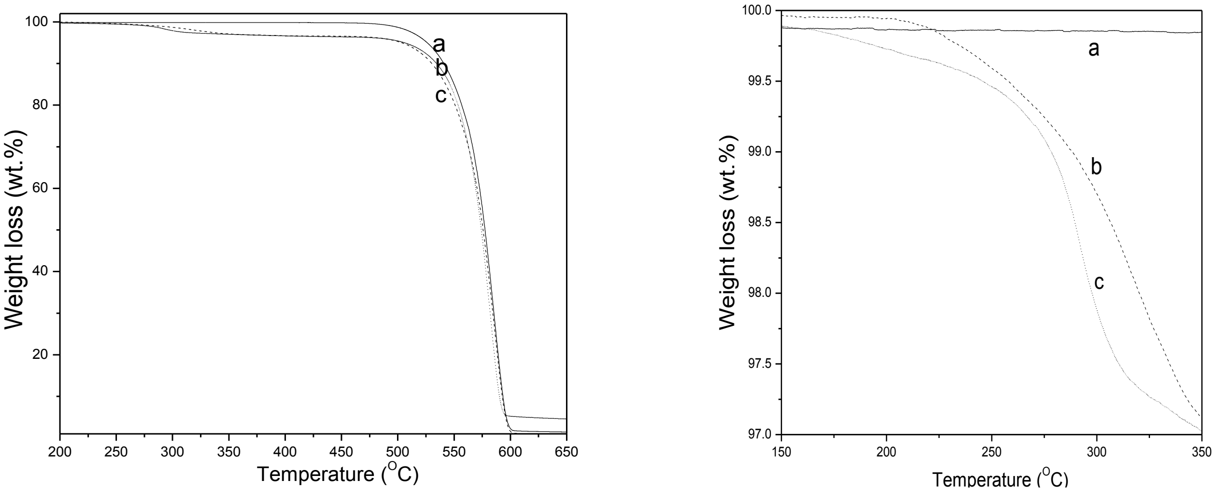

(A) (B)

Figure 4B.2. (A) Thermograms of pristine Teflon (curve a), G-g-T (curve b) and Ph-g-T (c): (B) Zoomed thermograms. Substrates heated up to 700°C at a heating rate of 10 °C min^{-1} under flowing purified argon atmosphere.

AFM analysis

The change in surface morphologies of grafted teflon substrates were studied by AFM analysis. It is evident from the representative AFM images given in Figure 4B.3 that the surface became rough after grafting and chemical modification. This was expected due to formation of thin poly(GMA) layer on Teflon surface due to grafting.

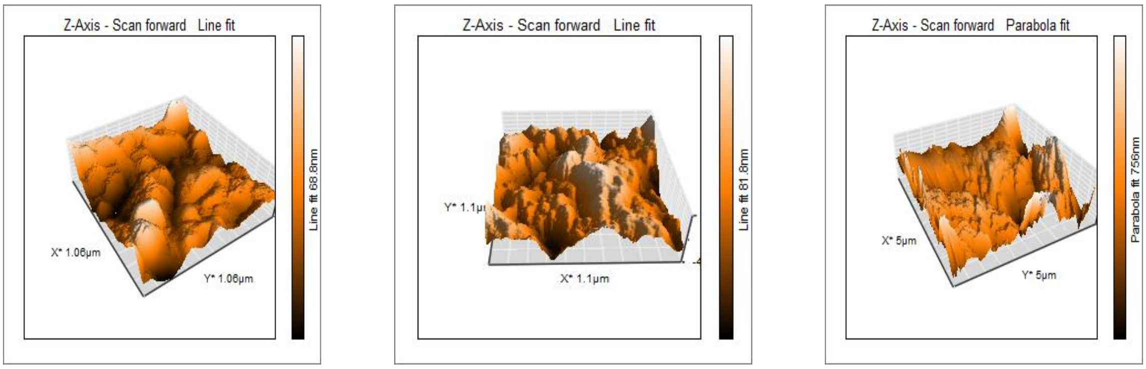

(a) (b) (c)

Figure 4B.3. Images obtained by AFM showing surface morphologies of pristine Teflon (a), G-g-T (b) and Ph-g-T (c) substrates.

4B.3.3. Pu and U sorption studies

The acidic phosphates are known to have affinity toward actinide ions [S Chappa et al. 2016; S Chappa et al. 2016]. Therefore, the Ph-g-T sheets were equilibrated in the solutions having UO_2^{2+} ions at pH=2 and Pu^{4+} ions at 3 mol L^{-1} HNO_3. The Pu^{4+}-loaded Ph-g-T sheet was subjected to alpha radiography using CR-39 to study the distributions of Pu^{4+} ions bound with phosphate groups on grafted matrix. Representative image obtained by transmission optical microscope is shown in Figure 4B.4a. It was observed that alpha tracks were uniformly distributed (± 8%) indicating homogeneity of grafting, thus a small representative area could be counted for obtaining alpha track density. To study distribution of U(VI) ions, the UO_2^{2+}-loaded Ph-g-T sheet was kept in a 2π contact with Lexan and irradiated with reactor neutron to register the fission tracks. It was seen from developed fission tracks shown in Figure 4B.4b that U(VI) ions were also distributed uniformly on the grafted surface of Ph-g-T sheet.

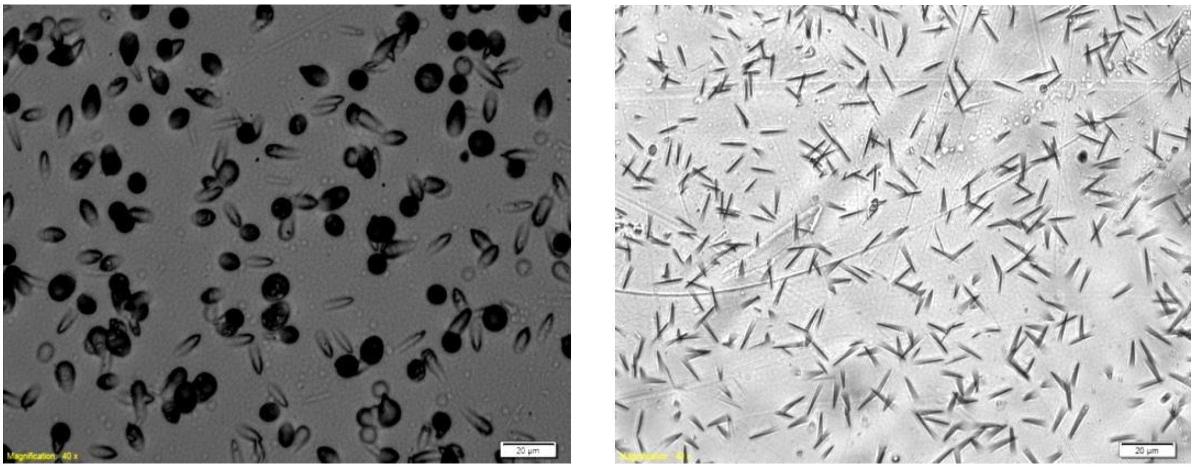

(a) (b)

Figure 4B.4. The representative images showing distributions of (a) alpha tracks and (b) fission tracks registered in CR-39 and Lexan plastic detectors exposed to the Pu^{4+}-loaded Ph-g-T and reactor neutron irradiated UO_2^{2+}-loaded Ph-g-T.

To optimize the maximum extent of surface grafting, the Ph-g-T substrates with different phosphate contents (0.5 - 2.1%) were prepared by controlled grafting extent of GMA through experimental parameters described elsewhere [C V Chaudhari et al. 2016]. These Ph-g-T substrates were loaded with Pu^{4+} ions from 3 mol L^{-1} HNO_3 and subjected to alpha spectrometry. From alpha spectrum of Pu^{4+} loaded Ph-g-T (Figure 4B.5) it was observed that, the characteristics alpha energy peaks corresponding to ^{239}Pu, ^{240}Pu and ^{238}Pu were well resolved with left-side tailing. This is an indicative of smaller extent of loss of kinetic energy of alpha particles in the grafted polymer matrix itself before emerging out. It was also observed that the extent of energy degradation of alpha particles increased with increase in the % phosphate content (i.e. polymer grafting). This could be attributed to increase in the thickness of phosphate bearing grafted layer with increase in grafting extent. The full width at half maxima (FWHM) from the alpha spectrum recorded was taken as indicative of the extent to which the alpha particles lose its energy while coming out from the matrix. It was observed that that FWHM value of 0.5% and 1% phosphate bearing Ph-g-T was similar (0.22 MeV). In case of 1.2 % phosphate, FWHM increased (0.26 MeV) which further increased in 2.1% phosphate content sample (0.40 MeV). This suggests significant deterioration of energies of alpha particles in the matrix having > 1 % phosphate bearing polymer layer on Ph-g-T. As evident from Figure 4B.5, there was significant contribution of alpha counts below 4 MeV in case of the 1, 1.2, 2.1% phosphate containing Ph-g-T samples due to left side tailing. Therefore, further studies were done using 0.5 % phosphate bearing Ph-g-T to avoid registering alpha particles in solid state nuclear track detector (SSNTD) having varying energies. As such, the track density is not affected by loss of small amount of kinetic energy of alpha particles in the source matrix. The alpha track density is used for quantification using SSNTD. In alpha spectrometry, the quantification would be affected by left side tailing due to erroneous integration of peak area.

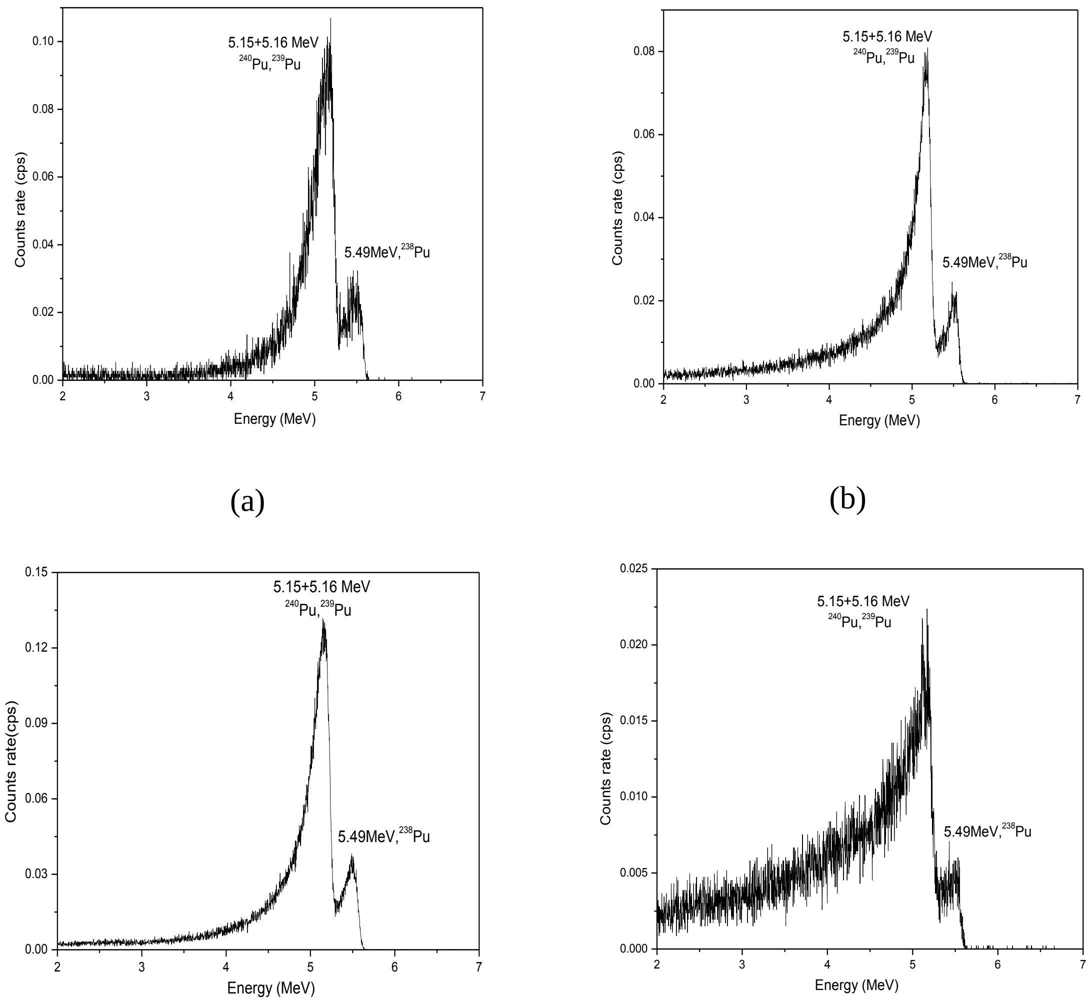

(a) (b)

(c) (d)

Figure 4B.5. Alpha spectra of Ph-g-T grafted matrix having different extent of phosphate conversion (a) 0.5 % (b) 1% (b) (c) 1.2% (d) 2.1%

The acidic phosphate groups are expected to bind with actinide ions via ion-exchange complexation with P-O- at pH range and complexation of neutral nitrate actinide salt with P=O at higher HNO_3 concentration. Thus, it is expected that Ph-g-T would exhibit a HNO_3 concentration dependent selectivity toward actinide ions. It is seen from the uptake profiles of the representative ions such as Am^{3+}, UO_2^{2+} and Pu^{4+} ions (Figure 4B.6) that Pu^{4+} ions sorb preferentially above 3 mol L^{-1} HNO_3. This could be attributed to ability of Pu^{4+} ions to coordinate with nitrate ions [S Chappa et al. 2016] and form neutral complex with P=O group. The trivalent actinide ions such as Am^{3+} ions bind with phosphate groups via ion-exchange mechanism, and, therefore, sorbs at pH range (1-3). However, it is interesting to note that UO_2^{2+} ions did not sorb at higher HNO_3 concentration. The acidic phosphate groups are expected to bind with actinide ions via ion-exchange complexation with $P\text{-}O^-$ at the pH range, and complexation of neutral nitrate actinide salt with P=O at higher HNO_3 concentration. The quantitative sorption of Pu(IV) at HNO_3 concentration could be attributed to ability of Pu^{4+} ions to coordinate with nitrate ions and form a neutral complex with P=O group. The trivalent actinide ions such as Am^{3+} ions bind with phosphate groups via ion-exchange mechanism and, therefore, sorbs in a pH range. The sorption Am^{3+} ions were higher than UO_2^{2+} ions at given pH as it has higher charge than UO_2^{2+} ions and ion-exchange is highly dependent on the charges. It was interesting to note that UO_2^{2+} ions did not sorb at higher HNO_3 concentration. This suggested that there was no stable complex formation of UO_2^{2+} with P=O group due to unsatisfied coordination with nitrate ions. The geometrical constraint did not allow UO_2^{2+} ions to bind with multiple P=O groups to satisfy its coordination numbers. Therefore, the Ph-g-T substrate developed in the present work exhibits remarkable selectivity towards Pu(IV) ions that are known for forming stable complex with nitrate ions.

However, UO_2^{2+} was found to sorb quantitatively from seawater and ground water (88 ±2 %) and thus can be used for preconcentration of UO_2^{2+} ions from these aqueous matrices. The attainment of optimum uptake of Pu^{4+} ions in the Ph-g-T from 3 mol L^{-1} HNO_3 solution as a function of time was studied, and observed that the Pu^{4+}-uptake reached optimum value (92±2 %) in 4.5 h, and remained constant thereafter. The Pu^{4+}-ions preconcentrated in the Ph-g-T could be de-loaded after two equilibrations with 0.2 mol L^{-1} hydrazine hydroxyl amine in 1 mol L^{-1} HNO_3.

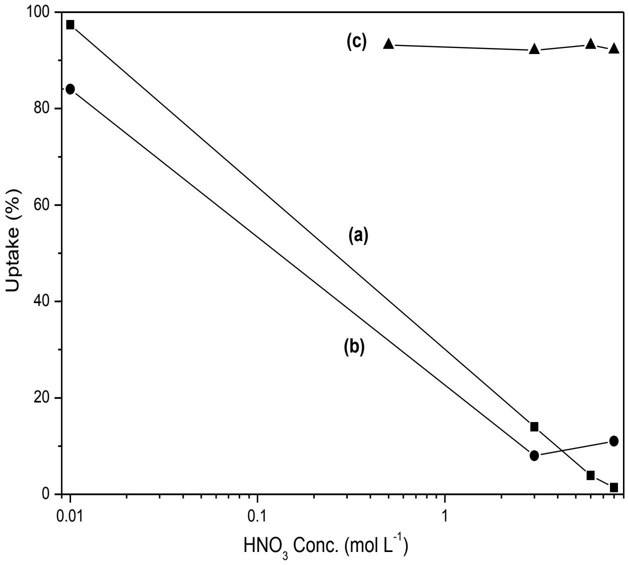

Figure 4B.6. Uptake profiles of Ph-g-T as a function of HNO_3 concentrations of ^{241}Am (a), ^{233}U (b) and ^{mix}Pu (c) . X-axis is in $\log_{10}$ to exhibit data at pH range.

The Pu^{4+}-uptake efficiency of Ph-g-T substrate must not expected to vary over a wide concentration range if the calibration plot or standard comparison method has to be used for the quantification. Therefore, the calibration plots were constructed by equilibrating Ph-g-T substrates in the solutions having varying Pu^{4+} concentration (4-222 Bq mL^{-1}). These Pu^{4+}-loaded samples were subjected to alpha tracks analysis by exposing these to CR-39 for a fixed period of time. It is evident from the calibration plot given in Figure 4B.7 that the alpha track densities in CR-39 varied linearly with the amount of Pu^{4+} ions in the equilibrating solution. Similar observation was made using the fission track analysis. This suggested that the uptake efficiency remained constant over the concentration range studied.

Ph-g-T was studied for its applicability in the estimation of uranium in water sample of natural origin using the fission track measurement. Ph-g-T (1 cm^2 size) was equilibrated with 5 mL of sample of natural water and U standard solutions for overnight. The fission track densities of samples were correlated with the standards. The concentration obtained for two samples were 42.9 ± 2.3 and 252.3 ± 21.2 ng g^{-1} which were in a good agreement with that obtained by LASER fluorometric measurements i.e. 40 and 249 ng g^{-1}, respectively. As SSNTD are more sensitive, Ph-g-T based SSNTD method could be used for quantifying ppb level concentration (2-100 ppb) of UO_2^{2+} ions in the natural water as observed from the calibration plots.

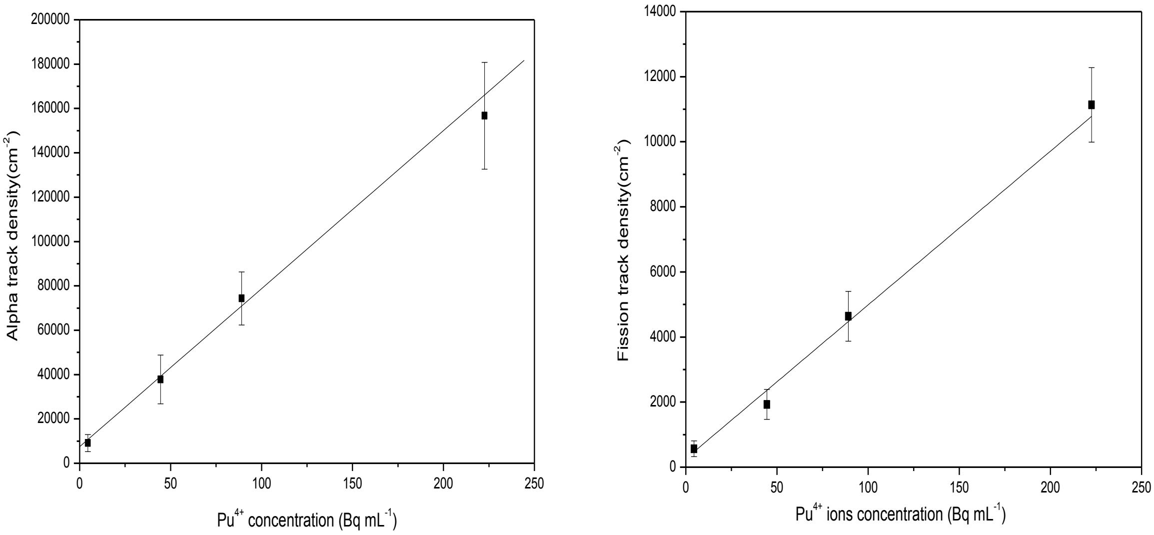

(a) (b)

Figure 4B.7. Variations of alpha and fission track densities recorded in CR-39 (a) and Lexan (b), respectively, exposed to different concentrations of Pu^{4+} ions loaded in Ph-g-T (1x2 cm^2). CR-39 exposure time was kept 30 min, and fission tracks were recorded by exposing to neutron flux of order of 4×10^7 n cm^{-2} sec^{-1} for 2 h.

For radionuclide derived from fission molly for medical objective, the total alpha activity in nano-Curie range has to be determined in the presence of curie level β-activity. In these cases, the SSNTD are best suited as β-particles do not form tracks and there is no possibility of electronic noise for a long exposure of detectors to accumulate sufficient alpha tracks. The easiest way is to immerse CR-39 detector in solution for desirable period (15-30 days) to record the alpha tracks. However, the alpha tracks registration efficiency in the solution is very low (K_{wet} =5 x 10^{-4} cm^{-1}, unit of efficiency is from balancing the dimension in equation= Td (track density)(tracks cm^{-2}) / N λ (activity concentration in Bq cm^{-3}) x t (

exposure time in sec)) as compared to thin solid source [R H Iyer et al. 1997].This is due to shorter range of alpha particles in the solution medium. Therefore, most of the alpha particles do not reach to the detector with suffiecient energy to form the tracks. Only those alpha particles emitted by radionuclides in a close proxmity of the detector form tracks. This is evident from the images given in Figure 4B.8 where high alpha track density is seen in CR-39 exposed to alpha activity preconcentrated in the Ph-g-T with respect to CR-39 immersed in the 4.5 mL solution of Sr^{90}-Y^{90} having 0.1 mol L^{-1} HCl. For the exposure time of 21.70 days of CR-39 in solution, the track density was 230 tracks cm^{-2} day^{-1}. For the exposure time of 15.92 days of CR-39 kept on Ph-g-T in 2π contact, the track density was 59883 tracks cm^{-2} day^{-1}. The alpha activity determined in this sample was determined to 1.04 Bq mL^{-1} by standard comparison method having known alpha activity of ${}^{mix}Pu$ (0.5-1.0 Bq mL^{-1}). It is seen from Figure 4B.8b that < 0.10 Bq mL^{-1} alpha activity could be easily quantified by using this method.

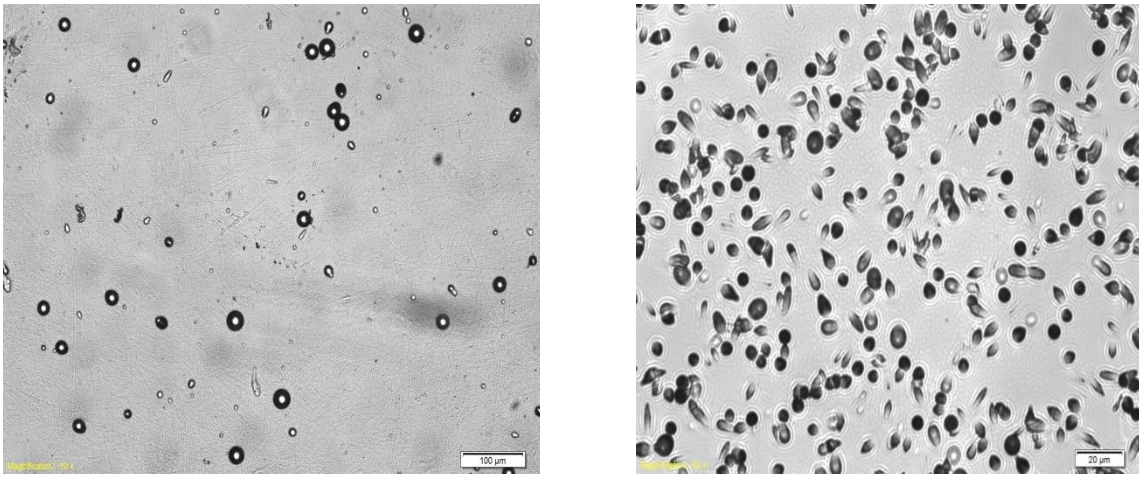

(a) (b)

Figure 4B.8.Alpha tracks recorded from solution medium in CR-39 (a), immersed for 21.70 days (b) alpha tracks recorded from Ph-g-T (immersed in same 4.5 mL solution for overnight with stirring) in CR-39 exposed for same 15.92 days. It should be noted that scale bars in image “a” is 100 μm and in “b” is 20 μm.

4B.4. Conclusions

Teflon was grafted with thin GMA polymer layer by mutual grafting technique and epoxide groups of poly (glycidyl methacrylate) were chemically modified to phosphate functionality. Teflon substrate with phosphate functionality was found to be selective towards Pu(IV) ions at higher concentration of nitric acid (3-8 mol L^{-1}). It was demonstrated that the Ph-g-T substrate could be used for Pu(IV) ions quantification in the aqueous samples by chemically selective alpha or fission tracks registration based SSNTD. The selective preconcentration of Pu(IV) would also enhance the detection limit to sub-ppb conc. Using this method, nano-Curie alpha activity in the ^{90}Sr-^{90}Y sample, having curie level of beta activity for medical objective, was quantified. U(VI) was found to preconcentrate in the phosphate group anchored Teflon from natural water, and used for its quantification using fission tracks based SSNTD.

CHAPTER-5: FUNCTIONALIZED GLASS FIBER FILTER MEMBRANES FOR FISSION RADIONUCLIDE MEASUREMENTS

The many of fission products of environmental interests are β/γ-emitters, and can be quantified unambiguously by HPGe detector based γ-rays spectrometry. This is because of the fact that these fission product radionuclides emit γ-rays with reasonably good abundances. However, the concentrations of these fission products released accidently in the environment are very low and γ-rays counts rate is not sufficient for their statistically meaningful quantifications. Thus, a preconcentration method is needed to bring the concentration of the fission products nuclides in the environmental samples within the analytical range of the γ-rays spectrometry. Therefore, for the high fission yields products such as iodine and caesium, the glass fibres membranes have been chemically modified to generate highly selective functional moieties for their selective preconcentrations and subsequent quantifications with γ-spectrometry. This chapter has been divided to two section dealing with radioiodine (section A) and radioactive cesium (section B). The contents of these sections are discussed briefly below.

SECTION 5A. Functionalized glass fiber membrane for iodine species

Poly(vinylpyrrolidone) (PVP) has been anchored on the glass fiber membrane for capturing radioiodine in gaseous state and dissolved in water. First, precursor alkoxy silane monomer was anchored by sol-gel method on the glass fiber membrane and its polymerizing double bond was used subsequently for the anchoring of PVP by UV graft-polymerization. Thus formed PVP membrane was characterized by Fourier transform infrared spectroscopy, field emission scanning electron microscopy with EDS and thermo-gravimetric analysis. The I_2 sorption efficiency and loading capacity of the membrane and stability of I_2 complexed in the membrane were studied by UV-Vis spectrophotometry and ^{131}I radiotracer method.

SECTION 5B. Functionalized glass filter membrane for radiocesium

Silicotungstate, a heteropoly acid, is known for its selectivity towards Cs^+ ions. Therefore, it has been anchored on poly(3-(trimethoxy silyl)propyl acrylate) grafted glass fibers membrane. The glass fiber membrane has been anchored with coupling monomer 3-(trimethoxysilyl) propyl acrylate (TMSPA) on a hydrolyzed glass fiber by a sol–gel process, and simultaneously utilized the double bonds of TMSPA by the UV-initiator-induced graft polymerization of TMSPA itself. Thereafter, the grafted glass membrane has been treated with silicotungstic acid. This membrane has been equilibrated with cesium salt solution followed by thermal treatment leading to condensation and formation of Cs^+-selective matrix. The Cs^+ ions have been deloaded in 3 mol L^{-1} HNO_3. Thus formed membranes have been characterized and used for capturing radioactive cesium ions for different aqueous samples for their quantification with γ-spectrometry.

SECTION 5A: FUNCTIONALIZED GLASS FIBER MEMBRANE FOR IODINE SPECIES

5A.1 Introduction

Iodine species such as molecular iodine, iodide, iodate and organically bound iodine are found naturally in the food, drinking water and seawater etc. In general, iodate and iodide are added to the table salt and processed food products for supplementing the dietary intake [P R Bhagat et al. 2009]. Thyroid glands in humans are known to accumulate the most of the necessary iodine. It is important to note that the molecular iodine has germicidal activity against a wide range of bacteria and viruses. Thus, the uses of iodine are extended to medical applications and disinfection [S Punyani et al. 2006]. Iodine species are also find applications in technological applications such as synthetic chemistry [S Das et al. 2008] and the Sulfur-Iodine thermo-chemical cycle for hydrogen production from splitting of water [A Singhania et al. 2018]. Though iodine is essential for human, the excess of iodine adversely affects thyroid function [WHO. 661, Iodine [WHO Food Additives Series 24]; WHO: Geneva]. Iodine exists in both gaseous (I_2) and aqueous soluble (I^-, IO_3^- , HOI, I_3^- and I_2) chemical forms.

Radioiodine is gaseous fission product (^{129}I and ^{131}I) that may be released during nuclear operations or accidents. ^{131}I is also produced form the nuclear reaction involving neutron irradiation of natural tellurium target. Apart from ^{131}I, there are other iodine isotopes such as ^{123}I and ^{125}I are also used either in medical diagnostic or as nuclear medicine. These isotopes need to be captured or extracted before releasing in to the environment. Once the ground water contaminated with iodide, then it enters in to the food chain and accumulates in the body and dysfunctions the thyroid gland; and cause severe health hazards especially long lived radioiodine isotopes having long-lived beta-emitting activity ($^{129}I = 1.6\times10^7 y$). A review of speciation of anthropogenic and natural ^{129}I in the environmental and biological systems highlights the bioavailability and radiation toxicity aspects that necessitate the need of the selective isolation and remediation of radioiodine [B J Riley et al. 2016, S U Nandanwar et al. 2016]. It should be noted that the monitoring of iodine isotopes in the environmental samples also requires a preconcentration and separation step [L A Metz et al. 2011]. There are several sorbents developed for capturing the radioiodine in the gaseous state or dissolved in water. These are activated carbon [J Zhou et al. 2014], silver nanoparticle-containing submicron-in-size mesoporous silica [N Mnasri et al. 2014], silver-mordenite [T M Nenoff et al. 2014], nanoporous materials (activated charcoals, zeolites, and metal-organic frameworks (MOFs) [D F S Gallis et al. 2017], chalcogen-based aerogels [B J Riley et al. 2011] and polyacrylonitrile-chalcogelhybridsorbents [B J Riley et al. 2014] etc. The review on the iodine complexes with polymer seems to suggest that the iodine can bind with the skeleton of several natural and synthetic polymers [S Moulay et al. 2013]. Amongst these, poly(vinylpyrrolidone) (povidone or PVP) complex with molecular iodine exhibits distinctly disinfecting properties, and commercially available as various trade names such as Betadine [S Moulay et al. 2013]. The polymer–iodine tablet having appropriate formulation with PVP-I_2 has been developed for slow iodine release for disinfection of untreated surface water [N Mazumdar et al. 2010]. The PVP-I_2 grafted magnetic nanoparticles have been developed that exhibit significant bactericidal rate and can be reused [A N Au-Duong et al. 2015]. To provide structural integrity, Bhagat et al. have anchored PVP in the membranes for capturing and quantifying iodine species in the aqueous samples [P R Bhagat et al. 2008]. However, for efficient and fast sorption of radioiodine species in gaseous and aqueous forms, PVP has to be anchored on highly porous substrate. There are several other materials such as silver iodide metaphosphate glasses and ZnO nanolayers formed inside the air capillaries of a silica photonic crystal fibers that can be adopted for making the sensing devices for making gaseous radionuclides [I Konidakis et al. 2014].

In this section of chapter 5, the polymerizing double bond bearing 3-(trimethoxysilyl) propyl acrylate has been anchored on glass fiber filter by the sol-gel method, and its polymerizing double was used subsequently for grafting PVP on the glass fibers by UV-initiator induced polymerization. Thus, formed PVP-grafted glass fiber membrane have been appropriately characterized and subjected to I_2 sorption studies in aqueous as well as in gaseous state. ^{131}I radiotracer has been used for studying the sorption and stability of iodine on the PVP-grafted glass fiber membrane.

5A.2 Experimental

5A. 2.1. Reagents and apparatuses

The details of reagents and apparatus used are given in Chapter 2.

5A. 2. 2. Grafting of PVP on glass fibre membrane

First, the glass fiber membranes were treated with piranha solution (H_2O_2:H_2SO_4, 1: 3 v/v) for 15 min to remove the organic impurities, and then washed with distilled water followed by ethanol. These hydrolyzed glass fiber membranes were immersed in 20 mL of ethanol solution containing 2 g of 3-(trimethoxysilyl) propyl acrylate (TMSPA) for overnight with constant stirring. Thus treated glass fiber membranes were air dried.

For PVP grafting, the polymerizing solution was prepared by dissolving the monomer 1-vinyl-2-pyrrolidone (VP) (2g), cross-linker ethylene glycol dimethyl acrylate (EGDMA) (0.18g), and UV-initiator α,α'-dimethoxy-α-phenylacetophenone (DMPA) in 5 mL *N,N'*-dimethyl formamide (DMF). The amounts of cross-linker and monomer were adjusted in the polymerization solution to get 5 mol% cross-linking, and the amount of UV-initiator was taken as 2 wt.%. For PVP-grafting, the TMSPA anchored host glass fibre membrane was soaked in the polymerizing solution for overnight, taken out and removed excess of polymerizing solution by dripping, and sandwiched between two transparent polyester sheets to prevent any possible loss of grafting solution from the membrane. Finally, the polyester sheets covered polymerizing solution filled glass fibre membrane was exposed to 365 nm UV light in a photo reactor for a period of 30 min. After exposure in the photo reactor, the PVP-grafted glass fibre membrane was washed thoroughly with DMF and distilled water to remove the un-grafted material.

5A. 2. 3. Sorption-desorption and stability studies

The ion-exchange capacity of the PVP-membrane substrates were measured as described elsewhere using 0.1 M KI spiked with a known activity of ^{131}I [V Chavan et al. 2018]. The iodine capacity of the PVP-membrane was measured by dissolving a known amount of I_2 crystals in chloroform containing known activity of $^{131}I_2$. In measurement, two equilibration tubes containing standard solutions of I_2 (0.05M) (3mL) spiked with ^{131}I (radiotracer) was prepared. Among two stock standard solutions, one stock was treated as to measure initial activity and other stock was used to measure the leftover activity after an overnight equilibration of the pre-weighed PVP-membrane to get the I_2 loading capacity. Also for I_2 loading capacity measurement, two standards were prepared by spiking known amount of stock solution on 2×2cm filter paper. The amount of I_2 (mmol/g) ion in the sample was obtained by comparing the activity of ^{131}I in the membrane samples with standards having identical shape and size to the membrane samples from the stock solution containing same active ($^{131}I^-$) to stable iodide ($^{127}I^-$) ratioby using a well-type NaI(Tl) detector based gamma ray spectrometer.

To study the sorption efficiency of gaseous I_2 in PVP membrane, a stock containing chloroform spiked with $^{131}I_2$ tracer was prepared. 1mL of stock solution having measured γ-activity of $^{131}I_2$ was taken in the glass vial. The PVP-membrane having 2×2 cm dimensions was cut and fixed on the mouth of vial containing $^{131}I_2$ tracer in chloroform, and allowed the membrane for overnight exposure to evaporated I_2. After exposure, the PVP-membrane was removed sealed in polythene and subjected to measurement of activity loaded in membrane. The vial containing stock solution was checked for a residual γ-activity leftover by adding same volume of chloroform and measuring known volume of aliquot. The difference in the initial stock activity and residual γ-activity used to calculate the amount of activity converted to gaseous I_2. The extraction efficiency was calculated by knowing the activity in the membrane and fraction of activity converted to gaseous I_2.

To study extraction efficiency of iodine in I_2 form in the PVP membrane below its loading capacity, a stock containing chloroform spiked with ^{131}I tracer was prepared. 2 mL of stock solution was taken in the vial. The stock was measured by taking 100 µL aliquot for initial activity measurement. The PVP-membrane (2×2 cm) was cut and immersed in the vial containing ^{131}I tracer solution in chloroform for overnight equilibration. The vial containing stock solution was checked for the γ-activity leftover after the equilibration by measuring same volume of aliquot.

The de-loading study was carried out by equilibrating I_2 loaded PVP functionalized glass fibre membrane with 10 mL 0.5M NaOH solution. After 1h, the PVP-membrane was removed from NaOH solution, wiped with tissue paper and measured for the leftover activity in the membrane by using a well-type NaI(Tl) detector. Again the I_2 loaded PVP membrane was put back in the NaOH solution for overnight equilibration for complete de-loading.

For monitoring the stability of I_2 complexed in the PVP-membrane, the pin holed polythene packet containing $^{131}I_2$-loaded PVP-membrane was monitored as function of time. The activities of ^{131}I (radiotracer) were monitored by using a well-type NaI(Tl) detector based gamma ray spectrometer. The sample was counted for sufficient time interval to have sufficient counts accumulated in the ^{131}I region of interest. The decay corrected γ-activity in the PVP-membrane was evaluated for the possibility of loss of I_2 from the PVP-membrane during storage.

5A. 3. Results and discussion

5A. 3. 1. Synthesis of PVP-grafted glass fiber membrane

The grafting of PVP on the glass fiber membrane involved two steps. In the first step, the polymerizing double bond bearing silane TMSPA was anchored on the surface of glass fibers by sol-gel method. In subsequent step, the UV-initiator induced graft-polymerization was used to form PVP chains on the glass fiber membrane. The use of cross-linker ensured that homo-polymerized PVP chains were also linked with the PVP chains grafted on the glass fibers. Thus, the cross-linked PVP linked with glass fibres were expected to form in the voids in the glass fiber membrane. The chemical reactions involved in both the steps are depicted in Scheme 5A.1. The presence of expected functional groups, as expected from Scheme 5A.1., was confirmed by FTIR spectroscopy of the untreated pristine glass membrane, TMSPA-anchored membrane, and final PVP-grafted membrane. It is seen from Figure 5A.1 that the FTIR spectrum of TMSPA-anchored membrane consisted of broad peak around 3400 cm^{-1}, at 1700 cm^{-1} and 2900 cm^{-1} corresponding to –OH group, carbonyl, and aliphatic carbon, respectively, as expected from Scheme 5A.1. After grafting, the FTIR spectrum exhibited much smaller peak 3400 cm^{-1} indicating most of the –OH groups were consumed in the formation of silicon oxide. The peaks at 1750 cm^{-1} was associated to carbonyl stretching of the five-member cyclic lactam structure, and other peaks related to C-H, C-H_2 and C-N groups were also seen in the FTIR spectrum of PVP-grafted glass fiber membrane. This confirmed the expected chemical structure of the PVP-grafted membrane.

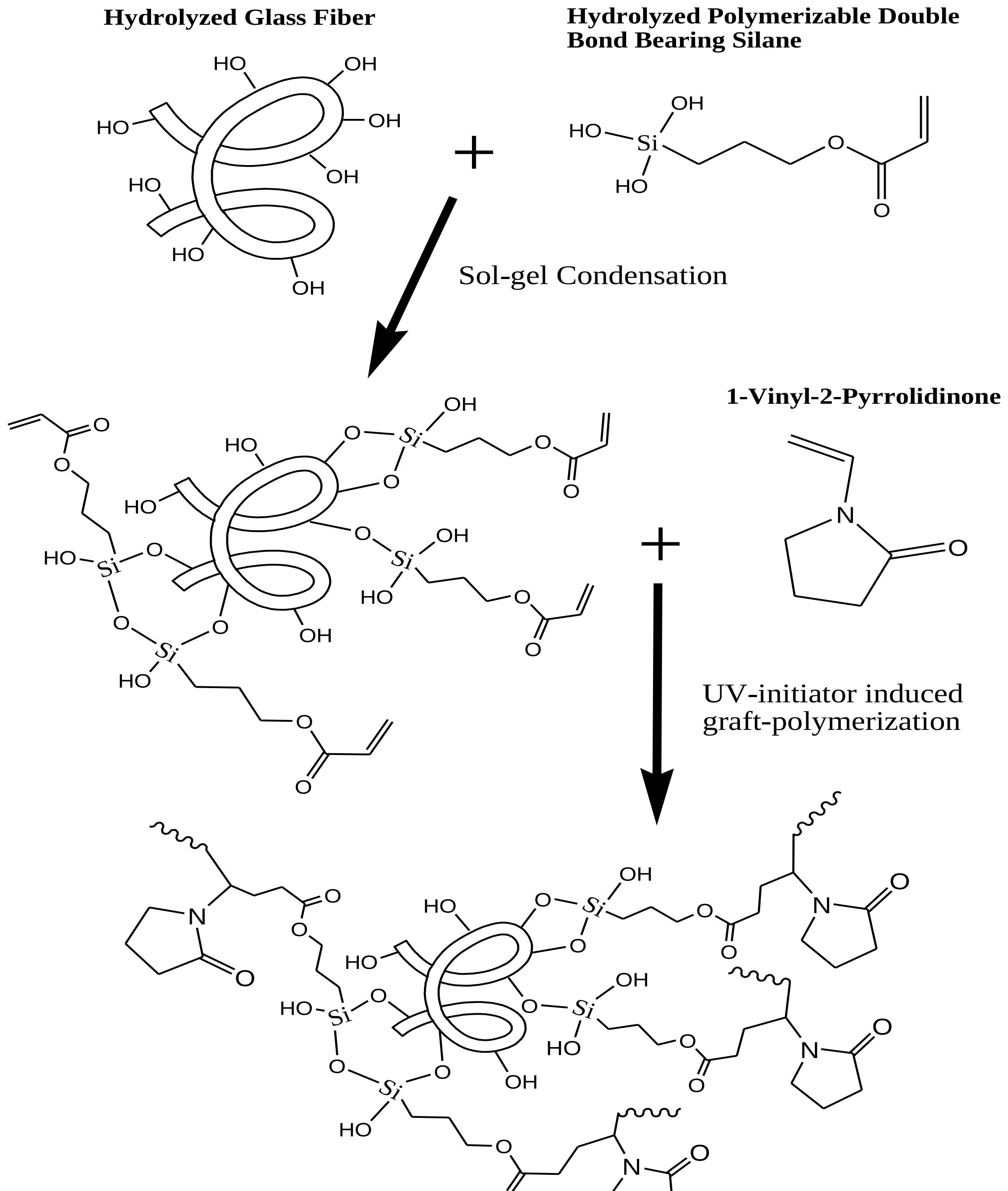

Scheme 5A.1. The chemical reactions involved in the grafting of PVP in the glass fiber membrane.

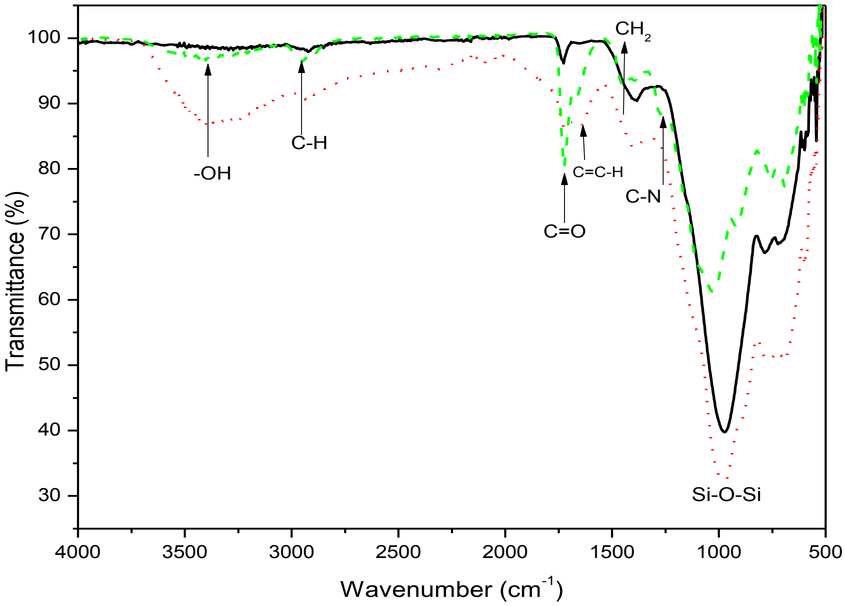

Figure 5A.1. FTIR spectra of the pristine glass fiber membrane (solid black line), TMSPA-anchored membrane (dotted red line), and final PVP-grafted membrane (dashed green line).

In present work, the PVP grafted filters were used to study iodine absorption from solution containing trace level concentration of iodine. However, smaller is the size of the fibres/rods available in the membrane/filter, more (3-(trimethoxysilyl) propyl acrylate (TMSPA) can be anchored due to more surface area available on individual fibre. Increase in TMSPA sites would result in increase in the PVP grafting, which is responsible for the iodine loading capacity. From gas phase radioiodine sorption, the porosity (flow rate) and accessible binding are important for iodine sorption. In the present work, commercially available glass fibers membrane was used to study the feasibility. In actual application, these properties can be tuned depending upon the requirements. The storage performance would be depended solely on the binding mechanism of PVP with iodine. The size of the PVP grafted rods as such would not have any role in the iodine storage.

5A. 3. 2. Characterizations of PVP-grafted glass fiber membrane

The physical characterization of the PVP-grafted glass membrane was done by SEM and FE-SEM imaging. It is seen from the comparison of SEM images of pristine and PVP-grafted glass fiber membrane that physical structure was significantly changed in terms of surface roughness/thickness of glass fibers and material incorporated in the spaces of overlapping fibers, see Figure 5A.2a & b. The high-resolution FE-SEM images showed that the grafted cross-linked PVP gels were also formed in voids of the glass fibers membrane and possessed nanoporous structures, see Figure 5A.2c & d.

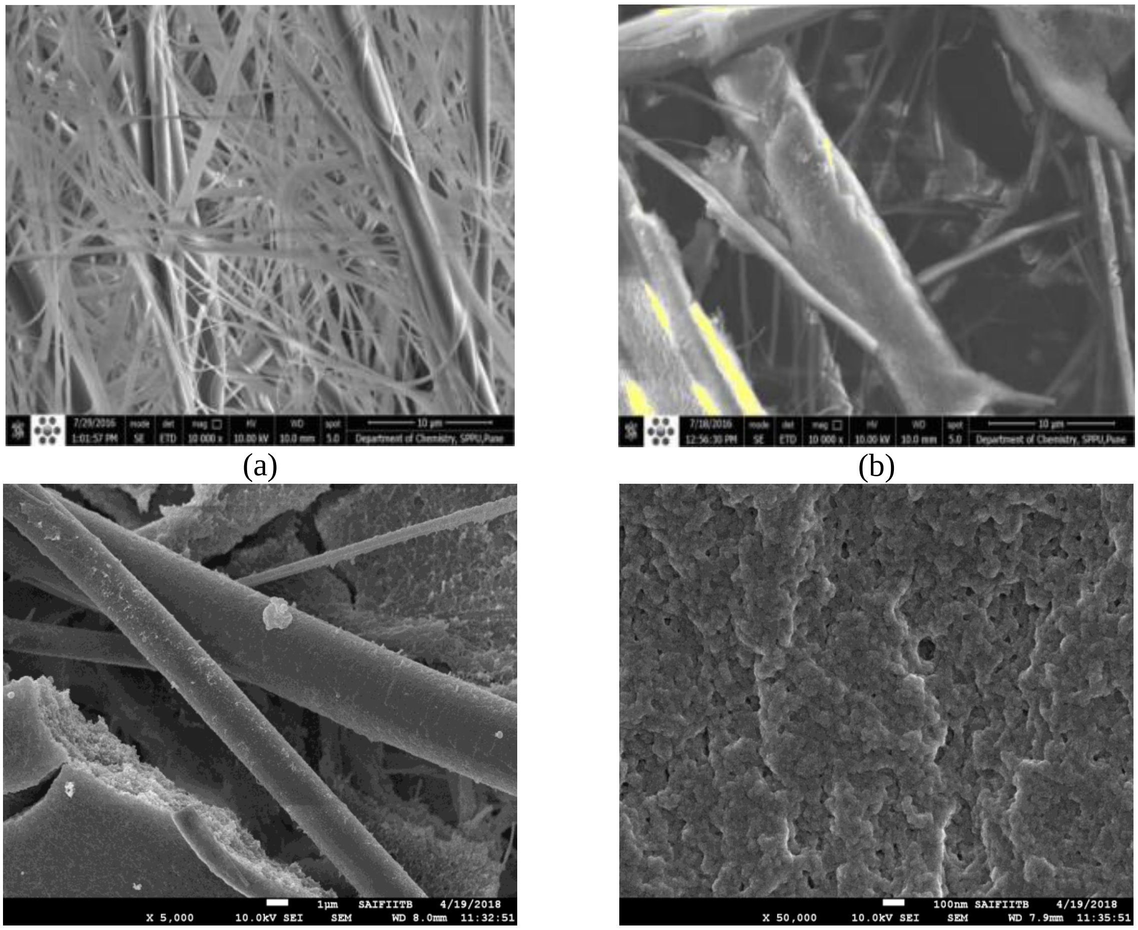

(a) (b)

(c) (d)

Figure 5A.2. SEM images of the pristine glass fiber membrane (a) and the PVP-grafted glass fiber membrane (b). The images (c) and (d) are high resolution images of the PVP-grafted glass fiber membrane obtained by FESEM.

To understand the distribution of PVP grafted in the membrane, elemental mappings of Si, O, C and N were carried out using the energy dispersive X-ray spectroscopy (EDX) attached to FESEM. The Si and O elemental mappings given in Figure 5A.3 suggested that Si and O atoms were distributed in the rod shapes as these are major constituents of the structural material of glass fibers. As can be seen form Figure 5A.3, the Si atoms were confined to the glass fibers only suggesting that TMSPA was grafted and did not deposit in the spaces in the glass fiber membrane. As expected from final structure of PVP-grafted membrane given in Scheme 5A.1, the O atoms distribution was extended to outside the glass fibers in the grafted PVP region. Contrary to Si and O elemental mappings, the N and C atoms were distributed throughout indicating the bulk of cross-linked PVP were formed in the spaces between the glass fibers as expected from Scheme 1, see Figure 5A.3.

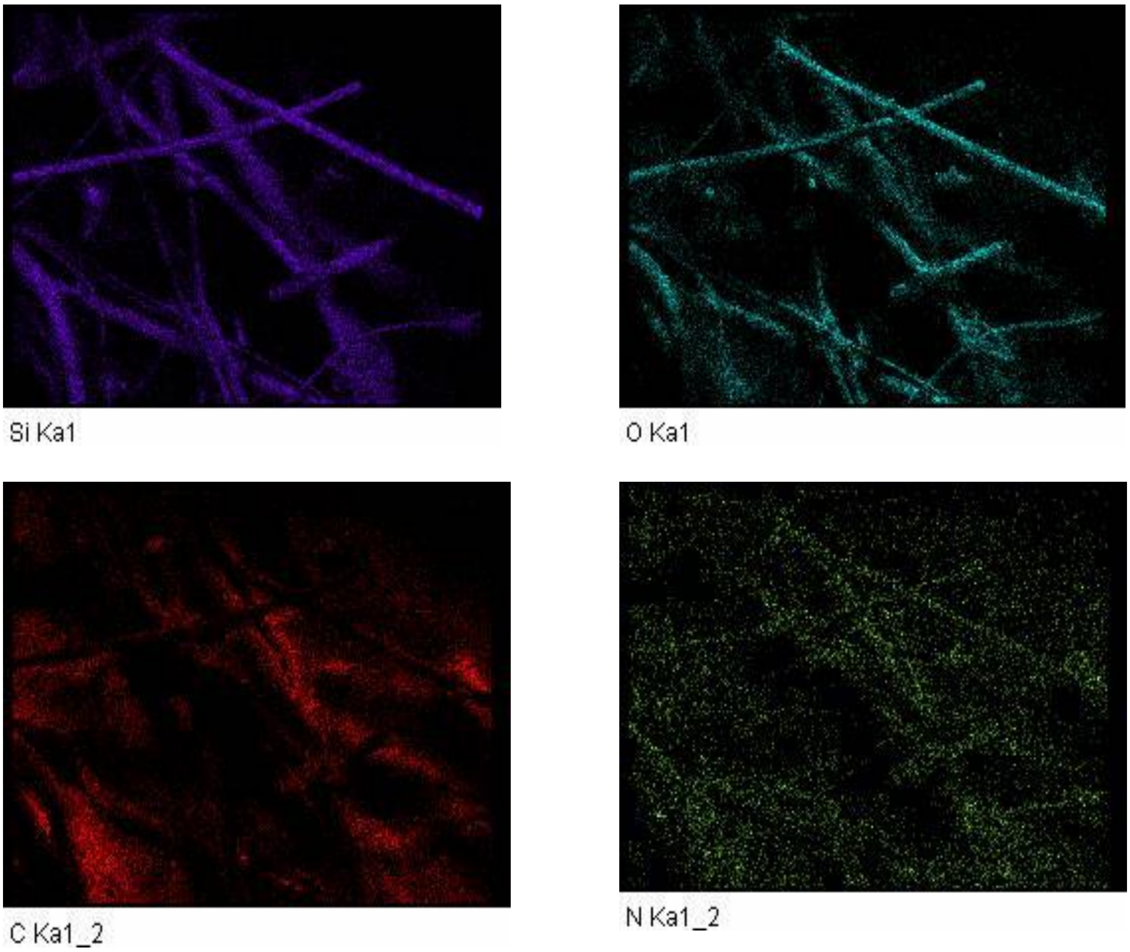
Si Ka1

O Ka1

C Ka1_2

N Ka1_2

Figure 5A.3. Elemental mappings of Si, O, C and N in the PVP-grafted glass fibers membrane by the energy dispersive X-ray spectroscopy (EDX) attached to FESEM.

The thermal stability and amount of TMPSA and PVP grafted in the glass fiber membrane were studied by thermo-gravimetric analysis (TGA). The thermograms of pristine, TMPSA-anchored membrane, and PVP-grafted glass fiber membranes are given in Figure 5A.4. It is seen from the thermogram that the TMPSA-anchored glass membrane decomposed at multiple steps. These steps can be assigned to bound water, condensation of hydroxyl group to form Si-O-Si bonds and finally decomposition of the anchored TMPSA moiety. Contrary to this, the final PVP-grafted membrane thermal decomposition had single step starting from 350 to 500 °C. Thus, the weight of grafted PVP can be obtained from weight loss from 350-500 °C which corresponded to be ≈23 wt.%. Also, the PVP-grafted membrane was thermally stable up to 350°C.

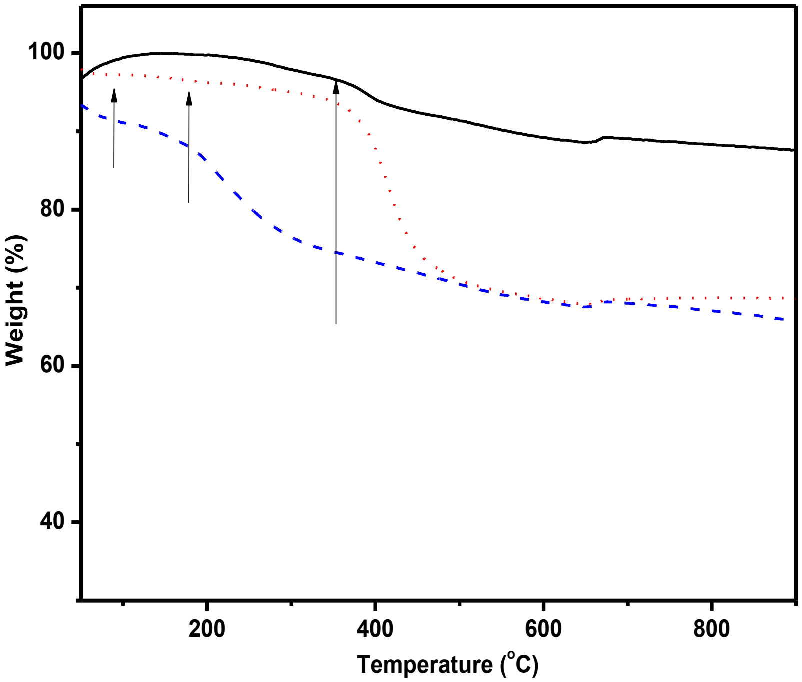

Figure 5A.4. Thermograms of pristine (solid black line), TMPSA- anchored membrane (dotted blue line), and PVP-grafted (dashed red line) glass fiber membranes recorded at the heating rate of 10^0C min^{-1} from 30^0C to 900^0C, under dynamic condition and in air atmosphere (50 mL min^{-1}).

5A. 3. 3. Iodine sorption studies

Molecular iodine hydrolyzes in which water results in the existence of several iodine species the aqueous solution such as I^-, I_2, I_3^- and HOI. The possible bindings of PVP with different iodine species are shown in Scheme 5A.2. I_3^- anionic species bind with PVP as shown in structure (a) of Scheme 5A.2 [S Moulay et al. 2013]. It is also possible that the tertiary amine nitrogen of PVP may get quaternized in acidic solution and bind with I_3^- anions as shown in structure (b). The neutral molecular iodine is expected to bind as shown in the structure (c).

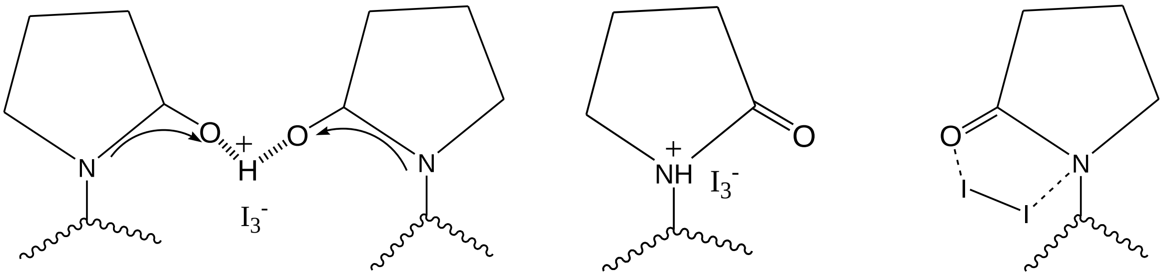

(a) (b) (c)

Scheme 5A.2. Iodine species possible binding modes in PVP-grafted glass fiber membrane.

To understand the sorption of iodine species, the UV-Vis spectra of molecular iodine dissolved in the distilled water and chloroform were obtained as shown in Figure 5A.5. The absorption peaks at 288.8 nm and 351.7 nm corresponding to I_3^- and 461.3 nm at corresponding to I_2 were observed in the UV- vis absorption spectrum of iodine dissolved in water. This is similar to that reported in literature [P R Bhagat et al. 2008, D B Gazda et al. 2004]. The molecular iodine absorbance peak at 516 nm was observed in the UV- vis spectrum of I_2 dissolved in chloroform.

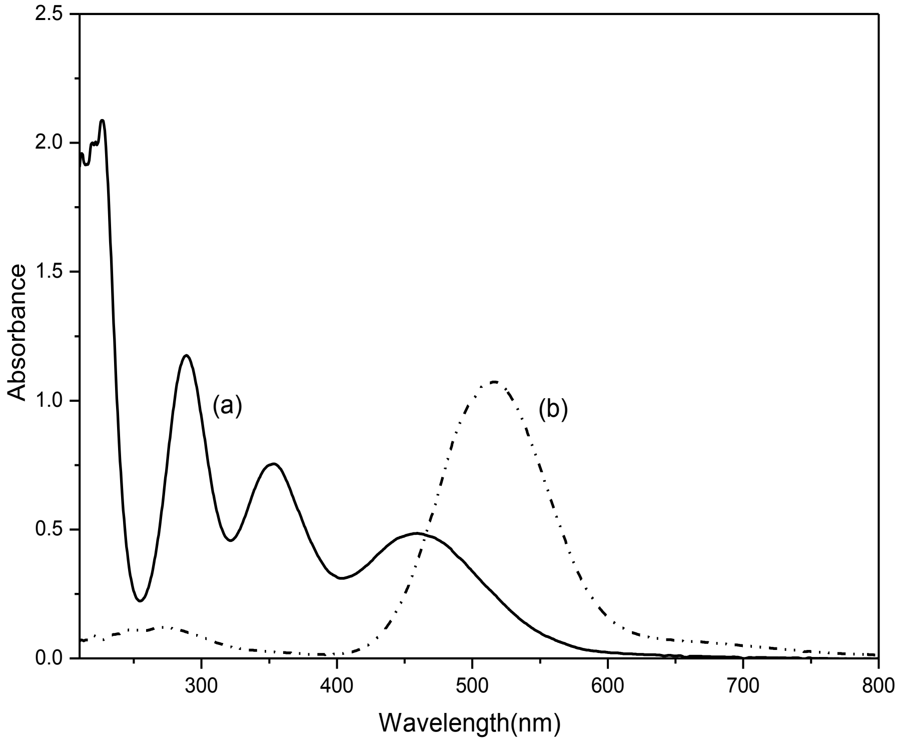

Figure 5A.5. UV-Vis spectra of molecular iodine dissolved in water (a) and in chloroform (b).

To study the sorption of iodine species, the PVP-grafted glass fiber membrane samples were equilibrated for a fixed in the solutions formed by dissolving molecular iodine in water and chloroform. The UV-Vis spectra were recorded before equilibration and after equilibration of the membrane sample for a fixed period of time with a constant stirring. It is seen from Figure 5A.6a that, the absorbance of peaks corresponding of I_2 and I_3^- species are significantly decreased in UV-Vis spectrum of molecular iodine dissolved water and recorded after equilibration of the PVP-membrane sample for 3 h. This seems to suggest that both I_2 and I_3^- species sorbed quantitatively in the PVP-membrane. In case of molecular iodine dissolved in chloroform, the absorbance peak corresponding to I_2 decreased to some extent after 1 h equilibration of the PVP-membrane (Figure 5A.6b) but did not decrease significantly thereafter. This could be attributed to fact that the molecular iodine affinity towards chloroform is significant with respect to aqueous solution.

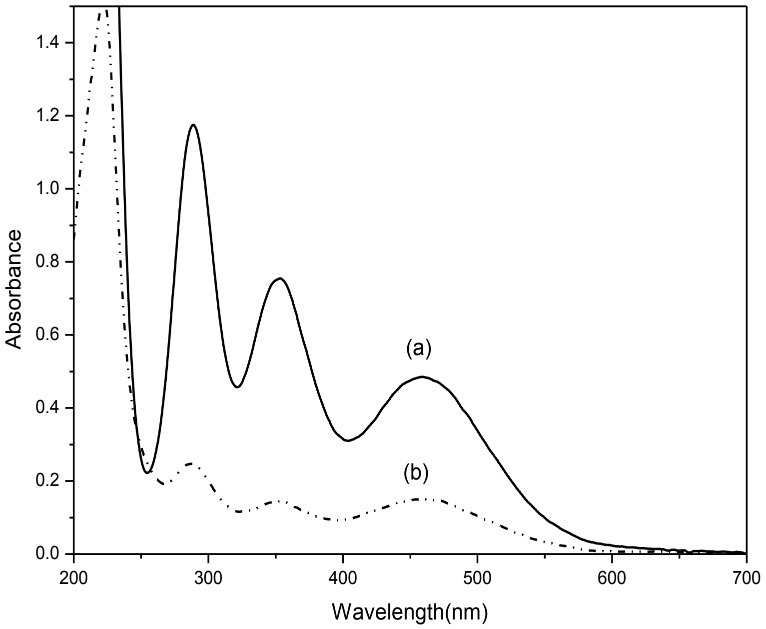

(a)

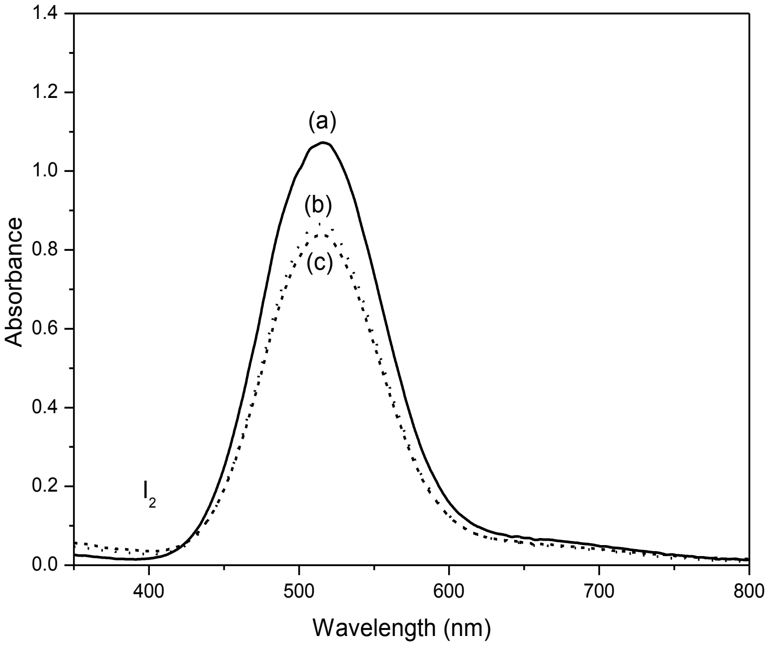

(b)

Figure 5A.6. (a) UV-Vis spectra of water containing dissolved molecular iodine initially (curve a) and after equilibration of the PVP-membrane sample for 3 h (curve b), and (b) UV-Vis spectra of molecular iodine dissolved in chloroform before equilibration (curve a) and after equilibration of the PVP-membrane sample for 1 h (curve b) and 3 h (curve c).

5A. 3. 4. Radiotracer Studies

The radiotracer ^{131}I was used to measure the loading capacities of I^- and I_2 in the PVP glass fiber membrane as described in the experimental section. Molecular iodine loading capacity of the PVP-glass membrane was measured using ^{131}I tagged I_2 dissolved in chloroform in which no other species of iodine is formed as observed from UV-Vis spectrum given in Figure 5A.5. The I^--loading capacity was measured using ^{131}I tagged I^- dissolved in water. The I^- and I_2 loading capacities were found to be 0.1 mmol g^{-1} and 1.13 mmol g^{-1}, respectively. This clearly suggest that the existence of quaternary ammonium sites shown in structure-b of Scheme 5A.2 in the PVP-membrane was not a major binding sites leading to very low (0.1 mmol g^{-1}) loading of I^- by ion-exchange interactions. The major binding sites appears to be that shown in structures a & c in Scheme 5A.2. The extraction efficiency of molecular iodine in ^{131}I tracer form, which was considerably lower than the loading capacity, was measured by measuring the γ-activity in the membrane and fraction of activity converted to gaseous I_2. The extraction efficiency of gaseous radiotracer I_2 in the PVP glass membrane was found to be 45%. However, the extraction efficiency of radiotracer I_2 form direct equilibration of the PVP glass membrane chloroform was found to be 31%. This could be attributed to fact that the molecular iodine has higher affinity towards chloroform. It was observed that 97% I_2 could be de-loaded during 1 h equilibration with 0.5M NaOH solution. The PVP - membrane sample was again tested for de-loading of the leftover I_2 in the PVP-membrane after overnight equilibration with 0.5M NaOH solution. However, it was observed that 2% I_2 activity remained intact in the PVP-membrane. This could be due to the formation of I^- during de-loading and the PVP-membrane had 0.1 mmol g^{-1} loading capacity of I^- as described earlier. The stability of the loaded I_2 in the PVP grafted glass membrane was tested by monitoring the γ-activity of ^{131}I of the radiotracer tagged I_2 loaded PVP-membrane. It is seen from the Figure 5A.7 that the decay corrected γ-activity of ^{131}I in the PVP-membrane did not decrease in the membrane kept under ambient conditions for 12 d. Thus, the molecular iodine loaded in the PVP-membrane has reasonably good stability and could be used for its storage.

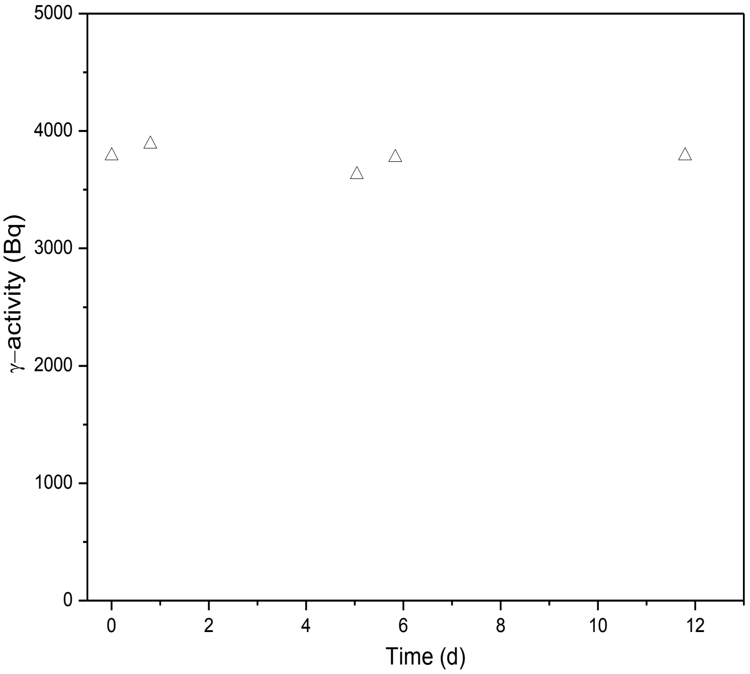

Figure 5A.7. Variation of the decay corrected γ-activity of ^{131}I in the PVP-membrane as function of time kept under ambient condition.

The storage depends on the stability of I_2-PVP complex under given condition. It was observed from the thermal analysis that the decomposition temperature for PVP grafted membranes was around 350-500 ^{0}C. The PVP-grafted membrane was thermally stable up to 350 ^{0}C. As shown in Scheme 5A.2, the possible bindings of PVP with different iodine species where PVP structure plays an important in the binding mechanism with iodine.

5A. 4. Conclusions

A new synthetic route has been developed for grafting the crosslinked PVP chains on the glass fiber membrane. Thus formed PVP-membrane has been characterized for its chemical and physical structures. The TGA studies showed that the extent of PVP grafting was order of ≈23 wt.%, and thermally stable up to 350 ^{o}C. The UV-Vis absorbance spectra revealed that the iodine species formed by dissolving molecular iodine such as I_2 and I_3^- were sorbed quantitatively in the PVP-membrane. The I^- and I_2 loading capacities were found to be 0.1 mmol g^{-1} and 1.13 mmol g^{-1}, respectively. This membrane was found to capture gaseous radioiodine with 45% efficiency and remained intact in the membrane for 12 days indicating its reasonably good stability in the membrane for a long time storage. The molecular iodine sorbed in the membrane could be de-loaded by 1h equilibration in the 0.5M NaOH solution.

SECTION 5B: FUNCTIONALIZED GLASS FILTER MEMBRANE FOR RADIOCESIUM

5B.1. Introduction

Radiocesium is one of the important fission products produced with significant yield, some of its isotope such as ^{137}Cs has long half-life, and mobile in the aquatic environment. From nuclear waste remediation point of view, long lived fission products such as ^{137}Cs and ^{90}Sr have to be isolated to avoid thermal load for better handling of radioactive waste before disposal. During confinement of radioactive waste in different solid matrices, it is observed that cesium gets separated from the matrices due to leaching and evaporation. Main reason for Cs in environment is due to its association with the particulates [P G Appleby et al. 2008, Q He et al. 1996, F Zapata et al. 2003, D E Walling et al. 1993, M E Ketterer et al. 2004]. The direct estimation ultratrace concentration of radiocesium is often difficult using routinely used γ-spectrometry. Hence, the isolation of radiocesium from the environmental, biological and geological samples and its preconcentration is very important before detection and quantification.

There are several methods reported in the literature for selective separation of Cs form actinide and fission products [S Peper et al. 2005]**.** The inorganic materials have been used for the cesium partitioning and quantification [B F Rider et al. 1960, N Yamagata et al. 1965, L E Glendemn and C M. Nelson, Paper 283, Nat1 Nuclear Energy Serves Div. 4. 9, book 3, 1942 (1951), J C Langford 1957, R B Hahn 1956, G M Alhson et al. 1951, A L Born et al. 1966, H G Petrow et al. 1957]. Membranes having macrocyclic functionalities are also reported for the cesium detection [M B Saleh et al. 2003, A S Attiyat et al. 1988, M G Fallon et al. 1996, M Shamsipur et al. 2001, A V Bogatsky et al. 1984, M Bochenska et al. 2003, A Cadogan et al. 1990**].** Cs^+-selective membrane electrodes based on 1,3-dialkyloxy calix[4]arene have been developed **[** C D Gutsche et al. 1987, C D. Gutsche et al. 1983, A Casnati et al. 1995, R Ungaro et al. 1994, E Ghidini et al. 1990, Z Asfari et al. 1992, Z Asfari et al. 1993, J S Kim et al. 2000; J S Kim et al. 1998**]**. With an objective of disposal of radioactive waste, several Cs-selective extractants have been developed. **[**Y Choi et al. 2004]**.** Heteropolyacids (HPAs) have been reported as one of the matrix modifiers due to its thermal stability [H Tian et al. 2006]**.** HPA such as silicotungstic ($H_4SiW_{12}O_{40}$, HSiW), phosphotungstic ($H_3PW_{12}O_{40}$, HPW) and phosphomolybdic ($H_3PMo_{12}O_{40}$, HPMo) are considered as highly attractive solid acid catalysts, having superior acidic characteristics. Many salts of heteropolyacid including cesium has been prepared by the ion-exchange mechanism and studied.**[** L Degirmenci et al. 2011]**.** It is observed that the complex of cesium with heteropolyacid is stable in acidic and oxidising conditions. **[**Z L Liuzhongqun et al. 1996**].** Cesium- silicotungstate anchored on Al_2O_3 has been developed, and evaluated for the catalytic dehydration of glycerol **[**M H Haider et al. 2012**]**. It is interesting to note from the literature that most of the HPAs have remarkable selectivity toward cesium (Cs) ions. However, it is difficult to desorb the Cs from HPAs, and therefore cannot be used for developing the reusable solid phase substrate having reproducible geometry which can be directly subjected to quantification for ^{137}Cs using γ-spectrometry.

In the present work, for selective preconcentration of Cs, silicotungstic acid was immobilized in poly(3-(trimethoxy silyl)propyl acrylate) matrix grafted glass fibers formed by sol-gel route and UV-initiator-induced graft polymerization, Thus formed glass substrate has been characterized by several techniques such as FTIR, FESEM, EDS, and XRD. The chemical affinity of the silicotungstic acid functionalized glass fibres membrane toward Cs ions has been studied in the presence of representative competing ions such as Na^+, Ba^{2+} and Sr^{2+} in aqueous solution using γ-spectrometry.

5B.2. Experimental

The details of reagents and apparatus used are given in Chapter 2.

5B.2.1. TMSPAgrafting on glass fibre membrane

First, the glass fiber membranes were treated with piranha solution (H_2O_2:H_2SO_4, 1:3 v/v) for 15 min to remove the organic impurities, and then washed with excess of distilled water followed by ethanol. For poly(3-(trimethoxysilyl) propyl acrylate) grafting, the monomer solution was prepared by dissolving 3-(trimethoxysilyl) propyl acrylate (TMSPA) (2g), and UV-initiator α,α'-dimethoxy-α-phenylacetophenone (DMPA) dissolved in 5 mL *N,N'*-dimethyl formamide (DMF). The amount of UV-initiator was taken as 2 wt.%. Glass fiber membranes samples were soaked in the polymerizing solution for overnight, taken out and removed excess of solution clinging on the surface. These membranes were sandwiched between two transparent polyester sheets to prevent any possible loss of grafting solution from the membrane. Finally, the polyester sheets covered and polymerizing solution filled glass fibre membranes were exposed to 365 nm UV light in a photoreactor for a period of 30 min. After UV-exposure, the poly(3-(trimethoxysilyl) propyl acrylate)grafted glass fibre membranes(poly(TMSPA)@GFM) were washed thoroughly with DMF and distilled water to remove the un-grafted material.

5B.2.2. Formation of SiWH –poly(TMPSA)@GFM

Anchoring of cesium selective functionality, the silicotungstic acid (SiWH), was done by soaking the poly(TMPSA)@GFM in the solution containing 2g ssilicotungstic acid dissolved in 50 mL water for overnight. The excess solution was removed, washed with water and subsequently equilibrated with 0.1 M caesium salt solution for overnight to load Cs^+ ions by ion-exchange. After loading Cs^+ ions, these samples were washed thoroughly and subjected to thermal treatments by heating at 120^0C, 150^0C, 200^0C for 2-3 h in air for templating the Cs^+ sorption geometry.

5B.2.3. Sorption-desorption experiments

The extent of Cs-sorptions in the untemplatedand Cs^+ ions templated SiWH-poly(TMPSA)@GFM at different temperature from solutions having pH-7 and 0.5M NaCl were quantified by counting of aqueous samples (100 μL) taken from solutions before and after overnight equilibrations of the membrane samples in well-type NaI(Tl) detector based γ-ray spectrometer connected to a multichannel analyzer. The sorption efficiency (uptake) of cesium was obtained from equation (1):

$$\text{Uptake (\%)} = [A_b - A_f] / [A_b] \times 100 \qquad \textbf{(1)}$$

where A_b and A_f were gamma count rates of ^{137}Cs in the solution before and after equilibration with the SiWH-poly(TMPSA)@GFM sample (1×2 cm).

The interference of monovalent ions and acidity on the extent of Cs-sorption were also studied in varying concentration of sodium chloride solution (0.01-1M) and HNO_3 (0.01-3M), respectively. The sorption rate of ^{137}Cs was measured by monitoring uptakes as a function of time of equilibration.

The Cs^+-exchange capacity of the Cs^+ ions templated SiWH-poly(TMPSA)@GFM was measured as described elsewhere using 0.1 M CsCl spiked with a known activity of ^{137}Cs **[**V Chavan et al. 2018**].** For the ion-exchange capacity measurement, two standards were prepared by spiking known amount of stock solution on 1×2 cm filter paper. The amount of Cs^+ (mmoles) per unit weight of the substrate was obtained by comparing the activity of ^{137}Cs in the membrane samples with standards having identical shape and size to the membrane samples from the stock solution containing same active $^{137}Cs^+$ to stable Cs^+ ratio by using a well-type NaI(Tl) detector based gamma ray spectrometer. The Cs^+exchange capacity in the presence of interfering monovalent and bivalent ions was also measured in 0.5M NaCl, $BaCl_2$ and $Sr(NO_3)_2$ solutions spiked with ^{137}Cs radiotracer.

5B.3. Results and discussion

Silicotungstic acid (also known as tungstosilicic acid) has chemical structure $H_4[Si(W_3O_{10})_4]$. x H_2O, and x may be as high as 26. Silicotungstic acid has Keggin structure of heteropoly acid consisting of one Si surrounded by four oxygen atoms to form a tetrahedron. This unit is at centre and surrounded by 12 octahedral WO_6 units linked to one another by the neighbouring oxygen atoms arranged on a sphere almost equidistant from each other, in four M_3O_{13} units, giving the complete structure an overall tetrahedral symmetry. It is important to note that silicotungstic acid self-assembles in acidic aqueous solution to form polyoxometalate by hydrogen bonding. In the presence of Cs^+ ions, highly selective precipitate of cesium silicotungstate is formed, and it is difficult to take out Cs^+ ions from the precipitate. It may be attributed to geometrical arrangement of Keggin units in the self assembled structure in the presence of Cs^+ ions. Therefore, a new route was explored in the present work to first anchor the silicotungstate on the polymer matrix, and thereafter controlled rearrangement of the matrix in the presence of Cs^+ ions by heat treatment.

5B.3.1. Synthesis of SiWH-poly (TMPSA)@GFM

The preparation of SiWH-poly (TMPSA)@GFM involved two steps. In first step, 3-(trimethoxysilyl)propyl acrylate (TMSPA) was coupled on a hydrolyzed glass fiber by a sol-gel process, and simultaneously utilizing the double bonds of TMSPA for the UV-initiator-induced graft polymerization of TMSPA dissolved in DMF using UV-light (350 nm) to form poly(TMPSA) matrix inside the fibrous architecture of the glass membrane. In second step, the silicotungstic acid (SiWH) was immobilized in the poly(TMPSA@GFM) matrix utilizing one of the four H^+ exchangeable sites by sol-gel method. For making this matrix selective to Cs^+ ions, thus formed samples were equilibrated with CsCl solution to load Cs^+ ions by the ion-exchange mechanism. During heat treatments below decomposition temperature of silicotungstic acid, the water molecules were removed and condensation occurred which led to freezing of geometrical arrangement of the SiWH-poly(TMPSA)@GFM matrix. Decomposition behaviour of heteropolyacids were studied in literature using DTA technique **[** H. Atia 2008**].**The chemical reactions involved are depicted in Scheme 5.2.1.

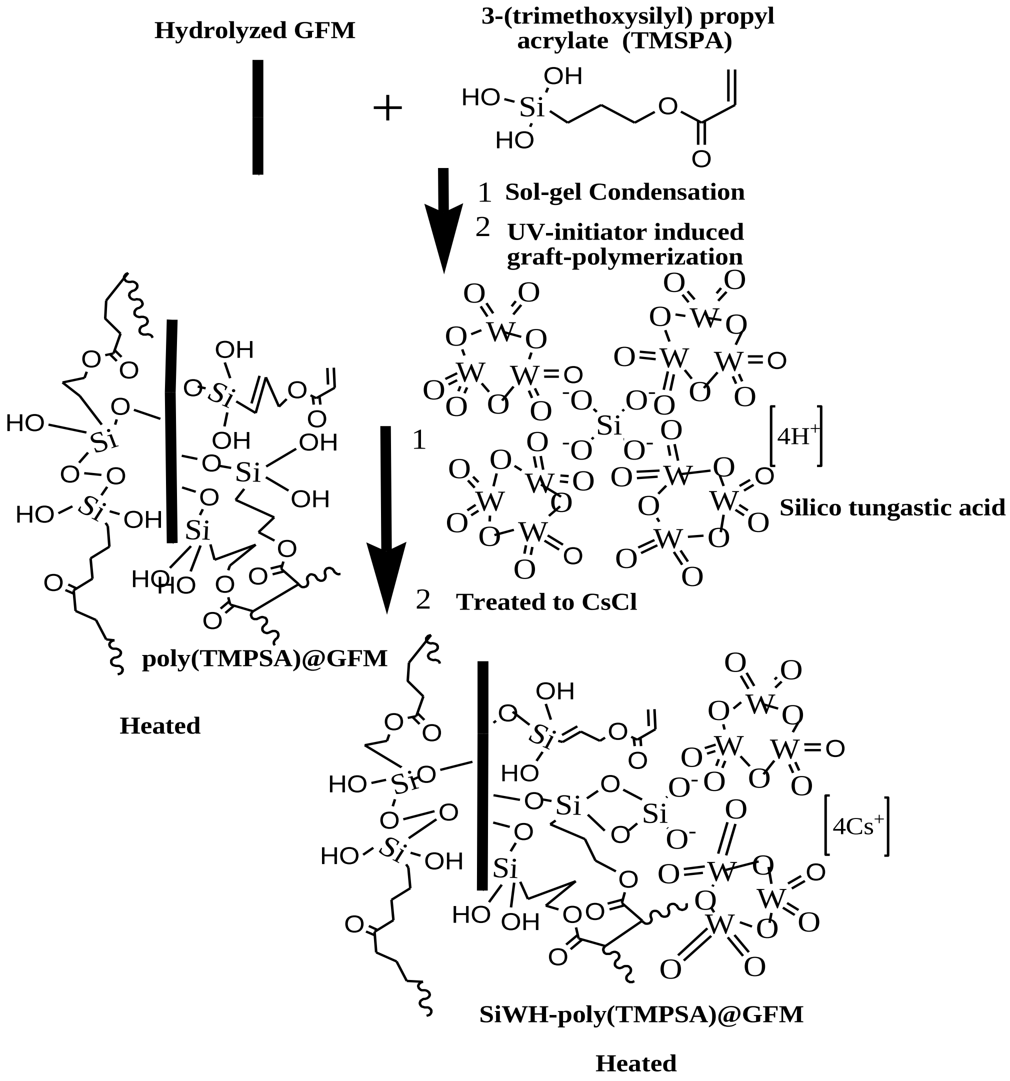

Scheme 5B.1. The chemical reactions involved in the preparation of SiWH-poly(TMPSA)@GFM.

5B.3.2. Characterizations of SiWH-poly(TMPSA)@GFM

FTIR measurements

Figure 5B.1 shows the FTIR absorptionspectra of the pristine glass fiber membrane (a), poly(TMPSA)@GFM (b), and SiWH-poly(TMPSA)@GFM(c) recorded in the 4000 to 400 cm^{-1}wavenumber range. It is seen from Figure 5B.1 (b) that TMSPA-anchored membrane consisted of broad peak around 3400 cm^{-1}, at 1700 cm^{-1} and 2900 cm^{-1} corresponding to –OH group, carbonyl, and aliphatic carbon, respectively, as expected from Scheme 5B.1. SiWH-poly(TMPSA)@GFM showed a strong absorption band centered at 3209 cm^{-1}with a prominent shoulder at 3355 cm^{-1} assigned to OH vibrations, see Figure 5B.1 (c). In addition to this, an absorption band appeared at 1708 cm^{-1} assigned to H_2O vibration, as already reported by Misono and co-workers, Highfield and Moffat**,** Bielanski et al.**,** and Essayem et al.**[**N Essayem et al. 2001**].** The Keggin anion vibration bands at 1079 cm^{-1}due to the asymmetric Si-O vibration. 795, 887 and 975 cm^{-1} bands were assigned to asymmetric W–O–W vibrations. Weaker absorption bands appeared at 596 and 525 cm^{-1} were due to symmetric W–O–W vibrations**[**N Essayem et al. 2001**].**

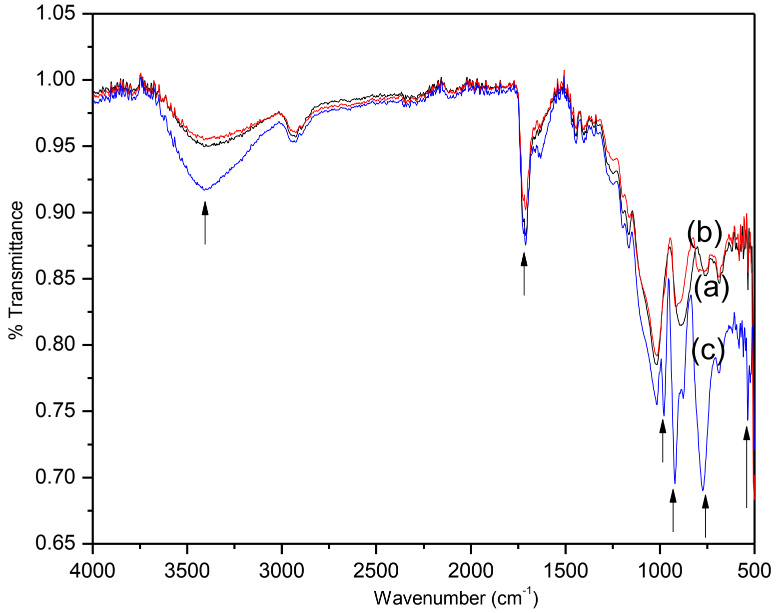

Figure 5B.1. FTIR spectra of the pristine glass fiber membrane (a), poly(TMPSA)@GFM(b), and SiWH-poly(TMPSA)@GFM(c).

To confirm the formation of SiWH-poly(TMPSA), a separate experiment was performed in which Cs salt of silicotungstic acid was prepared by adding stoichiometric amounts of an aqueous solution of caesium chloride to the desired volume of aqueous solution of silicotungstic acid as described elsewhere **[**N Essayem et al. 2001**].** The suspensions were stirred for 24 h at ambient temperature. Then, the precipitated salt was separated by centrifugation, washed twice with deionised water, and dried. The FTIR spectrum observed in case of Cs-silicotungstic acid salts shown in Figure 5B.2 (a) was comparable to SiWH-poly(TMPSA)@GFM as given in Figure 5B.2 (b). However, the intensity variation and some peak broadening were observed due to the matrix effects. Therefore, it was concluded that the Cs-silicotungastic acid complex of similar kind was formed in the SiWH-poly (TMPSA)@GFMas that of Cs-silicotungastic complex in the salt.

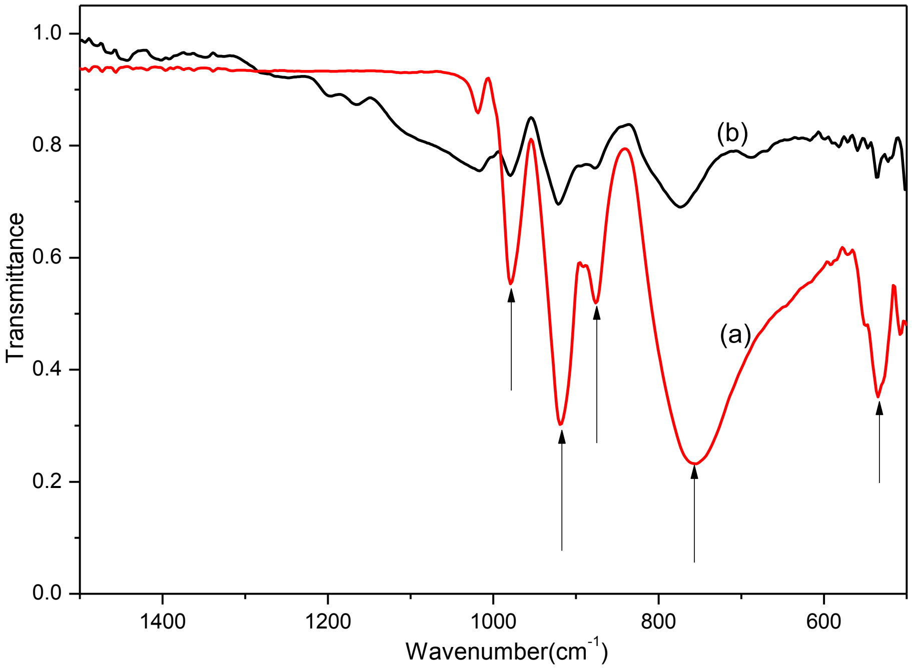

Figure 5B.2. FTIR spectra of the Cs-silicotugstic acid salt (a) and SiWH-poly(TMPSA)@GFM(b).

XRD study

The powder XRD patterns were studied to understand the formation of crystalline phase in the membrane. It is seen from the XRD patterns given in Figure 5B.3 that there were no peaks corresponding crystalline structure in the pristine glass fibre membrane (a), before condensation (heat treatment) of the poly(TMPSA)@GFM (b) and SiWH-poly(TMPSA)@GFM (c) samples. Only a broad peak corresponding to the polymer structure of the host membrane was seen.

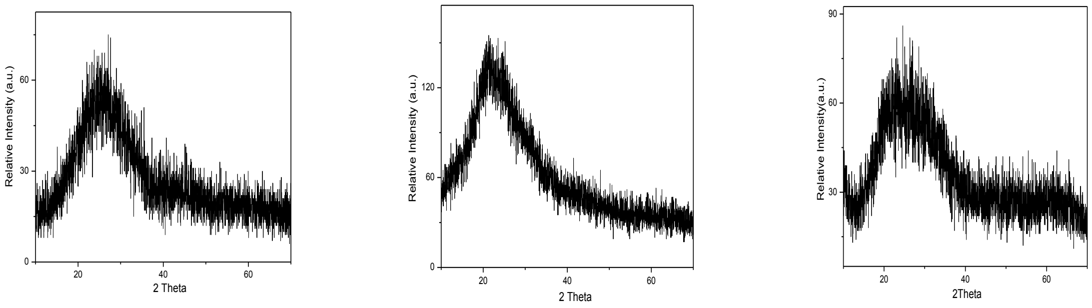

(a) (b) (c)

Figure 5B.3. Powder XRD patterns of the pristine glass fiber membrane (a), poly (TMPSA)@GFM(b) and SiWH-poly(TMPSA@GFM (c) before heat treatments.

Similarly, the powder XRD patterns were recorded after thermal treatment of SiWH-poly(TMPSA)@GFM before CsCl equilibrations at 150 ^{0}C and 200 ^{0}C to find out the formation of the crystalline phase during heating. It was observed that from Figure 5B.4 (a) and (b) that the XRD patterns obtained at 150 ^{0}C (a) and 200 ^{0}C (b) indicated the amorphous matrix with broad continuum and single peak consisting of crystalline silicon dioxide. There was a possibility that Keggin structure would be gradually decomposed. At higher temperature, the loss of water, the interaction with the support and the formation of new species were observed. However, the detailed structure evolution and the consequent activity changes with thermal treatment at elevated temperature are still not clearly unveiled. The polyoxoanions with Keggin structure were readily formed as degradation products and further increase in the calcination temperature caused total decomposition of Keggin structure **[**L. Liu et al.**].**

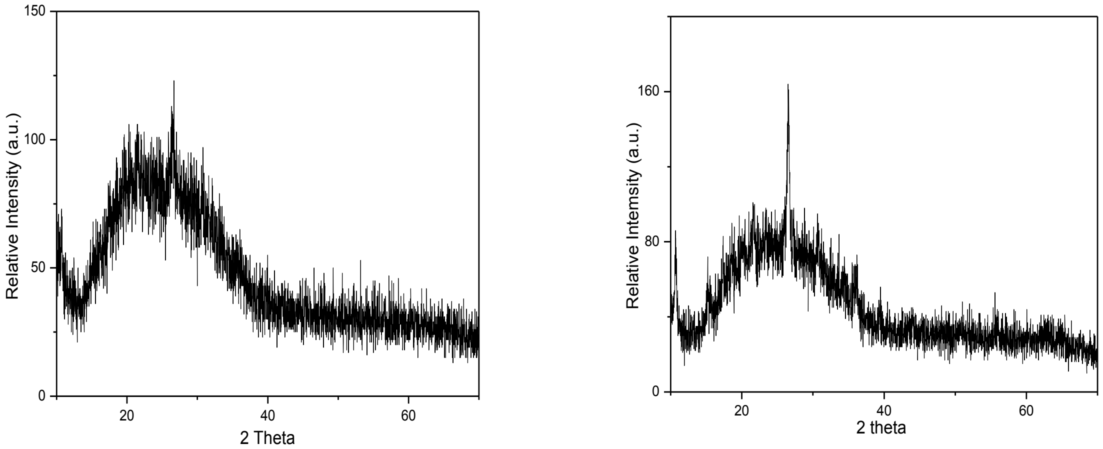

(a) (b)

Figure 5B.4. XRD patterns of the thermally treated SiWH-poly(TMPSA@GFM) at 150^{0}C (a) and 200^{0}C (b).

The XRD patterns were studied after loading Cs^{+} ions in the membrane and subjecting to thermal treatment at 120 ^{0}C. It was observed from the XRD pattern given in Figure 5B.5 that Kaggin crystalline structure was observed in the polymer matrix which was also supported by FTIR studies. The XRD pattern of the thermally treated Cs^{+}-SiWH-poly(TMPSA)@GFM was compared with the XRD pattern recorded for the Cs-silicotungstic precipitate. The XRD patterns obtained in both the cases were almost similar suggesting that the crystalline Keggin structure remained intact in the membrane. The XRD pattern of the membrane sample was compared with those reported in the literature for different Cs- silicotungstic acid compounds. The XRD pattern obtained in case of Cs^{+}-SiWH-poly (TMPSA)@GFM was in a good agreement with $Cs_4W_{12}O_{40}.12H_2O$.

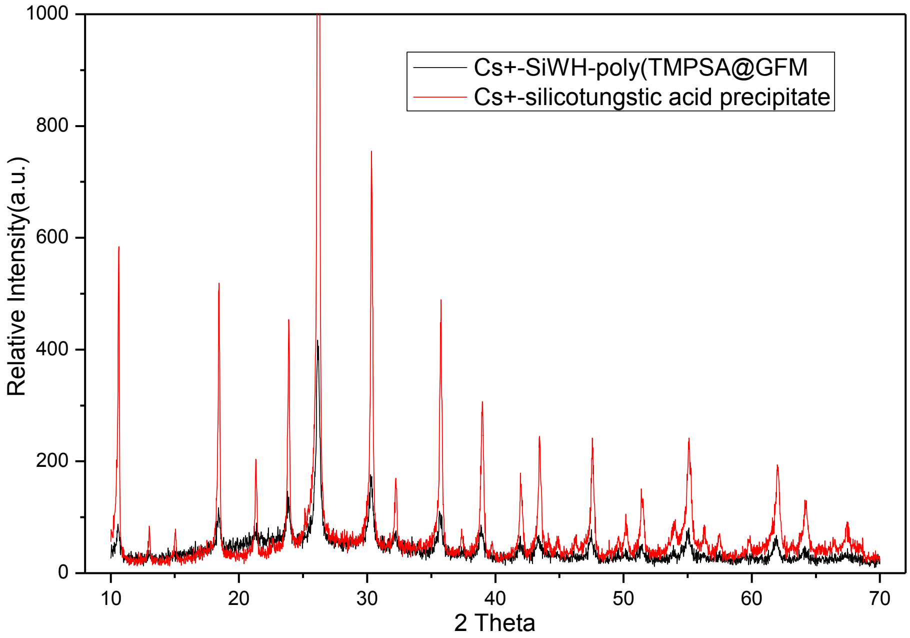

Figure 5B.5. The comparison of powderXRD patterns of the thermally treated Cs^+-SiWH-poly(TMPSA)@GFM at 120 ^{0}C with Cs^+-silicotungstic acid precipitate.

SEM Studies

The physical characterization of pristine glass membrane, thermally treated with and without Cs^+-loaded SiWH-poly(TMPSA)@GFM was done by SEM. It is seen from the comparison of SEM images of pristine glass membrane, SiWH-poly(TMPSA)@GFM that the physical structure was significantly changed in terms of surface roughness/thickness of glass fibers due to material incorporated in spaces of overlapping fibers, see Figure 5B.6 (a) & (b). In case of thermally treated without Cs^+loading in the SiWH-poly(TMPSA)@GFM it was observed (Figure 5B.6(c)) that the polymer matrix along with silicotungstic acid was decomposed indicating collapse of Kaggin crystalline structure after heating. In case of Cs^+ loaded SiWH-poly(TMPSA)@GFM, highly crystalline structure existed even after heating as can be seen from Figure 5B.6(d). This was also supported by XRD and FTIR studies.

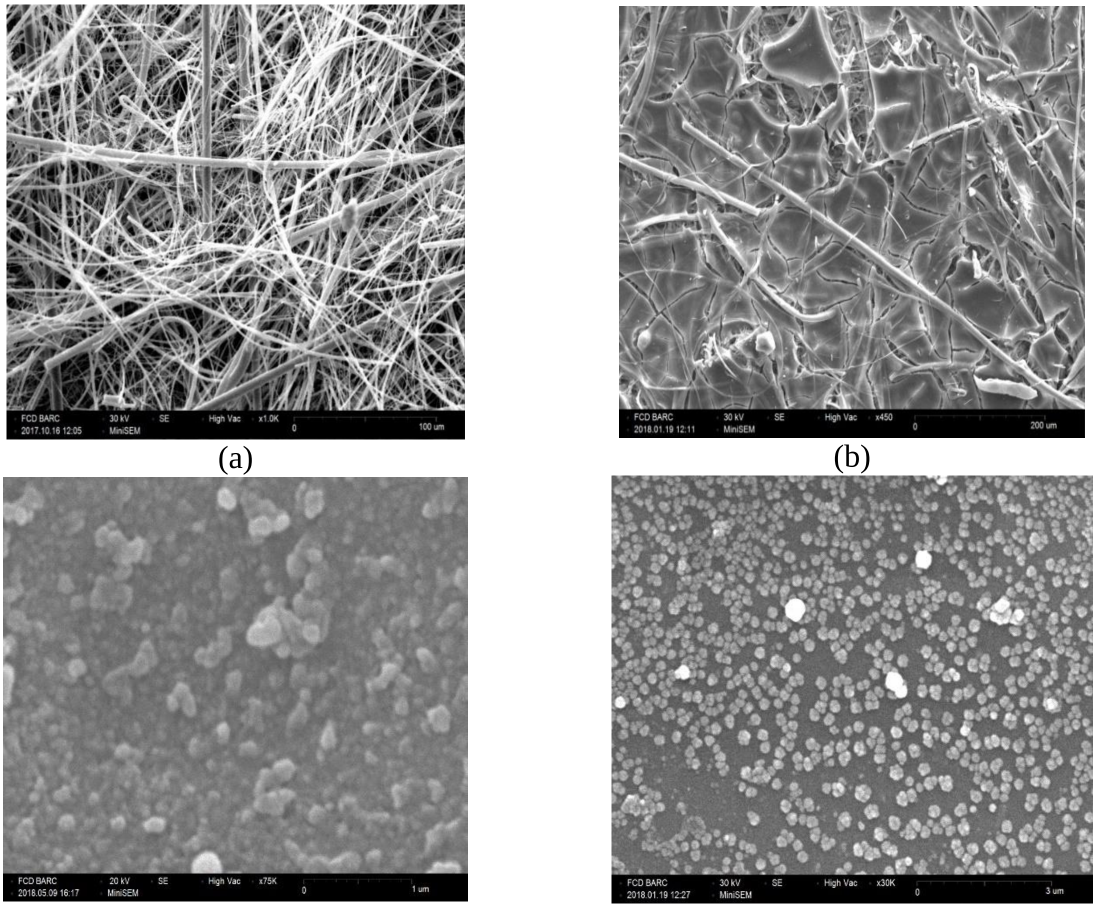

(a) (b)

(c) (d)

Figure 5B.6. SEM images of the pristine glass fiber membrane (a), thermally treated without Cs^+-loading (b) and corresponding zoomed image (c), and zoomed image of thermally treated Cs^+-loaded (d) SiWH-poly(TMPSA)@GFM.

5B.3.3. Radiotracer Studies

The radiotracer ^{137}Cs was used to measure the loading capacities (mmol/g) of Cs^+ in the final SiWH-poly(TMPSA)@GFM samples after Cs^+-loading and thermal treatmentas described in the experimental section. The obtained loading capacity was 0.15 mmol g^{-1}. Cs^+-loading capacities were also measured in the presence of very high concentration (0.5 M) of Na^+, Ba^{2+} and Sr^{2+} ions and was found to be 0.15, 0.13, 0.13 mmol g^{-1}, respectively, as shown in Table 5B.1. This seems to suggest that most binding sites were specific to Cs^+ ions and only less than 15% sites were not imprinted for the Cs^+ ions.

Table 5B.1. The ion-exchange capacity values for Cs^+ ions in the presence of Na^+, Ba^{2+} , Sr^{2+} ions (0.5 M).

ion	**Cs^+-loading capacity (mmol/g)**
Cs	0.15
Na	0.15
Ba	0.13
Sr	0.13

The radiotracer ^{137}Cs was used to measure Cs^+ uptake from pH 7 and 0.5 M NaCl solution in the thermally treated without Cs^+-loading in the SiWH-poly(TMPSA)@GFM samples as shown in Figure 5B.7. It is evident from this figure that the Cs^+-uptake efficiency was increased up to 120 ^{0}C, and thereafter decreased systematically with the increase in temperature. This could be attributed to the degradation of Keggin crystalline structure occurred at higher temperature as explained earlier. Also, it is seen that the Cs^+-loading efficiency was suppressed considerably from 0.5 M NaCl as compared to solution having pH-7. This suggested that the matrix did not have selectivity towards Cs^+ in the membrane matrix thermally treated in the absence of Cs^+ loading before heat treatment.

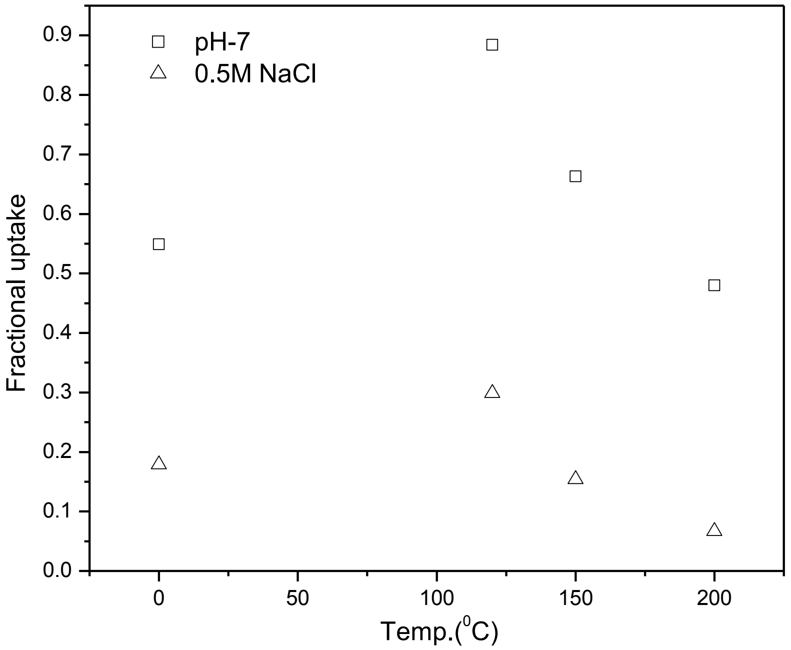

Figure 5B.7. The Cs^+-radiotracer uptake in the SiWH-poly(TMPSA)@GFM subjected to heat treatment without loading Cs^+-ions.

Contrary to this, the thermal treatment in the presence of Cs^+ ions loading did not deteriorate the Cs^+-ions radiotracer uptake efficiency beyond temp 120 ^{0}C but almost saturated to 90% as shown in Figure 5B.8. This could be attributed to enhance thermal stability of the Keggin ion crystalline temperature in the presence of Cs^+ ions. Also, the Cs^+ uptake efficiency of thermally treated Cs^+-SiWH-poly(TMPSA)@GFM from 0.5 M NaCl was similar to that from solution having pH-7. This clearly suggested the imprinting of SiWH-poly(TMPSA)@GFM for Cs^+ ions during the thermal treatment of Cs^+-SiWH-poly(TMPSA)@GFM sample.

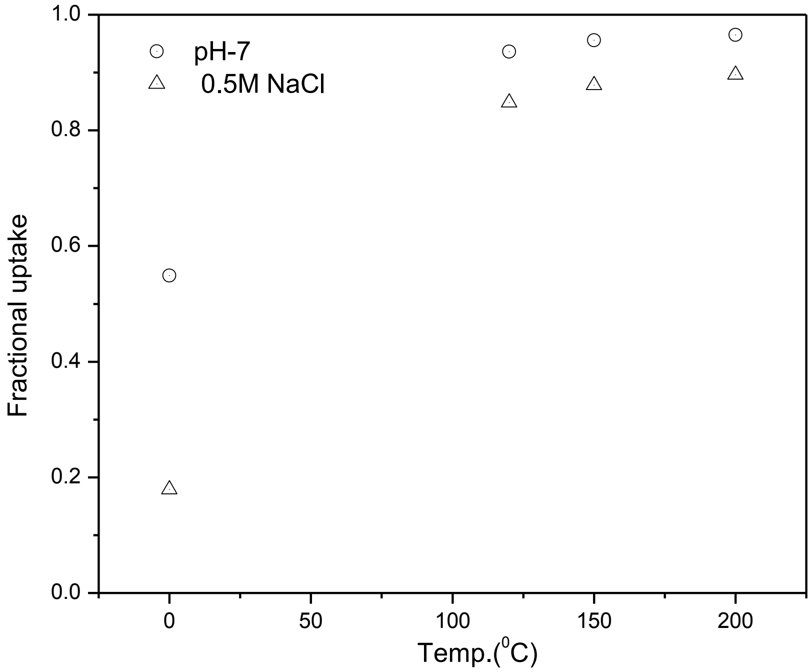

Figure 5B.8. The Cs^+-radiotracer uptake in the SiWH-poly(TMPSA)@GFM subjected to heat treatment after loading Cs^+-ions.

The sorption kinetics of Cs^+ ions in the imprinted SiWH-poly(TMPSA)@GFM is shown in Figure 5B.9 (a). It is seen from this figure that Cs^+-uptake reached optimum value 90% in 1 h, and remained constant thereafter. The uptake (%) of Cs^+ ions as function of HNO_3 concentration was also studied. It was observed from Figure 5B.9(b) that the maximum Cs^+ uptake is at the lower concentration of HNO_3 and reached lowest at 0.5 M indicating possibility of cesium deloading at higher concentration of HNO_3. The membranewas also studied for Cs^+-uptake in the concentration range 0.01-10 ppb. These Cs^+-loaded samples were subjected to gamma spectrometry. It is evident Figure 5B.9(c)**,** that the gamma count rates varied linearly with the amount of Cs^+ ions in the equilibrating solution.

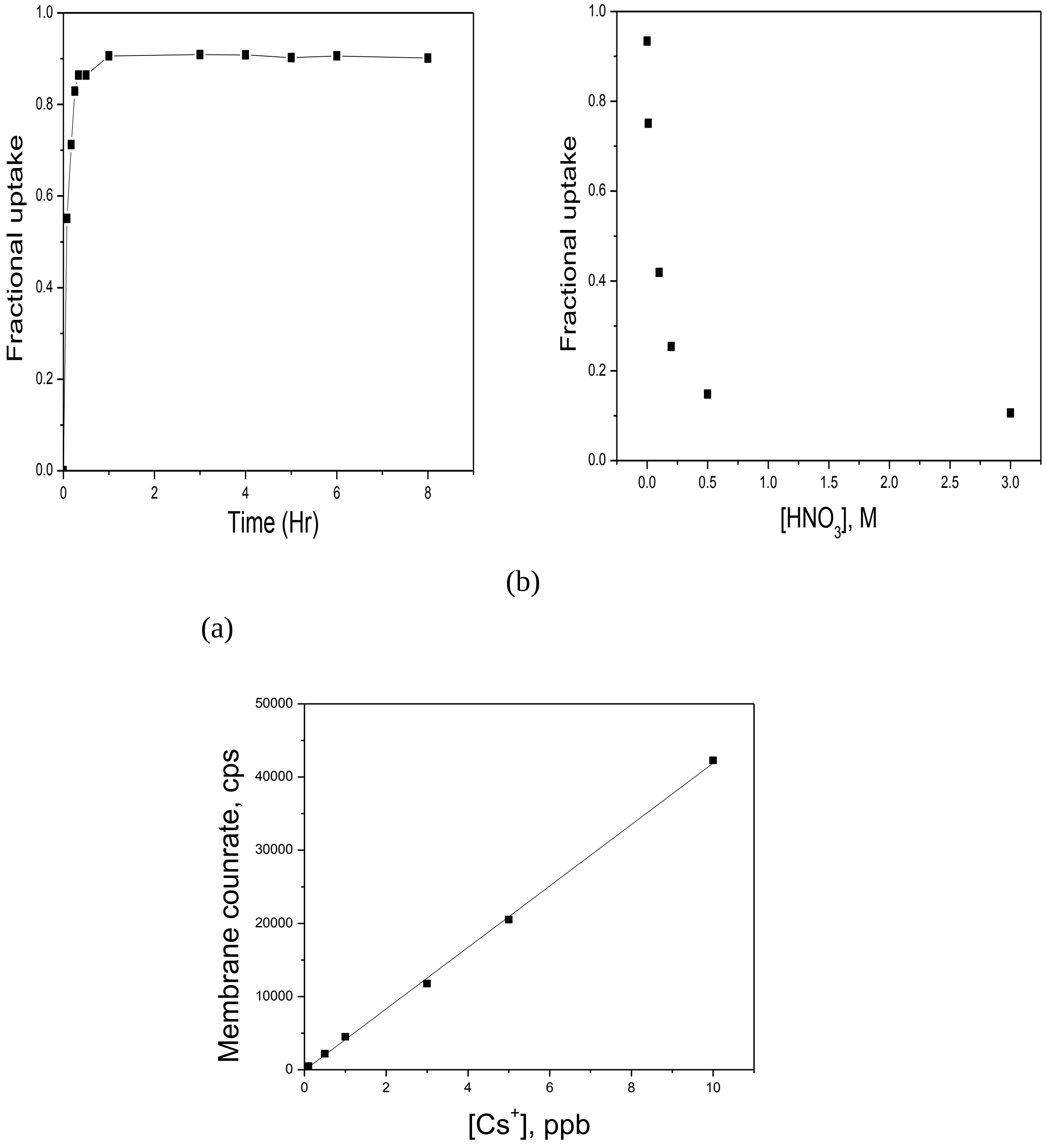

(b)

(a)

(c)

Figure 5B.9. Fractional uptake of Cs ions from pH=7 solution as a function of equilibration time(a), and from 0.01-3 mol L^{-1} HNO_3 medium (b). Calibration plot γ-count rate vs. concentration in the range of 0.01-10 ppb using imprinted SiWH-poly(TMPSA)@GFM (c).

5B.4. Conclusions

A new synthetic route has been developed for functionalization of silicotungstic acid on the glass fiber membrane. Thus formed SiWH-poly(TMPSA)@GFMhas been characterized for its chemical and physical structures. The XRD pattern of thermally treated Cs^+-SiWH-poly (TMPSA)@GFM exhibits Kaggin ion crystalline structure in the grafted matrix similar to that formed direct precipitation of Cs-silicotungstic salt responsible for high Cs^+ selectivity. The Cs^+-loading capacity was found to be 0.15 mmole g^{-1}. This membrane was found to be efficient for capturing Cs^+ in the presence of competing monovalent and divalent ions such as Na^+, Sr^{2+} and Ba^{2+} ions. The Cs^+ sorbed in the membrane could be de-loaded by equilibration in 0.5 M HNO_3.

CHAPTER 6: SUMMARY AND FUTURE SCOPE

6.1. Summary

The work carried out in this thesis involves development of polymer ligand sorbents anchored on the different host matrices such as glass, membrane, Teflon sheet and glass fiber filters. The developed substrates can be used in the ultratrace level measurements of alpha emitting actinides and β/γ-emitting fission products in the aqueous samples such as environmental samples, radiopharmaceutical samples derived from fission molly, fuel reprocessing aqueous waste samples and nuclear forensic samples using the alpha spectrometry, nuclear track detection, and gamma spectrometry. For α-spectrometry, the thin films of the polymer ligands on the host substrates were formed to minimize the degradation of alpha particles energies in the matrix itself.

The substrates developed in the present thesis can be used directly for the quantification by α-spectrometry or γ-spectrometry. The polymer ligands based methods offer several advantages over radioanalytical methods where the sample is to be subjected to multistep treatments like purification, preconcentration step for bringingthe concentration of analyte in the measurement range and also to avoid interferences of matrices in the measurements processes followed by source preparation. The functionalized thin polymer film substrates address these issues by combining the sample purification, preconcentration and source preparation in a single step. This avoids the multisteps sample treatment and also possibility of the cross-contaminations, which is important for the sample having ultratrace concentration of target radionuclide. The developed substrates also show application in the selective charge particle detection form target source by SNNTD, which is most sensitive for recording the energetic charge particles. Also, the track registration efficiency from the thin film would be considerably higher as compared to solution medium generally used for the homogeneous track registration in SSNTD for the analytical applications. It also addresses the limitations of solid state nuclear track detection with respect to chemical selectivity and limited capability to distinguish the particles based on their energies. In γ-spectrometry applications, highly porous fibrous architecture with bulk functionalized matrix of flat sheet/disc sorbents would produce materials with a large surface area and densely packed ligating sites. The applications of such materials in the conventional instrumental methods would not only exhibit rapid kinetics, high exchange capacity and capability of the selective extraction of fission products from solution but also would have well-defined counting geometry.

6.2. Conclusions

The major conclusions of the present thesis are:

(i) The phosphate bearing thin polymer film was anchored covalently on the glass substrate, which obviated the need for sample purification and source preparation for alpha spectrometry applications. The glass@poly(BMEP) substrate was found to have reasonably good selectivity towards Pu^{4+} ions with respect to Th^{4+} and UO_2^{2+} ions in a competing mode, and the representative trivalent actinide Am^{3+} did not sorbs from 3 mol L^{-1} HNO_3, even in the absence of competing ions. The overall summary of this work is shown in Scheme 6.1.

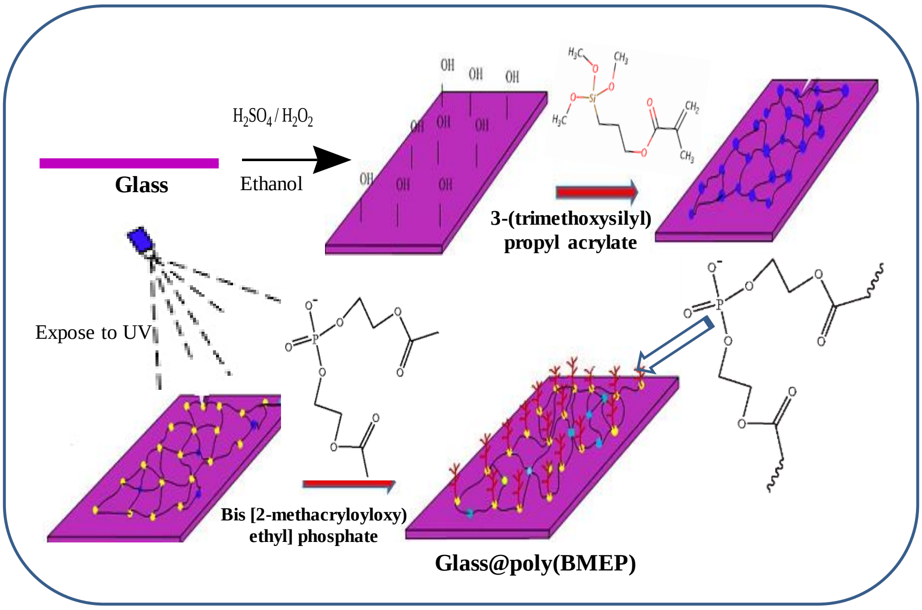

Scheme 6.1. Formation of phosphate bearing polymer grafted glass for Pu(IV) ions selective α-spectrometry.

(ii) It was observed that theglass@poly(BMEP) substrate sorbed Pu(IV) ions from 3 mol L^{-1} HNO_3 solution with a high efficiency; and could be used for their quantification by registering the alpha particles tracks in CR-39. The glass@poly(BMEP) based isotope-dilution alpha spectrometric method was successfully applied to Pu determination in seawater and ground water samples. The graphical representation of this work is illustrated in Scheme 6.2.

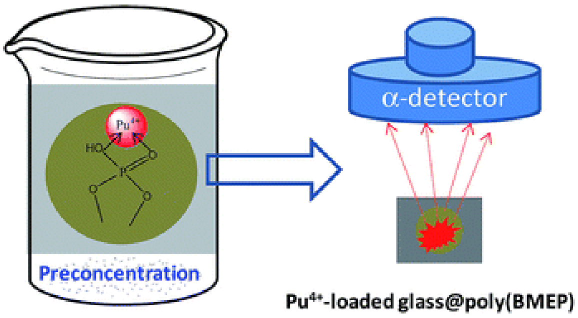

Scheme 6.2. Graphical illustration of thin ligand bearing polymer grafted substrate based α-spectrometry and SSNTD.

(iii) The polymer phosphate ligand bearing thin film on the PES membrane (Scheme 6.3)and Teflon (Scheme 6.4)substrates could be used for Pu(IV) ions quantification in the aqueous samples by chemically selective alpha or fission tracks registration based SSNTD. The selective preconcentration of Pu(IV) could enhanced the detection limit to sub-ppb conc. U(VI) was found to preconcentrate in the phosphate group anchored Teflon from natural water, and used for its quantification using fission tracks based SSNTD.

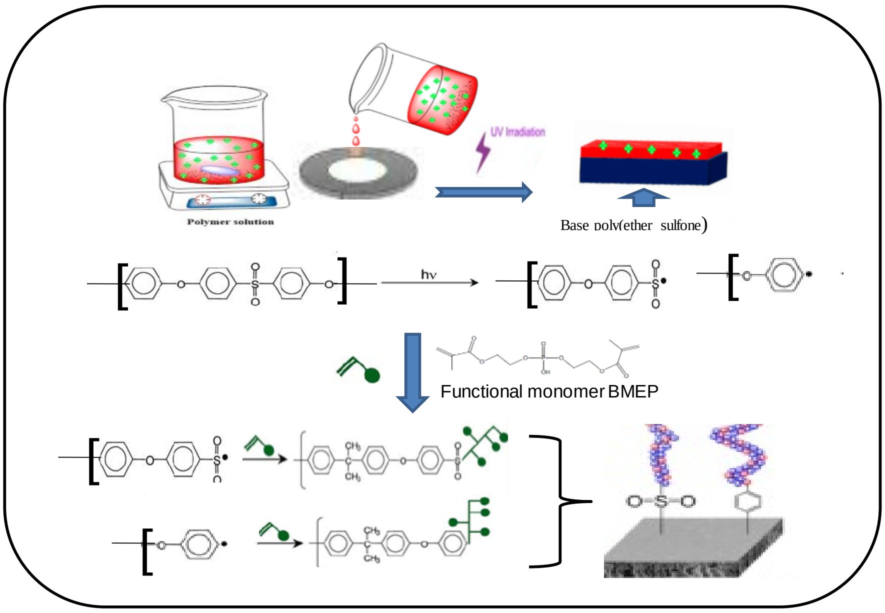

Scheme 6.3. Anchoring of thin film of poly(bis[2-(methacryloyloxy) ethyl] phosphate on PES membrane.

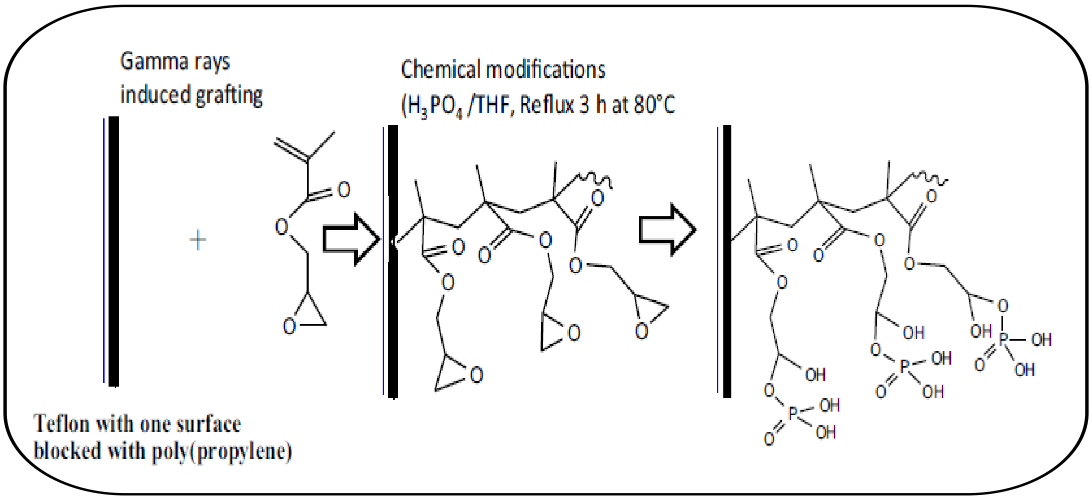

Scheme 6.4. Chemical steps involved in functionalization of radiation grafted Teflon.

(iv) A new synthetic route has been developed for grafting the crosslinked PVP chains on the glass fiber membrane Scheme 6.5. This substrate was found to capture gaseous radioiodine which remained intact in the membrane indicating its reasonably good stability in the membrane for long time storage.

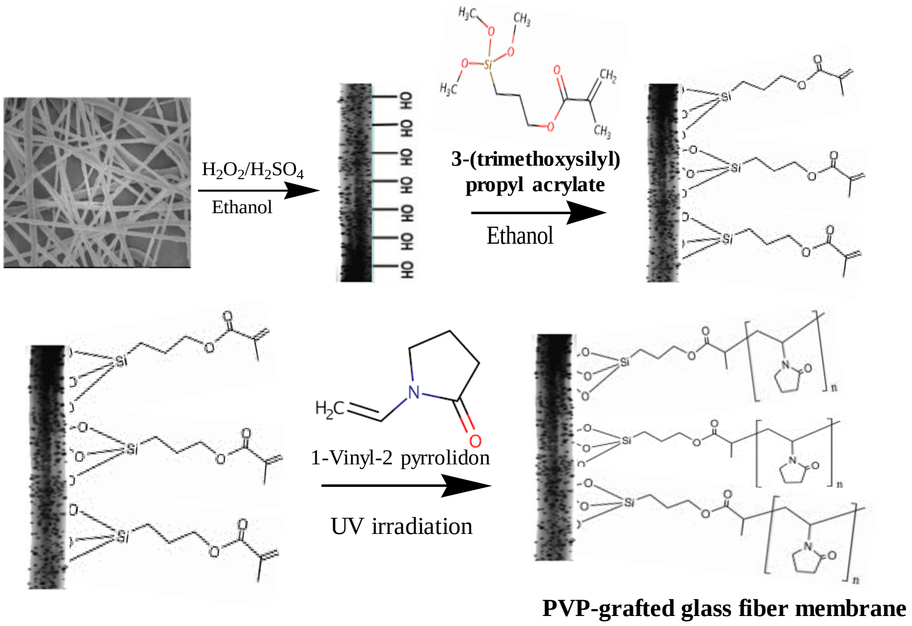

Scheme 6.5. Chemical steps involved in PVP grafted glass membrane for I_2 – sorption

(V) The cesium selective silicotungstic acid was immobilized and organized in alkoxysilane grafted glass fiber filters to capture radiocesium as shown in Scheme 6.5. The functionalized glass membrane sorbed ^{137}Cs efficiently from aqueous samples in the presence of the competing ions such as monovalent alkali and divalent alkaline ions, and could be desorbed quantitatively in 3 mol L^{-1} HNO_3.

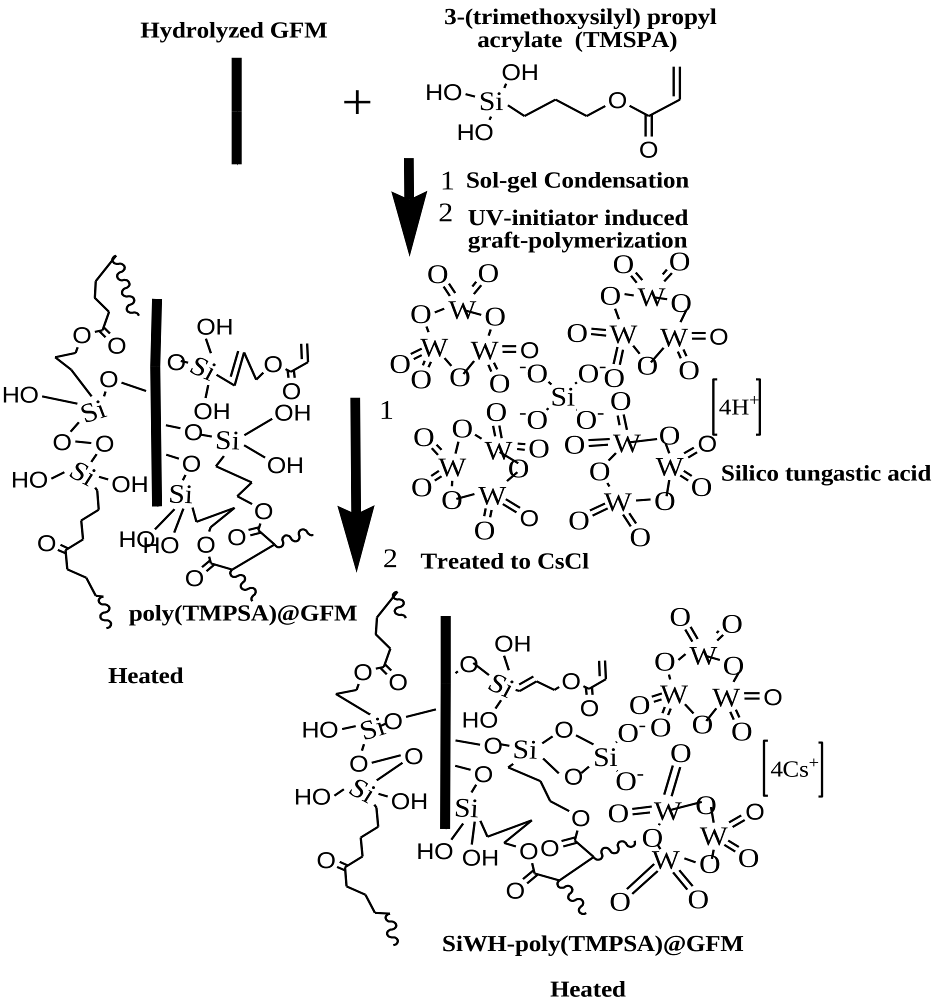

Scheme 6.6. Anchoring of silicotungastate in glass membrane for Cs^+- ions imprinting.

6.3. Future Scope

Future work could be related to the fine-tuning of the developed substrates, integration with instrumently method, using low-pressure filtration for processing of a large volume of contaminated solutions. The anchoring of actinide selective functionality on surface of organic thin film used as solid state nuclear track detectors such as CR-39 and Lexan would be very effective for the nuclear forensic applications as both detector and source would serve the purpose in ultratrace level estimation.

REFERENCES

A

Abdelouas A (2006) Uranium mill tailings: geochemistry, mineralogy, and environmental impact. Elements 2:335–341.

Addleman RS, O’Hara MJ, Grate JW, Egorov OB (2005) Chemically enhanced alpha-energy spectroscopy in liquids. J Radioanal Nucl Chem 263:291–294.

Agarwal C, Pandey AK, Das S, et al (2012) Neck-size distributions of through-pores in polymer membranes. J Memb Sci 415:608–615.

Aggarwal SK (2016) Alpha-particle spectrometry for the determination of alpha emitting isotopes in nuclear, environmental and biological samples: past, present and future. Anal Methods 8:5353–5371.

Akbari A, Desclaux S, Rouch JC, et al (2006) New UV-photografted nanofiltration membranes for the treatment of colored textile dye effluents. J Memb Sci 286:342–350.

Amero C, Golzarri JI, Izerrouken M, Espinosa G (2001) ^{148}Gd, ^{238}U, ^{239}Pu and ^{244}Cm alpha particle energy analysis using tracks in solids. Radiat Meas. 34:341–343.

AnthonyáMcKervey M (1990) Caesium-selective poly (vinyl chloride) membrane electrodes based on calix [6] arene esters. Analyst 115:1207–1210.

Asai S, Magara M, Shinohara N, et al (2008) Separation of U and Pu in spent nuclear fuel sample using anion-exchange-group-introduced porous polymer sheet for ICP-MS determination. Talanta 77:695–700.

Asfari Z, Abidi R, Arnaud F, Vicens J (1992) Synthesis and complexing properties of a double-calix [4] arene crown ether. J Incl Phenom Mol Recognit Chem 13:163–169.

Asfari Z, Weiss J, Pappalardo S, Vicens J (1993) Synthesis and properties of double-calix [4]-arenes, doubly-crowned calix [4]-arenes, and double-calix-crowns. Pure Appl Chem 65:585–590.

Atia H, Armbruster U, Martin A (2008) Dehydration of glycerol in gas phase using heteropolyacid catalysts as active compounds. J Catal 258:71–82.

Attiyat AS, Ibrahim YA, Christian GD (1988) Potentiometric selectivity study of TMC-crown formazane lonophore for cesium. Microchem J 37:122–128.

Au-Duong A-N, Vo D-T, Lee C-K (2015) Bactericidal magnetic nanoparticles with iodine loaded on surface grafted poly (N-vinylpyrrolidone). J Mater Chem B 3:840–848.

B

Bhagat PR, Acharya R, Nair AGC, et al (2009) Estimation of iodine in food, food products and salt using ENAA. Food Chem 115:706–710.

Bhagat PR, Pandey AK, Acharya R, et al (2008a) Molecular iodine selective membrane for iodate determination in salt samples: chemical amplification and preconcentration. Anal Bioanal Chem 391:1081–1089.

Bhagat PR, Pandey AK, Acharya R, et al (2008b) Molecular iodine preconcentration and determination in aqueous samples using poly(vinylpyrrolidone) containing membranes. Talanta 74:1313–1320.

Bhattacharya A, Misra BN (2004) Grafting: a versatile means to modify polymers: techniques, factors and applications. Prog Polym Sci 29:767–814.

Biaglow JE, Farhataziz MA, Rodgers J (1987) Radiation chemistry: principles and applications. VCH, New York 527.

Bocheńska M, Zielińska A, Pomećko R, et al (2003) Lower Rim Substituted tert-Butyl Calix [4] Arenes (Part IV). Calix [4] Arene-Crown Ethers as Ionophores in Plasticized PVC-Membrane Electrodes. Electroanal An Int J 15:1307–1313.

Bogatsky AV, Lukyanenko NG, Golubev VN, et al (1984) Cation selectivity of liquid-membrane electrodes based on macrocyclic lactones and lactonelactams. Anal Chim Acta 157:151–156.

Bondarenko OA, Onishchuk YN, Berezhnoy A V, et al (2000) Low level measurement of plutonium content in bioassay using SSNTD alpha-spectrometry. J Radioanal Nucl Chem 243:555–558.

Boni AL (1966) Rapid ion exchange analysis of radiocesium in milk, urine, seawater, and environmental samples. Anal Chem 38:89–92.

Boukhalfa H, Peterson DS, Gonzales ER, et al (2017) Extraction of plutonium using DIPEX immobilized in polystyrene thin films. React Funct Polym 113:31–39.

Boulyga SF, Kievitskaja AI, Kievets MK, et al (1999) Nuclear track radiography of “hot” aerosol particles. Radiat Meas 31:191–196.

Boulyga SF, Testa C, Desideri D, Becker JS (2001) Optimisation and application of ICP-MS and alpha-spectrometry for determination of isotopic ratios of depleted uranium and plutonium in samples collected in Kosovo. J Anal At Spectrom 16:1283–1289.

Brinker CJ, Scherer GW (2013) Sol-gel science: the physics and chemistry of sol-gel processing. Academic press.

Bull RK, Durrani SA (1987) Solid state nuclear track detectors, principles, method and applications Pergamon Press, Oxford.

C

Casnati A, Pochini A, Ungaro R, et al (1995) Synthesis, complexation, and membrane transport studies of 1, 3-alternate calix [4] arene-crown-6 conformers: a new class of cesium selective ionophores. J Am Chem Soc 117:2767–2777.

Chamizo E, Jiménez-Ramos MC, Wacker L, et al (2008) Isolation of Pu-isotopes from environmental samples using ion chromatography for accelerator mass spectrometry and alpha spectrometry. Anal Chim Acta 606:239–245.

Chappa S, Das S, Debnath AK, et al (2016a) Spacer Monomer in Polymer Chain Influencing Affinity of Ethylene Glycol Methacrylate Phosphate toward UO_2^{2+} and Pu^{4+} Ions. Ind Eng Chem Res. 55: 8992-9002

Chappa S, Mhatre AM, Adya VC, Pandey AK (2017) Egg-shell membrane mimicking synthetic polymer membrane supported palladium nanoparticles for catalyzing reduction of uranyl(VI) ions. Appl Catal B Environ. 203: 53-64.

Chappa S, Singha Deb AK, Ali SM, et al (2016b) Change in the Affinity of Ethylene Glycol Methacrylate Phosphate Monomer and Its Polymer Anchored on a Graphene Oxide Platform toward Uranium(VI) and Plutonium(IV) Ions. J Phys Chem B. 120: 2942–2950.

Chaudhari CV, Guin JP, Dubey KA, et al (2016) Radiation induced grafting of glycidyl methacrylate on teflon scrap for synthesis of dual type adsorbent: Process parameter standardisation. Environ Prog Sustain Energy 35:1367–1373.

Chavan V, Agarwal C, Adya VC, Pandey AK (2018) Hybrid organic-inorganic anion-exchange pore-filled membranes for the recovery of nitric acid from highly acidic aqueous waste streams. Water Res 133:87–98.

Chavan V, Agarwal C, Pandey AK (2016) Pore-filled scintillating membrane as sensing matrix for α-emitting actinides. Anal Chem 88:3796–3803.

Chavan V, Paul S, Pandey AK, et al (2013) Thin extractive membrane for monitoring actinides in aqueous streams. J Hazard Mater 260:53–60.

Choi Y, Kim H, Lee JK, et al (2004) Cesium ion-selective electrodes based on 1, 3-alternate thiacalix [4] biscrown-6, 6. Talanta 64:975–980.

Crespo MT (2012) A review of electrodeposition methods for the preparation of alpha-radiation sources. Appl Radiat Isot 70:210–215.

Currie LA (1968) Limits for qualitative detection and quantitative determination. Application to radiochemistry. Anal Chem 40:586–593.

D

Das S, Borah R, Devi RR, Thakur AJ (2008) Molecular iodine in protection and deprotection chemistry. Synlett 2008:2741–2762.

De Benoist B, Andersson M, Egli IM, et al (2004) Iodine status worldwide: WHO global database on iodine deficiency, Geneva,2004, ISBN 92 4 159200 1.

Degirmenci L, Oktar N, Dogu G (2011) Activated carbon supported silicotungstic acid catalysts for ethyl-tert-butyl ether synthesis. AIChE J 57:3171–3181.

Dozol M, Hagemann R (1993) Radionuclide migration in groundwaters: review of the behaviour of actinides (technical report). Pure Appl Chem 65:1081–1102.

Durrani SA, Bull RK (2013) Solid state nuclear track detection: principles, methods and applications. Elsevier.

Duval CE, Darge AW, Ruff C, et al (2018) Rapid sample preparation for alpha spectroscopy with ultrafiltration membranes. Anal Chem 90:4144–4149.

E

Eikenberg J, Jäggi M, Beer H, et al (2009) Separation techniques for low-level determination of actinides in soil samples. Appl Radiat Isot 67:776–780.

Essayem N, Holmqvist A, Gayraud PY, et al (2001) In situ FTIR studies of the protonic sites of $H_3PW_{12}O_{40}$ and its acidic cesium salts $M_xH_{3-x}PW_{12}O_{40}$. J Catal 197:273–280.

F

Fábián F, Csordás A, Sas Z, Kovács T (2017) Preparation of a radon-free thoron source for a thoron calibration chamber. J Radioanal Nucl Chem 311:1169–1175.

Fallon MG, Mulcahy D, Murphy WS, Glennon JD (1996) Cesium ion-selective electrodes based on crowned benzoquinones. Analyst 121:127–131.

Fink D (2013) Fundamentals of ion-irradiated polymers. Springer Science & Business Media

Fischer BE, Spohr R (1983) Production and use of nuclear tracks: imprinting structure on solids. Rev Mod Phys 55: 907-944.

Fleischer RL, Price PB, Walker RM, Leakey LSB (1965) Fission-Track Dating of Bed I, Olduvai Gorge. Science 148:72–74.

Fleischer RL, Price PB, Walker RM, Walker RM (1975) Nuclear tracks in solids: principles and applications. Univ of California Press., page 1-597.

Fleisher RL, Price PB, Walker RM (1979) Nuclear Tracks in SolidsUniversity of California Press.

Friedlander G, Kennedy JW, Macias ES (1981) Nuclear and radiochemistry. John Wiley & Sons.

G

GarciaáAlonso JI (1995) Determination of fission products and actinides in spent nuclear fuels by isotope dilution ion chromatography inductively coupled plasma mass spectrometry. J Anal At Spectrom 10:381–393.

Gavrilescu M, Pavel LV, Cretescu I (2009) Characterization and remediation of soils contaminated with uranium. J Hazard Mater 163:475–510.

Gazda DB, Lipert RJ, Fritz JS, Porter MD (2004) Investigation of the iodine–poly (vinylpyrrolidone) interaction employed in the determination of biocidal iodine by colorimetric solid-phase extraction. Anal Chim Acta 510:241–247.

Ghidini E, Ugozzoli F, Ungaro R, et al (1990) Complexation of alkali metal cations by conformationally rigid, stereoisomeric calix [4] arene crown ethers: a quantitative evaluation of preorganization. J Am Chem Soc 112:6979–6985.

Glad B, Irgum K, Hörstedt P (1995) Photopolymerization and characterization of methacrylate-based reactive composite membranes. J Memb Sci 100:171–179.

Goel NK, Kumar V, Pahan S, et al (2011) Development of adsorbent from Teflon waste by radiation induced grafting: Equilibrium and kinetic adsorption of dyes. J Hazard Mater 193:17–26.

Gorden AE V, Xu J, Raymond KN, Durbin P (2003) Rational design of sequestering agents for plutonium and other actinides. Chem Rev 103:4207–4282.

Grate JW, O’Hara MJ, Farawila AF, et al (2011) Extraction chromatographic methods in the sample preparation sequence for thermal ionization mass spectrometric analysis of plutonium isotopes. Anal Chem 83:9086–9091.

Gray J, Jones SR, Smith AD (1995) Discharges to the environment from the Sellafield site, 1951-1992. J Radiol Prot 15:99.

Guérin N, Calmette R, Johnson T, Larivière D (2011) Multi-dimensional extraction chromatography of actinides for alpha and mass spectrometry. Anal Methods 3:1560–1567.

Gutsche CD, Dhawan B, Levine JA, et al (1983) Calixarenes 9: Conformational isomers of the ethers and esters of calix [4] arenes. Tetrahedron 39:409–426.

Gutsche CD, Izatt RM, Christensen JJ (1987) Synthesis of Macrocycles: The Design of Selective Complexing Agents.

H

Habibi A, Boulet B, Gleizes M, et al (2015) Rapid determination of actinides and ^{90}Sr in river water. Anal Chim Acta 883:109–116.

Haider MH, Dummer NF, Zhang D, et al (2012) Rubidium-and caesium-doped silicotungstic acid catalysts supported on alumina for the catalytic dehydration of glycerol to acrolein. J Catal 286:206–213.

Hanson SK, Mueller AH, Oldham Jr WJ (2014) Kläui Ligand Thin Films for Rapid Plutonium Analysis by Alpha Spectrometry. Anal Chem 86:1153–1159.

Hassan NM, Hanafy MS, Naguib A, El-Saftawy AA (2017) Controlling alpha tracks registration in Makrofol DE 1-1 detector. Nucl Instruments Methods Phys Res Sect B Beam Interact with Mater Atoms 407:230–235.

He D, Ulbricht M (2006) Surface-selective photo-grafting on porous polymer membranes via a synergist immobilization method. J Mater Chem 16:1860–1868.

He Q, Walling DE (1996) Interpreting particle size effects in the adsorption of ^{137}Cs and unsupported ^{210}Pb by mineral soils and sediments. J Environ Radioact 30:117–137.

Hepburn C, Windle AH (1980) Solid state nuclear track detectors. J Mater Sci 15:279–301.

Hernández-Mendoza H, Chamizo E, Delgado A, et al (2011) Comparison of methods and application of alpha spectrometry and mass spectrometry techniques for ^{239}Pu determination in biological samples. J Anal At Spectrom 26:1509–1513.

Hofstadter R (1949) The detection of gamma-rays with thallium-activated sodium iodide crystals. Phys Rev 75:796.

Huang CP, Lin TY, Chiao LH, Chen HB (2012) Characterization of radioactive contaminants and water treatment trials for the Taiwan Research Reactor's spent fuel pool. J Hazard Mater 233:140–147.

I

Iqbal MS, Jamil Y, Kausar T, Akhtar M (2009) Thermal degradation study of glycidyl methacrylate acrylonitrile copolymers. J Therm Anal Calorim 96:225–233.

Iyer RH, Chaudhuri NK (1997) Development of the track registration technique in solid state nuclear track detectors from solution media and its applications. Radiat Meas 27:529–548.

Iyer RH, Pandey AK, Kalsi PC, Sharma RC (1991) Excitation functions for the helium-ion-induced fission of holmium and erbium. Phys Rev C 44:2644.

Iyer RH, Pandey AK, Kalsi PC, Sharma RC (1993) Helium-ion-induced fission excitation functions of terbium and ytterbium. Phys Rev C 48:87.

J

Jackson D, Zimmerman CH, Gray J (1998) Discharges of krypton from Sellafield, 1951-1997, and the resultant doses to members of the public. J Radiol Prot 18(2):111-118.

Jagtap RN, Ambre AH (2006) Overview literature on atomic force microscopy (AFM): Basics and its important applications for polymer characterization.

Jalili N, Laxminarayana K (2004) A review of atomic force microscopy imaging systems:

application to molecular metrology and biological sciences. Mechatronics 14:907–945.

Jenkins R (1995) Quantitative X-ray spectrometry. CRC Press., volume 20.

K

Kalal J, Švec F, Maroušek V (1974) Reactions of epoxide groups of glycidyl methacrylate copolymers. In: Journal of Polymer Science: Polymer Symposia. Wiley Online Library, pp 155–166

Karamanis D, Ioannides KG, Stamoulis KC (2006) Determination of ^{226}Ra in aqueous solutions via sorption on thin films and α-spectrometry. Anal Chim Acta 573:319–327.

Ketterer ME, Hafer KM, Jones VJ, Appleby PG (2004) Rapid dating of recent sediments in Loch Ness: inductively coupled plasma mass spectrometric measurements of global fallout plutonium. Sci Total Environ 322:221–229.

Khan HA (1973) An important precaution in the etching of solid state nuclear track detectors. Nucl Instruments Methods 109:515–519.

Kim G, Burnett WC, Horwitz EP (2000a) Efficient preconcentration and separation of actinide elements from large soil and sediment samples. Anal Chem 72:4882–4887.

Kim J, Suh I, Kim J, Cho M (1998) Selective sensing of caesium ions by novel calix [4] arene bis (dibenzocrown) ethers in an aqueous environment. J Chem Soc Perkin Trans 1 2307–2312.

Kim JS, Lee WK, Suh I-H, et al (2000b) Heterogeneous binuclear complexation of 1, 3-alternate calix [4]-bis-crown bearing two different crown rings. J Org Chem 65:7215–7217.

Klemenčič H, Benedik L (2010) Alpha-spectrometric thin source preparation with emphasis on homogeneity. Appl Radiat Isot 68:1247–1251.

Knoll GF (2010) Radiation detection and measurement. John Wiley & Sons

Konidakis I, Pissadakis S (2014) Optical spectra tuning of all-glass photonic bandgap fiber infiltrated with silver fast-ion-conducting glasses. Materials (Basel) 7:5735–5745.

Krtil J, Bezděk M (1968) Comparison of quantitative and substoichiometric determination of caesium from fission products with nitrobenzene solution of lithium dipicrylaminate. Talanta 15:1423–1433.

L

Labrecque C, Whitty-Léveillé L, Larivière D (2013) Cloud point extraction of plutonium in environmental matrixes coupled to ICPMS and α spectrometry in highly acidic conditions. Anal Chem 85:10549–10555.

Lariviere D, Benkhedda K, Kiser S, et al (2010) Rapid and automated sequential determination of ultra-trace long-lived actinides in air filters by inductively coupled plasma mass spectrometry. Anal Methods 2:259–267.

Law YL, Nikezic D, Yu KN (2008) Optical appearance of alpha-particle tracks in CR-39 SSNTDs. Radiat Meas 43:S128–S131.

Lebed PJ, de Souza K, Bilodeau F, et al (2011) Phosphonate-functionalized large pore 3-D cubic mesoporous (KIT-6) hybrid as highly efficient actinide extracting agent. Chem Commun 47:11525–11527.

Lebed PJ, Savoie J-D, Florek J, et al (2012) Large pore mesostructured organosilica-phosphonate hybrids as highly efficient and regenerable sorbents for uranium sequestration. Chem Mater 24:4166–4176.

Lee EH, Lewis MB, Blau PJ, Mansur LK (1991) Improved surface properties of polymer materials by multiple ion beam treatment. J Mater Res 6:610–628.

Leo WR (2012) Techniques for nuclear and particle physics experiments: a how-to approach. Springer Science & Business Media

Li C, Lariviere D, Kiser S, et al (2008) Method intercomparison for the analysis of $^{239/240}$Pu in human urine. J Anal At Spectrom 23:521–526.

Liu Z-M, Xu Z-K, Wan L-S, et al (2005) Surface modification of polypropylene microfiltration membranes by the immobilization of poly(N-vinyl-2-pyrrolidone): a facile plasma approach. J Memb Sci 249:21–31.

Locklair WD, Mannion JM, Husson SM, Powell BA (2016) Uptake of plutonium on a novel thin film for use in spectrometry. J Radioanal Nucl Chem 307:2333–2338.

Love S, Filby R, Glover S, et al (1998) Use of combined alpha-spectrometry and fission track analysis for the determination of ^{240}Pu/^{239}Pu ratios in human tissue. J Radioanal Nucl Chem 234:189–193.

M

Ma H, Bowman CN, Davis RH (2000) Membrane fouling reduction by backpulsing and surface modification. J Memb Sci 173:191–200.

Mannion JM, Locklair WD, Powell BA, Husson SM (2016) Alpha spectroscopy substrates based on thin polymer films. J Radioanal Nucl Chem 307:2339–2345.

Manos MJ, Kanatzidis MG (2012) Layered metal sulfides capture uranium from seawater. J Am Chem Soc 134:16441–16446.

Mazumdar N, Chikindas ML, Uhrich K (2010) Slow release polymer–iodine tablets for disinfection of untreated surface water. J Appl Polym Sci 117:329–334.

McCurdy D, Lin Z, Inn KGW, et al (2005) Second interlaboratory comparison study for the analysis of ^{239}Pu in synthetic urine at the μBq (100 aCi) level by mass spectrometry. J Radioanal Nucl Chem 263:447–455.

Meinke WW (1957) Reviews of articles published late 1955 to late 1957 on applicationsof radioisotopes to analysis.

Mekki S, Bouvier-Capely C, Jalouali R, Rebière F (2010) The extraction of thorium by calix [6] arene columns for urine analysis. Radiat Prot Dosimetry 144:330–334.

Metz LA, Payne RF, Engelmann MD (2011) Optimizing separation of iodine from halogen interferences in preparation for TIMS analysis. Sep Sci Technol 46:2451–2455.

Milliard A, Durand-Jézéquel M, Larivière D (2011) Sequential automated fusion/extraction chromatography methodology for the dissolution of uranium in environmental samples for mass spectrometric determination. Anal Chim Acta 684:40–46.

Misdaq MA, Aitayoub A, Chaouqi A (2018) Analysis of ^{238}U, ^{232}Th, ^{222}Rn, and ^{220}Rn in Fresh and Canned Marine Fish Samples Using Solid State Nuclear Track Detectors and Resulting Alpha Radiation Doses to Adult Consumers. Health Phys 114:436–449.

Mishra R, Tripathy SP, Dwivedi KK, et al (2003) Effect of electron irradiation on polytetrafluoro ethylene. Radiat Meas 37:247–251.

Mnasri N, Charnay C, De Menorval LC, et al (2014) Silver nanoparticle-containing submicron-in-size mesoporous silica-based systems for iodine entrapment and immobilization from gas phase. Microporous Mesoporous Mater 196:305–313.

Moulay S (2013) Molecular iodine/polymer complexes. J Polym Eng 33:389–443.

N

Nandanwar SU, Coldsnow K, Utgikar V, et al (2016) Capture of harmful radioactive contaminants from off-gas stream using porous solid sorbents for clean environment–A review. Chem Eng J 306:369–381.

Nenoff TM, Rodriguez MA, Soelberg NR, Chapman KW (2014) Silver-mordenite for radiologic gas capture from complex streams: Dual catalytic CH_3I decomposition and I confinement. Microporous Mesoporous Mater 200:297–303.

Nouh SA, Wahab LA, Eissa HM (1998) The effect of alpha particle dose on the thermal degradation of some SSNTDs. Radiat Meas 29:465–471.

P

Patterson MS, Greene RC (1965) Measurement of Low Energy Beta-Emitters in Aqueous Solution by Liquid Scintillation Counting of Emulsions. Anal Chem 37:854–857.

Paul S, Pandey AK, Kumar P, et al (2014) Tailored bifunctional polymer for plutonium monitoring. Anal Chem 86:6254–6261.

Paul S, Pandey AK, Shah R V, et al (2016) Polymer based sorbent materials for thermal ionization mass spectrometric determination of uranium (VI) and plutonium (IV) ions. J Anal At Spectrom 31:985–993.

Paul S, Pandey AK, Shah R V, Aggarwal SK (2015) Chemically selective polymer substrate based direct isotope dilution alpha spectrometry of Pu. Anal Chim Acta 878:54–62.

Peper S, Gonczy C, Runde W (2005) Cs^+-selective membrane electrodes based on ethylene glycol-functionalized polymeric microspheres. Talanta 67:713–717.

Peterson DS, Montoya VM (2009) Separation of actinides using capillary extraction chromatography-inductively coupled plasma mass spectrometry. J Chromatogr Sci 47:545–548.

Petrow HG, Levine H (1967) Ammonium hexacyanocobalt ferrate as an improved inorganic exchange material for determination of cesium-137. Anal Chem 39:360–362.

Pillai GS, Hameed PS, Khan SMMN (2016) Natural radioactivity levels in the soils and human risk assessment in Tiruchirappalli district (Tamil Nadu, India). J Radioanal Nucl Chem 307:1265–1277.

Pommé S (2015) Typical uncertainties in alpha-particle spectrometry. Metrologia 52:S146.

Price PB (2005) Science and technology with nuclear tracks in solids. Radiat Meas 40:146–159.

Price PB (2008) Recent applications of nuclear tracks in solids. Radiat Meas 43:S13–S25.

Punyani S, Narayana P, Singh H, Vasudevan P (2006) Iodine based water disinfection: A review. Journal of scientific and industrial research. 65(2):116-120.

Q

Qiao B, Demars T, Olvera de la Cruz M, Ellis RJ (2014) How hydrogen bonds affect the growth of reverse micelles around coordinating metal ions. J Phys Chem Lett 5:1440–1444.

Qiao J, Hou X, Miró M, Roos P (2009) Determination of plutonium isotopes in waters and environmental solids: a review. Anal Chim Acta 652:66–84.

Qiao J, Hou X, Roos P, Miró M (2013) Bead injection extraction chromatography using high-capacity lab-on-valve as a front end to inductively coupled plasma mass spectrometry for urine radiobioassay. Anal Chem 85:2853–2859.

R

Reilly D, Ensslin N, Smith Jr H, Kreiner S (1991) Passive nondestructive assay of nuclear materials. Nuclear Regulatory Commission, Washington, DC (United States). LA-UR-90-732.

Riley BJ, Chun J, Ryan J V, et al (2011) Chalcogen-based aerogels as a multifunctional platform for remediation of radioactive iodine. RSC Adv 1:1704–1715.

Riley BJ, Pierce DA, Chun J, et al (2014) Polyacrylonitrile-chalcogel hybrid sorbents for radioiodine capture. Environ Sci Technol 48:5832–5839.

Riley BJ, Vienna JD, Strachan DM, et al (2016) Materials and processes for the effective capture and immobilization of radioiodine: A review. J Nucl Mater 470:307–326.

Rim JH, Armenta CE, Gonzales ER, et al (2016) Evaluating bis (2-ethylhexyl) methanediphosphonic acid (H2DEH [MDP]) based polymer ligand film (PLF) for plutonium and uranium extraction. J Radioanal Nucl Chem 307:2327–2332.

Roggenkamp HG, Kiesewetter H, Spohr R, et al (1981) Production of Single Pore Membranes for the Measurement of Red Blood Cell Deformability-Produktion von Einzelloch-Membranen zur Messung des Verformungsvermögens von roten Blutkörperchen. Biomed Tech Eng 26:167–169.

Roos P (2003) Analysing alpha particle emitters using semiconductor detectors. Detector operation and source preparation. In: Seminar on sampling techniques, radiochemical methods, detectors and measurements, Baltic-Danish Co-operation on Radiation Protection.

Risø National Laboratory, pp 77–88.

S

Saleh MB, Hassan SSM, Abdel Gaber AA, Abdel Kream NA (2003) PVC membrane cesium ion-selective sensor based on cephalexin antibiotic. Anal Lett 36:2367–2377.

Sava Gallis DF, Ermanoski I, Greathouse JA, et al (2017) Iodine gas adsorption in nanoporous materials: A combined experiment–modeling study. Ind Eng Chem Res 56:2331–2338.

Scott RPW (2000) Physical chemistry resources (Book 5. Thermal Analysis).

Shamsipur M, Kazemi S, Sharghi H, Niknam K (2001) Cesium-selective membrane electrode based on a recently synthesized 16-membered macrocyclic diamide. Fresenius J Anal Chem 371:1104–1108.

Sibbens G, Altzitzoglou T (2007) Preparation of radioactive sources for radionuclide metrology. Metrologia 44:S71.

Silva RJ, Nitsche H (1995) Actinide environmental chemistry. Radiochim acta 70:377–396.

Singhania A, Bhaskarwar AN (2018) TiO_2 as a catalyst for hydrogen production from hydrogen-iodide in thermo-chemical water-splitting sulfur-iodine cycle. Fuel 221:393–398.

Sodaye S, Tripathi R, Pandey AK, Reddy AVR (2004) Scintillating polymer inclusion membrane for preconcentration and determination of α-emitting actinides. Anal Chim Acta 514:159–165.

Spinks JWT, Woods RJ (1990) An introduction to radiation chemistry. radiation Research. 124(3):378-379.

Steinbauer E, Bauer P, Geretschläger M, et al (1994) Energy resolution of silicon detectors: approaching the physical limit. Nucl Instruments Methods Phys Res Sect B Beam Interact with Mater Atoms 85:642–649.

Steinhauser G (2014) Fukushima’s forgotten radionuclides: a review of the understudied radioactive emissions. Environ Sci Technol 48:4649–4663.

Sun Y, Shao D, Chen C, et al (2013) Highly efficient enrichment of radionuclides on graphene oxide-supported polyaniline. Environ Sci Technol 47:9904–9910.

Susanto H, Ulbricht M (2007) Photografted Thin Polymer Hydrogel Layers on PES Ultrafiltration Membranes: Characterization, Stability, and Influence on Separation Performance. Langmuir 23:7818–7830.

T

Talmadge C (2007) Deterring a nuclear 9/11. Wash Q 30:21–34.

Tian H, Savadogo O (2006) Silicotungstic acid Nafion composite membrane for proton-exchange membrane fuel cell operation at high temperature. J New Mater Electrochem Syst 9:61.

Tran QT, Pomorski M, de Sanoit J, et al (2014) Optimization of actinides trace precipitation on diamond/Si PIN sensor for alpha-spectrometry in aqueous solution. IEEE Trans Nucl Sci 61:2082–2089.

Tretyakova SP (1991) Observation of nuclear clusters in the spontaneous fission of heavy nuclei. Int J Radiat Appl Instrumentation Part D Nucl Tracks Radiat Meas 19:667–674.

Tretyakova SP, Bonetti R, Golovchenko A, et al (2001) Study of cluster decay of ^{242}Cm using SSNTD. Radiat Meas 34:241–243.

U

Ulbricht M, Matuschewski H, Oechel A, Hicke H-G (1996) Photo-induced graft polymerization surface modifications for the preparation of hydrophilic and low-proten-adsorbing ultrafiltration membranes. J Memb Sci 115:31–47.

Uma V, Srivastava BK, Chaudhuri NK, Iyer RH (1980) Nuclear track registration from solution media: alpha track registration in solid state track detectors in solutions of actinides. Nucl Instruments Methods 171:75–86.

Ungaro R, Casnati A, Ugozzoli F, et al (1994) 1, 3-Dialkoxycalix [4] arenecrowns-6 in 1,3-Alternate Conformation: Cesium-Selective Ligands that Exploit Cation-Arene Interactions. Angew Chemie Int Ed English 33:1506–1509.

V

Vajda N, Kim C-K (2011) Determination of transuranium isotopes (Pu, Np, Am) by radiometric techniques: a review of analytical methodology. Anal Chem 83:4688–4719.

Vajda N, Törvényi A, Kis-Benedek G, et al (2009) Rapid method for the determination of actinides in soil and sediment samples by alpha spectrometry. Radiochim Acta Int J Chem Asp Nucl Sci Technol 97:395–401.

Vasudevan T, Das S, Sodaye S, et al (2009) Pore-functionalized polymer membranes for preconcentration of heavy metal ions. Talanta 78:171–177.

W

Walling DE, He Q (1993) Use of cesium-137 as a tracer in the study of rates and patterns of floodplain sedimentation. IAHS Publ 319.

Wolf S (1998) Application of instrumental radioanalytical techniques to nuclear waste testing and characterization. J Radioanal Nucl Chem 235:207–212.

X

Xu Z-K, Dai Q-W, Liu Z-M, et al (2003) Microporous polypropylene hollow fiber membranes: Part II. Pervaporation separation of water/ethanol mixtures by the poly (acrylic acid) grafted membranes. J Memb Sci 214:71–81.

Xu Z, Wang J, Shen L, et al (2002) Microporous polypropylene hollow fiber membrane: Part I. Surface modification by the graft polymerization of acrylic acid. J Memb Sci 196:221–229.

Z

Zapata F (2003) The use of environmental radionuclides as tracers in soil erosion and sedimentation investigations: recent advances and future developments. Soil Tillage Res

69:3–13.

Zheng J, Tagami K, Homma-Takeda S, Bu W (2013) The key role of atomic spectrometry in radiation protection. J Anal At Spectrom 28:1676–1699.

Zhou J, Hao S, Gao L, Zhang Y (2014) Study on adsorption performance of coal based activated carbon to radioactive iodine and stable iodine. Ann Nucl Energy 72:237–241.

Zhu L, Liu Z, Cheng W, Cheng S (1996) Removing Cs from nuclear waste liquid by crown ether and heteropoly acid. ournal of Radioanalyfical and Nuclear Chemistry. 205: 49-56.

Zolotov YA, Tsysin GI, Morosanova EI, Dmitrienko SG (2005) Sorption preconcentration of microcomponents for chemical analysis. Russ Chem Rev 74:37–60.

Zorri V, Remetti R, Capogni M, et al (2017) Feasibility study on the application of solid state tracks detectors for fast surveys of residual alpha contamination in decommissioning activities. Radiat Meas 107:111–114.